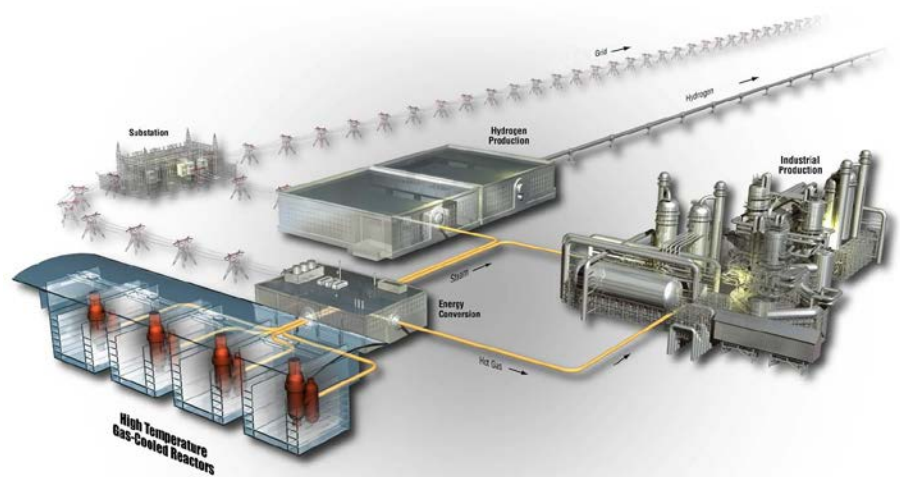# Role of Nuclear Grade Graphite in Controlling Oxidation in Modular HTGRs

W. Windes, G. Strydom, R. Smith, and J. Kane

November 2014

The INL is a
U.S. Department of Energy
National Laboratory
operated by
Battelle Energy Alliance

INL
Idaho National
Laboratory

Role of Nuclear Grade Graphite in Controlling Oxidation in Modular HTGRs

**W. Windes, G. Strydom, R. Smith,
and J. Kane**

November 2014

**Idaho National Laboratory
ART Program
Idaho Falls, Idaho 83415**

http://www.inl.gov

ART Program

Role of Nuclear Grade Graphite in Controlling Oxidation in Modular HTGRs
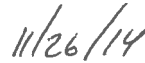
INL/EXT-14-31720
Revision 0

November 2014

Approved by:

_____
Travis Mitchell
INL ART Project Manager

_____11/26/14_____
Date

EXECUTIVE SUMMARY

The passively safe modular High Temperature Gas-cooled Reactor (mHTGR) design is one of the primary concepts considered for Generation IV and Small Modular Reactor (SMR) programs. The helium cooled, graphite moderated reactor design provides a high outlet temperature option for generating either industrial process heat or electricity generation at high efficiencies. While the nuclear grade graphite core provides neutron moderation, high temperature stability, thermal conductivity, and passively safe reactivity control for these high temperature reactors, graphite is a carbonaceous material and this has generated a persistent concern that the graphite core components could actually burn during accident conditions.

This report directly addresses the issue of uncontrolled, self-sustained oxidation (burning) of graphite and demonstrates that burning is not possible for high purity, nuclear graphite. The four conditions for self-sustained oxidation (fuel, oxygen, heat and chemical reaction) as defined by the National Fire Protection Association (NFPA) are introduced to define the parameters required for self-sustained burning. Using the four common NFPA requirements, the principles underlying graphite oxidation are summarized over a range of length-scales based upon the large international knowledgebase related to graphite oxidation. To illustrate the dissimilar oxidation behavior for different carbonaceous materials the physical and material differences between coal, a carbonaceous material that can burn, and graphite, a similar carbonaceous material that cannot burn, are summarized. This illustrates that while coal and graphite may seem outwardly similar; the unique atomic crystal structure of graphite eliminates three of the four requirements for self-sustained burning and is critical to limiting graphite oxidation.

A detailed explanation is presented for the concept that the unique crystal structure and microstructure of graphite eliminates one or more conditions for self-sustained oxidation at all graphite length-scales (atomic crystal structure length scales to the component length scales). Combustion or burning, as defined by the NFPA, is the sequence of chemical reactions between a carbonaceous fuel and an oxidant accompanied by the production of heat and conversion of chemical species. At the atomic scale, every carbon atom may be assumed to potentially be fuel for a carbon-oxygen self-sustaining chemical reaction. However, the carbon atoms in graphite are covalently bonded within graphene basal planes stacked within graphite crystallites. Only those atoms at specific atomic crystal position sites are actually available for the graphite-oxygen reaction. This severely limits the available fuel for the oxidation reaction, as reactive surface area (RSA) sites occur only on the outer edges of the crystallites and oxygen cannot diffuse inside the crystallite structure to react with central atoms. Thus only a fraction of the available carbon atoms react at even the smallest graphite length-scale, the crystallites, which severely limits the rate of reaction at any temperature.

Oxidation of graphite is a complex phenomenon requiring specific knowledge of the chemical reaction behavior as well as material properties of nuclear grade graphite at all length scales to determine the oxidation behavior. Oxygen transport theory at the atomic and crystallite length scale is the key parameter driving the behavior of graphite self-sustained oxidation but all mechanisms and factors underlying graphite-oxygen chemical reactions such as the graphite microstructure, the component size, and temperature affect the rate of graphite oxidation. The rate of graphite oxidation is dependent not just upon the theoretical oxidation rate at the crystallite length scale, which assumes unlimited oxygen available, but also the diffusion efficiency of the oxygen to the limited supply of available carbon atom sites throughout the entire volume of graphite.

The number of available RSA sites within the graphite microstructure provides an upper bound for the oxidation rate of graphite. Reactive sites within the microstructure can be increased by decreasing the crystallite size or creating less ordered stacked basal plane structure (i.e., more binder material used that has less graphitized order than the coke filler particles). However, it should be understood that any graphene plane within a crystallite will resist oxidation reactions of the covalently bonded interior carbon atoms leaving only the RSA sites along the edges of the basal plane available for chemical reaction. So long as there are intact graphene planes stacked within crystallites the chemical reaction is limited to only the outer edge sites which represent a fraction of the total carbon atoms within a graphite material. Thus, unlimited consumption of the carbon atoms within a graphitized graphite microstructure is not possible under any oxidizing condition.

While it is understood that the density of RSA sites within the graphite microstructure provides an upper bound to graphite oxidation the difficulty in transporting oxygen to the available RSA sites makes oxygen transport the central parameter in determining the actual (measurable) rate of graphite oxidation. To illustrate this point, in the case where the crystal structures may produce more RSA sites, thus increasing the amount of available carbonaceous fuel, the diffusion of oxygen to these sites through the tortuous open pore structures of graphite is severely restricted at the microscopic, bulk, and component length-scales. Additionally, at high temperatures oxygen diffusion is further impeded by diffusion of the reaction products, CO and CO_2, out of the microstructure. This reduced oxygen diffusion creates significant limitations on transporting oxygen to the regions with available RSA sites and limits the continuous chemical reaction. Even though there are more RSA sites available within the microstructure, the amount of oxygen that diffuses to these reactive sites is what actually controls the rate of reaction. This demonstrates oxygen transport is the rate limiting factor for this chemical reaction.

Finally, to sustain the graphite-oxygen chemical reaction, the chemical chain reaction requires a continuous supply of available carbon atoms, unrestricted oxygen to react with the carbon atoms, and a high temperature necessary for a high rate of reaction. Even if it is assumed that graphite components within a nuclear reactor may sustain high temperatures during an accident, satisfying one of the requirements for a chain reaction, neither a continuous supply of carbon atoms or unrestricted oxygen is possible. Even at the highest temperatures anticipated for an air or steam ingress accident, the oxidation of graphite is shown to be self-limiting at the crystallite length-scale level, and a chemical chain reaction cannot be maintained. A continuous chemical chain reaction, and thus self-sustained oxidation, is physically not possible due to these material restrictions.

However, while self-sustained oxidation is not possible in purified, nuclear graphite significant oxidation damage to nuclear core components can occur during an accident which introduces oxygen (either as steam or air) into the hot graphite reactor core. The overall design of mHTGRs integrates the major objectives of safe, reliable, economic generation of power and/or process steam with one of the primary design objectives being control of chemical attack.

Analysis of off-normal oxygen ingress events are required as part of the reactor licensing process. Sophisticated models are used to predict the total kinetic rate of oxidation in the graphite regions. These models utilize a combination of the kinetic mechanism equations discussed in the graphite-oxygen chemical reaction theory, accounting for the availability of oxygen due to the fluid flow characteristics, the graphite temperatures expected from the nuclear decay heat source, as well as the design of the core components and core configuration. An overview of several design-specific graphite oxidation simulations are presented for prismatic and pebble bed modular HTGRs (e.g., spatial distributions of gas compositions, mass flow rates, and temperatures). These examples illustrate the overall influence of the physical and chemical reaction limitations on graphite oxidation as well as the effects of reactor system design selections on the progression of graphite oxidation events .

Finally, despite the multiple length-scale and core design limitations on graphite oxidation, accidents which cause significant (but not self-sustained) oxidation of graphite are possible if the core components

are exposed to sufficient quantities of oxygen and heat during an accident. A discussion of the two historical examples of large scale severe graphite oxidation events in nuclear reactors, the October 1957 accident at Windscale Pile Number 1 and the Chernobyl accident in April 1986 is provided. In both cases it is shown that although massive oxidation of the graphite structures did occur, the presence of additional fuel sources in Chernobyl (roof tar and fuel rod cladding) and excess heat in the Windscale core (from a uranium metal fire) were the crucial parameters, and the oxidation was not self-sustained at any point, even with a continuous fresh air supply. Unwarranted assumptions and contradictory language used to explain these two most dramatic examples of large scale accidental graphite oxidation have contributed to common misconceptions about the role played by graphite in these accidents. This additional information, along with the fundamental principles of the graphite-oxygen chemical reaction theory, is provided as a specific counter argument to previous (erroneous) descriptions of these two graphite core reactor accidents as "graphite fires".

The paper concludes with a summary of the underlying chemical reaction principles which illustrate self-sustained oxidation is not physically possible for graphite nuclear components. All four components necessary for a sustained reaction (heat, carbon fuel, oxygen, and chain reaction) are severely restricted or eliminated at and above the crystallite length-scale within a graphite material precluding self-sustained oxidation.

CONTENTS

FIGURES

TABLES

ACRONYMS

AE	Anticipated Event
AGR	Advanced Graphite Reactor
BDBE	beyond design basis event
CCS	core conditioning system
DBE	design basis event
DLOFC	depressurized loss of forced coolant
HPB	helium pressure boundary
HPS	helium purification system
HTGR	High Temperature Gas-cooled Reactor
HTR-PM	High Temperature Reactor Pebble Bed Module
MHTGR	Modular High Temperature Gas-cooled Reactor
NFPA	National Fire Protection Association
PBMR	Pebble Bed Modular Reactor
PSIAD	Preliminary Safety Information Document
RCCS	Reactor Cavity Cooling System
RSA	reactive surface area
SMR	Small Modular Reactor
TRISO	tristructural isotropic
VHTR	Very High Temperature Reactor

Role of Nuclear Grade Graphite in Controlling Oxidation in Modular HTGRs

1. INTRODUCTION

The passively safe modular High Temperature Gas-cooled Reactor (MHTGR) design is one of the primary concepts considered for Generation IV and Small Modular Reactor (SMR) programs. The helium cooled, graphite moderated core achieves high operating temperatures for industrial process heat or electricity generation at high efficiencies. In addition to their neutron moderating properties, nuclear grade graphite reactor components provide excellent high temperature stability, thermal conductivity, and chemical compatibility with the high temperature nuclear fuel form. Graphite has been continuously used in nuclear reactors since the 1940s and has performed remarkably well over a wide range of core environments and operating conditions. Graphite moderated, gas-cooled reactor designs, predominantly cooled with carbon dioxide, have been safely used for research and power production purposes in multiple countries since the inception of nuclear energy development. To date, seven commercial operating High Temperature Gas-cooled Reactor (HTGR)s have operated in five countries with two more under construction in China.

Graphite is a carbonaceous material, however, and this has generated a persistent concern that the graphite components could actually burn during accident conditions[1,2].The common misconception is that graphite, since it is ostensibly similar to charcoal and coal, will chemically react in a similar manner. Combustion or burning, as defined by the National Fire Protection Association (NFPA), is the sequence of chemical reactions between a fuel and an oxidant accompanied by the production of heat and conversion of chemical species. According to NFPA there are four requirements to sustain a fire: fuel, heat, an oxidant, and sustaining a continuous chemical chain reaction (the fire tetrahedron). All four requirements (fuel, heat, oxidant, and chain reaction) of the fire tetrahedron must be in place to initiate and sustain the chemical reaction. Eliminating any one of the requirements will prevent or stop the sustained chemical reaction.

Graphite is an allotrope of carbon in which the carbon atoms should form a perfectly layered, planar crystal structure. Each layer is a graphene plane of covalently bonded carbon atoms arranged in a hexagonal lattice (a honeycomb or "chickenwire" appearance). The graphene planes (designated basal planes) are stacked in layers to form a dense, solid crystallite structure much like the pages stacked together inside a book. Nuclear grade graphite, like most graphite grades available commercially, is manufactured from a combination of carbonaceous materials that are heat treated to very high temperatures to form the ordered, layered graphitic crystal structure desirable in graphite material. In general, graphite with high purity (low levels of non-carbon impurities) that has undergone very high graphitization temperatures is required for nuclear applications.

Specific standards exist for manufacturing nuclear grade graphite that stipulate the chemical purity, minimum graphitization temperatures, and minimum material properties for nuclear applications[3]. Even trace impurities in the graphite microstructure can significantly alter the bulk oxidation rate of graphite. Additionally, formation of long, uninterrupted graphene basal planes within the formed crystallites is critical to the oxidation behavior of graphite. The formation of these highly graphitized crystallites can only occur if the carbonaceous material has been heat treated to graphitization temperature (above 2800°C) to realign the benzene-like ring structure in the carbonaceous preform materials into the hexagonal covalently bonded graphene plane structure. The addition of impurities will also disrupt the formation of continuous graphene planes leading to less perfect basal plane formation and dramatically different oxidation performance. For these reasons, nuclear grade graphite is usually assumed to be purified to reduce total impurity levels below 300 ppm and graphitized to temperatures of at least 2800°C. These specifications differentiate nuclear grade graphite from the less pure and less graphitized electrode and other carbonaceous material commonly produced by graphite vendors.

While charcoal, coal and other carbonaceous materials may have the appearance of graphite, the internal microstructure, entrained volatile organic (carbon-based) structures, and impurities within these carbonaceous materials are very different from graphite leading to dramatically different oxidation behavior. Coal and charcoal possess significant levels of long chained organic compounds, as well as volatile carbonaceous species (e.g., methane, ethane, etc.) and trapped moisture within their microstructure. These additions interrupt the formation of a stable uniform graphitic crystal structure. These shorter, disrupted carbon crystal structures within coal and charcoal enhances the carbon-oxygen reaction rather than suppressing it as seen in graphite which possess much higher amounts of the stable graphitic crystal structure. In addition, because of the volatile gases and moisture contained within the structure of coal and charcoal, there is a ready supply of oxygen and volatile carbonaceous material internal to the microstructure. These oxidation enhancing additions actively promote ignition and help sustain a carbon-oxygen chemical reaction. The fabrication process used to produce graphite eliminates these organic structures, volatile gases and moisture in addition to creating the dense, highly ordered crystal structures which suppress oxidation.

Graphite is formed from long chained, organic compounds similar to coal, charcoal, and other carbonaceous materials. However, these carbon pre-cursor materials are removed or transformed into long range, uniform graphitic crystal structures during the high temperature fabrication process. During the high temperature process the long organic (carbon-based) compounds are either volatilized and removed from the microstructure or the carbon atoms rearranged into the extremely stable hexagonal lattice graphene plane structure of graphite. In addition, nuclear graphite undergoes a purification step where non-carbon trace impurities are removed from the material yielding microstructures that have very pure, graphitic crystal structures. These highly graphitized crystallites formed within nuclear graphite possess structures of covalently bonded graphene planes that are extremely energetically stable and strong. These highly pure, energetically stable crystal structures within graphite without the addition of volatile gases, entrained organic compounds, and non-carbon impurities prove to be exceptionally resistant to oxidation producing a very slow reaction rate for the graphite-oxygen chemical reaction.

Oxidation of highly ordered graphite is naturally arrested by the constraints on the chemical reactants and the graphitic structure at the atomic scale. Mitigation of the oxidation reaction begins at the atomic lattice length scale and continues up to reactor component size Figure 1. Conditions at each length scale within the nuclear grade graphite structure acts to remove one or more or all of the requirements (fuel,

2

heat, oxidant, and chain reaction) within the fire tetrahedron necessary for a self-sustained chemical chain reaction. Even at an atomic lattice scale, all requirements of the fire tetrahedron are limited, preventing self-sustaining oxidation once the layered graphene crystal structure has been established. This resistance to ignition and oxidation, even at the crystallite length-scale, is the reason fine graphite powder is used as a fire suppressant material for one of the most dangerous classes of fires, Class D metal fires[4].
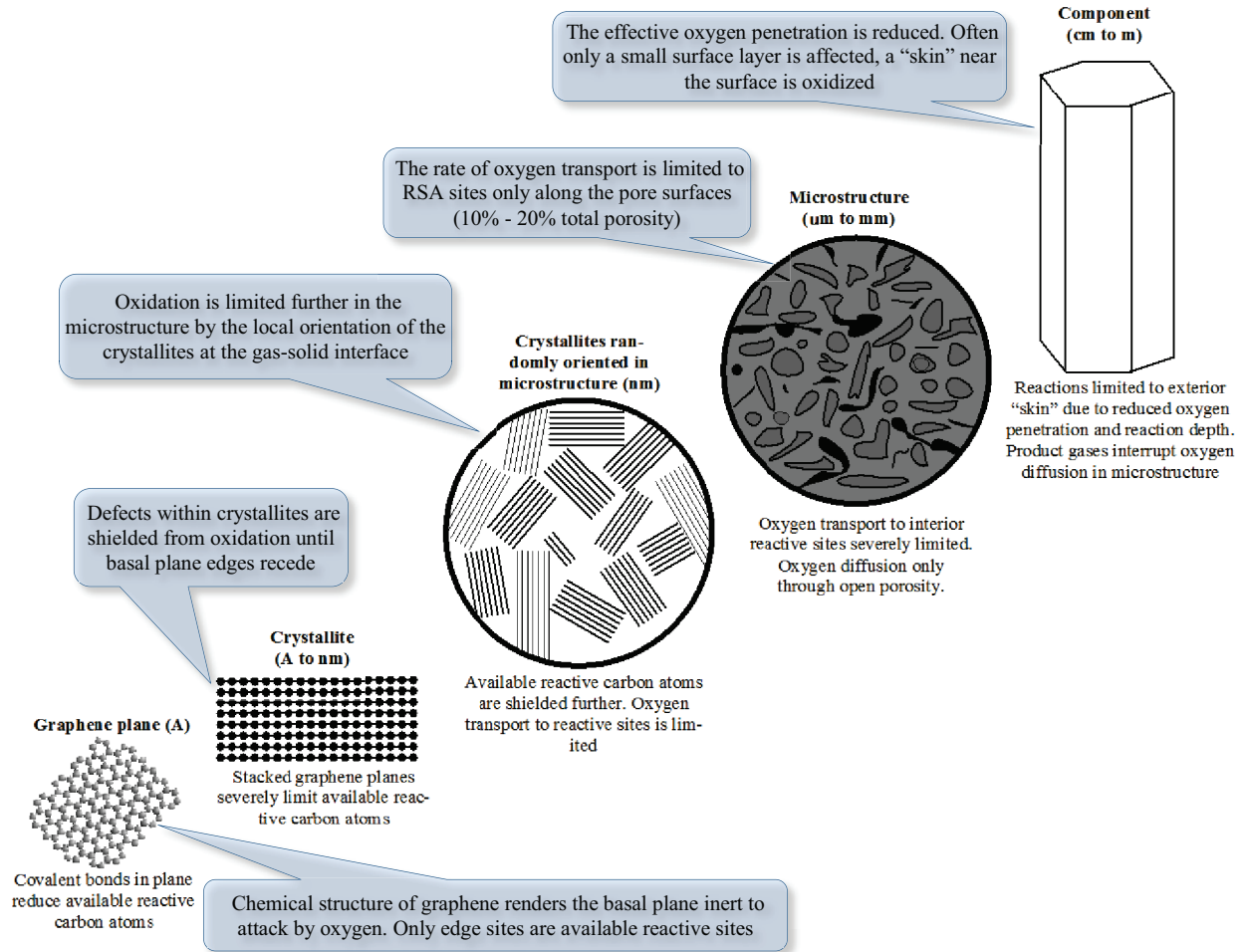
Figure 1. Mitigation of graphite-oxygen reaction for each microstructure length-scale within graphite.

Graphite oxidation must be limited in order to protect the fuel during off-normal events. Beginning at the atomic crystal lattice, the bonding and ordered structure of the atoms within a solid graphite structure impede the graphite-oxygen reaction process. This impediment is exacerbated at the crystallite length-scale, where access to reactive carbon atoms is limited to specific areas along the outer edges of the graphite crystallites. At the same time, oxygen access to these reactive carbon sites is restricted by the microstructure formed inside these graphitic components. The microstructural features within nuclear grade graphite (grains, binder material, and porosity) all restrict oxygen access to the reactive carbon sites inside the graphite. So while the reactive carbon atoms are less available within a graphitic structure, the microstructural features also restrict transport of oxygen to any reactive carbon atoms. This eliminates the possibility of self-sustained oxidation within graphite core components.

While the crystal structure of graphite material eliminates the possibility of self-sustained oxidation, the graphite components will still oxidize if oxygen is introduced to the hot core. Air or steam ingress accident events can allow oxygen to come in contact with the hot graphite components through a leak or break in the Helium Pressure Boundary (HPB) with a subsequent loss of helium pressure and an extended loss of forced cooling. This can lead to a helium-air mixture entering the reactor over an extended period of time. To mitigate oxidation of the graphite core components, the modular HTGR designs incorporate safety systems to reduce oxygen within the core region, as well as core cooling systems, to reduce the graphite temperature and thus the oxidation rate. Modular HTGR designs employ several overlapping safety systems such as the choice of high pressure helium as the coolant to the high integrity of the HPB that is composed of three vessels with only small diameter connections to the vessel system. Some designs also utilize a forced cooling system for heat removal that is designed for the full spectrum of fully pressurized to fully depressurized helium environments.

To illustrate the current scientific understanding of graphite oxidation, the physical mechanism underlying graphite oxidation are summarized. This summary is based upon the large international knowledgebase related to graphite oxidation studies as it pertains to the safety design approach of the modular HTGR. Since nuclear grade graphite is a multi-length scale composite structure, the basic thermodynamics of the graphite-oxygen reaction at the atomic and crystallite length scale are discussed initially followed by the critical oxidation parameters at successively larger length scales up to the component size, as shown in Figure 1.

Similarly, the safety systems for modular HTGR designs are described in the context of mitigating graphite oxidation during oxygen ingress accident events. Sophisticated simulations of various oxidation events based upon the fundamental graphite-oxygen chemical reaction theory allow an assessment of the magnitude and probability of oxidation within the graphite core. An overview of the oxidation behavior in typical Licensing Basis Events for modular HTGR designs is presented in Section 3 with a review of analyses performed with several different reactor simulation codes and for several representative modular HTGR designs. No new simulations were performed for this publication. The methodologies represent the current state-of-the-art in core-wide reactor graphite oxidation simulation, allowing a comprehensive understanding of the role played and risks posed by the use of graphite as a moderator in nuclear reactors.

While the rate of graphite-oxygen chemical reaction at the crystallite length scale level is shown to prevent self-sustained oxidation, the engineered safety systems of the HGTR designs are in addition used to mitigate significant oxidation of the graphite core components. This paper attempts to address both issues as they significantly impact the perceived safety risk of modular HTGR operation.

2.   GRAPHITE OXIDATION THEORY

The overall rate of oxidation depends upon a complex combination of temperature, the number of available reaction sites, and the availability of reactants. These are three of the four requirements needed for self-sustained oxidation in the fire tetrahedron. Increasing the temperature increases the oxidation rate, but the relationship is not a simple linear response due to the multiple oxidation pathways possible, each with different activation barrier energies to overcome. Under ideal conditions, with no restrictions of oxygen, temperature, or access to the graphite material, the reactive sites available for reacting at the crystallite length scale provide a maximum reaction rate for graphite with a highly ordered crystal structure. Under more realistic conditions, the amount of available reactive sites and the oxygen reactant availability are significantly more variable since the defect microstructure within specific graphite grades can dramatically increase or decrease the specific oxidation rates. To understand the overall oxidation

behavior of nuclear grade graphite, the effects of these complex elements must be understood at each graphite length scale.

The oxidation of graphite occurs by several thermodynamic chemical reactions fundamental to the unique graphite crystal structure. From the atomic scale, there is broad consensus regarding the relevant graphite-oxygen reaction chemistry. The overall thermodynamic reaction between carbon and oxygen can be succinctly written as:

$$C(s) + \left(1 - \tfrac{1}{2}x\right)O_2(g) \leftrightarrow xCO(g) + (1-x)CO_2(g) \tag{1}$$

where x is the molar fraction of gaseous CO product which can vary from 0 to 1.

The primary thermodynamic reactions comprising this overall oxidation reaction are generally accepted as the equations given below[5,6,6,7]:

$$C_{(s)} + O_{2\,(g)} \leftrightarrow CO_{2\,(g)} \qquad\qquad \Delta H_{298K} = -393.5 \text{ kJ/mol} \tag{2}$$

$$C_{(s)} + \tfrac{1}{2}\,O_{2\,(g)} \leftrightarrow CO_{(g)} \qquad\qquad \Delta H_{298K} = -110.5 \text{ kJ/mol} \tag{3}$$

$$C_{(s)} + CO_{2\,(g)} \leftrightarrow 2\,CO_{(g)} \qquad\qquad \Delta H_{298K} = +172.5 \text{ kJ/mol} \tag{4}$$

$$CO_{(g)} + \tfrac{1}{2}\,O_{2\,(g)} \leftrightarrow CO_{2\,(g)} \qquad\qquad \Delta H_{298K} = -283.0 \text{ kJ/mol} \tag{5}$$

$$C_{(s)} + H_2O_{(g)} \leftrightarrow CO_{(g)} + H_{2\,(g)} \qquad\qquad \Delta H_{298K} = +131.3 \text{ kJ/mol} \tag{6}$$

$$C_{(s)} + 2\,H_{2\,(g)} \leftrightarrow CH_{4\,(g)} \qquad\qquad \Delta H_{298K} = -74.6 \text{ kJ/mol} \tag{7}$$

$$H_2O_{(g)} \leftrightarrow \tfrac{1}{2}\,O_{(g)} + H_{2\,(g)} \qquad\qquad \Delta H_{298K} = +241.8 \text{ kJ/mol} \tag{8}$$
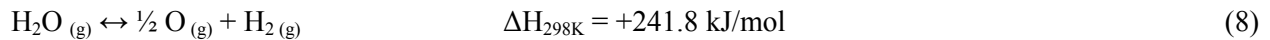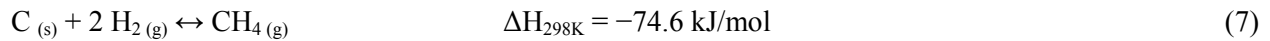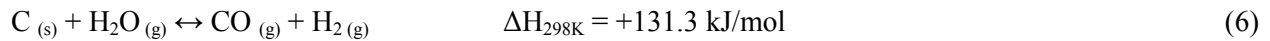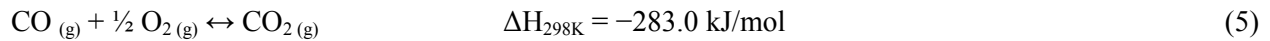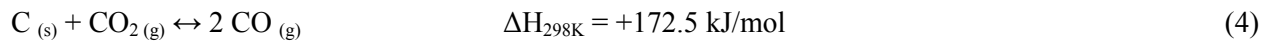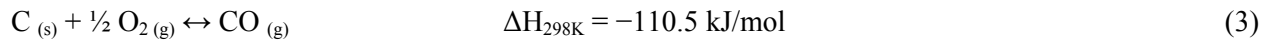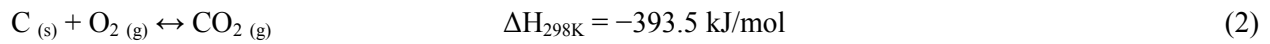
The thermodynamics of the oxidation reactions show 1) oxidation does occur spontaneously at atmospheric pressure for many of the reactions near room temperature, and 2) the net result is exothermic for the overall oxidation reaction. Figure 2 provides a cursory estimate of the potential for each carbon-oxygen reaction system based upon the free energy of the reaction. From this Gibbs Free Energy diagram, the reactions with the lowest energy values are the reactions with the most potential to occur, since products with greater stability (with a lower relative free energy of formation) will form in preference to those of lesser stability. As seen, the most likely reactions for graphite oxidation involve molecular oxygen (Equations 2, 3, and 4). Carbon reactions with water and hydrogen are not as energetically favorable, and the reactions involving molecular oxygen (Equations 7 and 8) will be the preferred oxidation reactions.

Change in Free Energy of Reactions with Temperature

ΔG_{RXN}, kJ/mol

$C + CO_2 \rightarrow 2CO$

$C + 2H_2 \rightarrow CH_4$

$CO + H_2O \rightarrow CO_2 + H_2$

$C + H_2O \rightarrow CO + H_2$

$C + \frac{1}{2}O_2 \rightarrow CO$

$CO + \frac{1}{2}O_2 \rightarrow CO_2$

$C + O_2 \rightarrow CO_2$
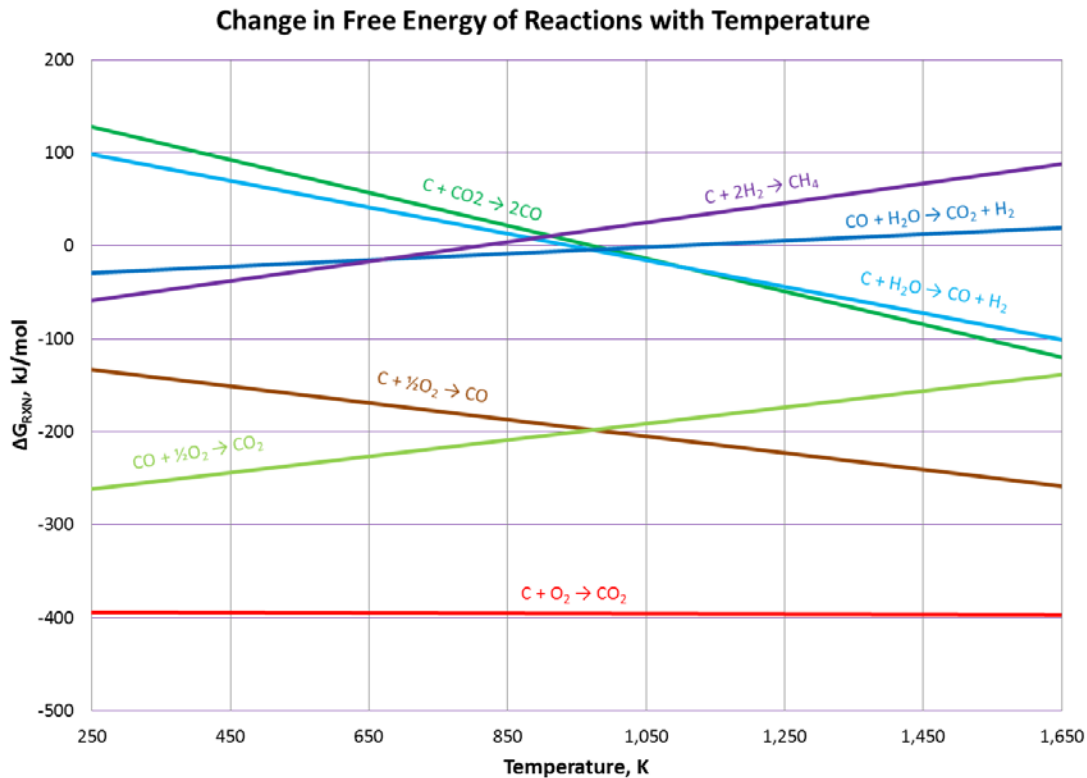
Temperature, K

Figure 2. Change in Gibbs free energy illustrates the equilibrium tendencies of the competing reactions: the relative tendencies change with temperature – the more negative the thermodynamic value of ΔG, the greater the progression of the forward reaction.

As illustrated in Figure 2, the molecular oxygen reactions will dominate graphite oxidation behavior as long as the oxygen available in air greatly exceeds available moisture. In the event of steam ingress during reactor operations, thermodynamic reactions 6 and 8 would be dominant regardless of their less energetically favorable reactions. However, water dissociates near 600°C, providing free oxygen for the more energetically favorable reactions involving oxygen. Water dissociation is an endothermic reaction which effectively cools the graphite. While the high temperatures in a nuclear core are expected to provide ample heat for this reaction to occur, the formation of additional hydrogen from water dissociation tends to suppress the rate of graphite oxidation significantly[9]. All other factors being equal, air ingress will provide more energetically favorable reactions and larger heat of formation than water ingress. Therefore the focus of this discussion is upon air oxidation reactions. Water ingress is a consideration under some design basis event conditions, but the extent and rate of oxidation will be significantly smaller than for a comparable air ingress event.

Nitrogen interaction (from air) with carbon is not appreciable below about 1400°C[10], so nitrogen will only become reactive with the graphite at the highest of accident temperatures. Oxygen still remains the preferred reactant even at these higher temperatures, reacting with any available carbon before nitrogen, so for simplicity the carbon-nitrogen reactions are excluded from this discussion.

Finally, at ambient pressure conditions, carbon monoxide does not dissociate to a meaningful extent into elemental carbon and oxygen even up to temperatures where graphite sublimes[5,7]. Oxygen from this

6

dissociation process will not be available for additional graphite-oxygen reactions. However, the incomplete reactions (Equation 3) or secondary reactions (Equation 4) can produce quantities of CO which can be oxidized further to CO_2 (Equation 5).

At the atomic level, with no consideration of crystalline bonding structures, given sufficient carbon, oxygen and heat to initiate reaction (ignition temperature), the net heat produced from simply combining carbon atoms to oxygen atoms is capable of perpetuating self-sustained oxidation. However, this idealized condition of free carbon atoms as the fuel in the fire tetrahedron does not exist, because the smallest unit available for graphite oxidation within nuclear components is the crystallite. Thus, graphite oxidation that occurs at the crystallite level is dependent upon the unique crystalline carbon bond structure of graphite. This dependence of graphite oxidation upon the dynamic reaction environment at the crystallite level is the critical consideration for determining the maximum overall rate of oxidation for nuclear grade graphite.

Even though the crystallite structure will provide the maximum number of available carbon atoms for the reaction, the actual oxidation rate will also be dependent upon the amount of oxygen readily available. For any thermodynamic reaction to occur, oxygen must first diffuse to these reactive carbon atom sites. Nuclear grade graphite is fabricated with significant porosity (up to 15%), and the oxygen can diffuse through this complex pore network to the reactive carbon sites. The defect pore structure is tortuous, however, limiting the diffusion rate of oxygen through the graphite structure to the reactive carbon sites. With the oxygen availability limited by the diffusion rate through the graphite pore network, the unique graphite microstructure also becomes a critical consideration in determining the overall oxidation rate of nuclear grade graphite.

The complex interrelationship among all of these factors must be understood at each length scale to determine the overall oxidation behavior of large nuclear grade graphite components. Oxidation rate theory addresses oxidation rate trends in graphite across the full range of temperatures from ambient conditions up to the highest credible accident temperature. These rate trends are conventionally described as three oxidation regimes to approximate the observed oxidation behavior of bulk graphite specimens, as shown in Figure 3. These overall oxidation trends are governed by the complex combination of the intrinsic graphite material structure, the chemical reactions, and environmental factors discussed previously. The trends on either extreme of Figure 3 depict simplified oxidation conditions: instantaneous reaction of the oxygen at the highest temperatures and nearly unreactive conditions at the lowest temperatures. For simplicity, oxidation is usually depicted as a linear rate within each regime.
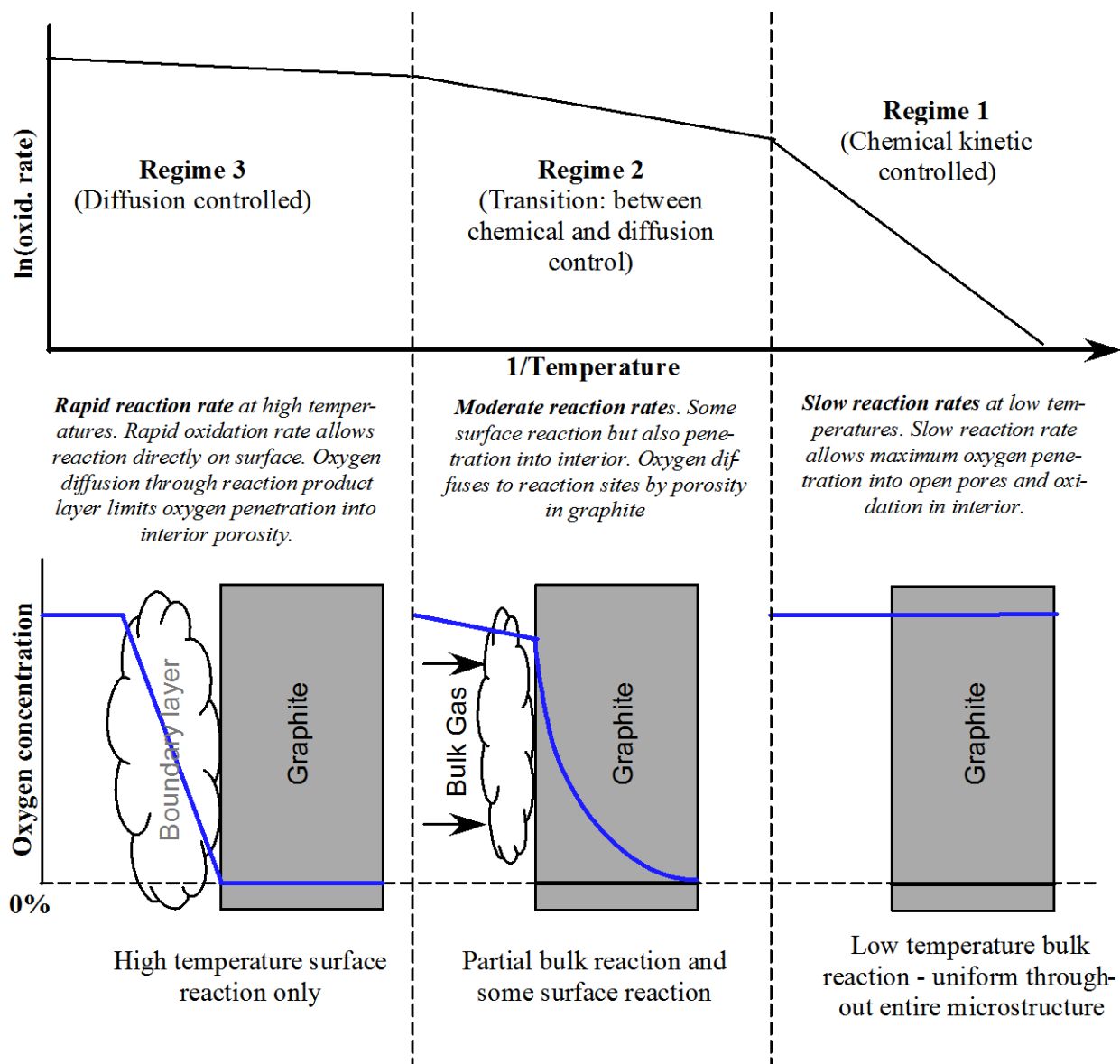
Figure 3. Three regime zones representing the variation in oxidation rate with temperature in bulk graphite[6,11]. Regimes are dependent upon flow conditions, temperature, and individual graphite microstructure.

At lower temperatures, the overall reaction rate trend can be estimated by a simple Arrhenius expression, given in Equation 9 below.

Rate (r) = k[O_2]^n (9)

where k (the overall oxidation rate constant) is represented as $k = A\ exp(-Ea/RT)$

In this relationship, r represents the oxidation rate; E_a, the effective activation energy; R, the gas constant; and T, the temperature. The linear coefficient, A, is understood to include k_0, the overall oxidation rate constant (bulk oxidation); but also varies with the extent of reaction because mass loss

contributes to the porosity and number of available active sites. The rate constant also varies to a lesser extent with the partial pressure of oxygen, depending on the order of the reaction *n* the value of which has been experimentally determined to be between 0.5 and 1.0 for various grades of graphite.

At lower temperatures (<650°C) the oxidation rate varies exponentially with temperature. This range is referred to as the *kinetic controlled* regime (Regime 1) since the chemical reaction kinetics are limited. The slow rate of chemical oxidation allows a larger amount of oxygen to diffuse into the pore structures as little oxygen reacts with the available active carbon sites. This higher diffusion permits the oxygen to come in contact with a larger quantity of reactive surface area (RSA) sites within the unique microstructure of each graphite grade, (i.e., grades with different pore structures and RSA sites will have distinctly different oxidation rates). Most bulk oxidation comparative studies are conducted at these lower temperatures because differences in the oxidation rate between different graphite grades result from differences in the microstructures. These different oxidation rates are most apparent during kinetic regime oxidation.

As the temperature increases ($\sim 650 - 750$°C) the overall reaction rate increases, and this limits the amount of oxygen diffusing into the graphite material since it is being consumed by the reactions near the graphite surface. The bulk oxidation becomes progressively more dependent on the reactant diffusion rate and enters into a *transition* regime (Regime 2) in which the effects of reactant transport restriction through the graphite microstructure begin to dominate the oxidation rate. In this transition regime, the oxidation rate begins to be governed by gaseous diffusion through the pore defect microstructure, into and out of pores in the solid material.

At the highest temperatures (>750°C) the chemical reactions occur much more rapidly than oxygen can diffuse through the defect microstructure. The *diffusion controlled* regime (Regime 3) is dominated by reactant and product diffusion rates across the gaseous boundary layer to and from the reactant sites. The rate of oxidation within the solid is dependent upon the limited oxygen penetration beyond the surface[12]. This diffusion rate limiting boundary layer may occur at the crystallite, the particle, or even the component solid surface, wherever there are reaction sites available. Within the diffusion controlled regime the majority of reaction occurs on the outer graphite surface rather than in the interior bulk.

These bulk oxidation trends are used to predict the oxidation rate and the extent of mass loss in the large graphite components comprising a modular HTGR graphite core during the spectrum of Licensing Basis Events involving an air or steam ingress (see Section 3). These reactor cores are quite large and have large temperature gradients from top to bottom and side to center of the core. In addition, the complex gas flow within these large core designs will tend to yield variations in oxygen concentration in different sections of the core during ingress events, as air/moisture flow to some areas will be less efficient. The oxidation rate in the core depends upon the specific temperature as well as local oxygen concentration in the components within each region of the core as well as the amount of oxygen in the helium-air gas mixture that can diffuse through/around the components making up the core. Further complicating the bulk oxidation rate is the potential for irradiation damage to change the thermal properties of the graphite as well as alter the complex microstructure inside the graphite, which may alter the oxidation rate. Similar to the overall oxidation response of the specific graphite material, the overall bulk oxidation response is a complex interrelationship between the material response, the available oxygen at the component position within the core, the temperature of the component within the core region, and any irradiation damage that may alter the microstructure and thermal properties of the graphite material.

The graphite-oxygen reaction kinetics and factors that affect the reactions from either physical or material properties have been studied in detail. A simplified kinetic mechanism model is presented to illustrate the active mechanism underlying graphite oxidation at the crystallite length scale. At the graphite microstructure length scale, the defect microstructure (porosity) is shown to dominate the degree of oxygen mass transport expected into the interior graphite-oxygen reaction sites. Finally, at the component length scale, the effects of irradiation damage, large component geometries, and specific issues surrounding the engineered components of the nuclear reactor core are discussed with respect to the graphite-oxygen reaction.

2.1   Atomic/Crystallite Level Oxidation

From a strictly thermodynamic viewpoint, self-sustained oxidation of nuclear grade graphite as a structure of carbon atoms appears to be favorable since the graphite-oxygen reactions are generally exothermic. While exothermic reactions may indicate graphite oxidation will occur spontaneously given a sufficient ignition temperature, thermodynamics yields no information about the reaction rate, which is the fundamental parameter for self-sustained oxidation. At the fundamental atomic level, any given occurrence of a reaction is usually regarded as instantaneous because the rearrangement of individual bonds is not directly observed for a single such event. The reaction rate is only meaningful at a length scale where the frequency of occurrence of the reaction can be observed and where oxygen transport, available reactive sites, temperature, and competing mechanisms influence the net outcome over time. A simplified oxygen transfer mechanism model is presented for the graphite-oxygen reaction kinetics.

2.1.1   The Graphite Crystal Structure

Pure graphite consists of layers of graphene planes with the carbon atoms in each layer arranged in a hexagonal shaped ring (similar to an aromatic benzene ring structure) which is extended into a honeycomb shaped lattice, Figure 4. The covalent bonding produces a relatively short 0.142 nm separation between carbon atoms within the graphene planes, and weak electronic bonding between planes yields a rather long 0.335 nm plane separation. Single and double bonds between the atoms comprising the graphene basal planes generally form the theoretical sp^2 bonding structure shown in Figure 5. Standard AB planar stacking yields a theoretical density of 2.23 g/cm^3 per hexagonal unit cell of the crystal structure.

(a)   (b)
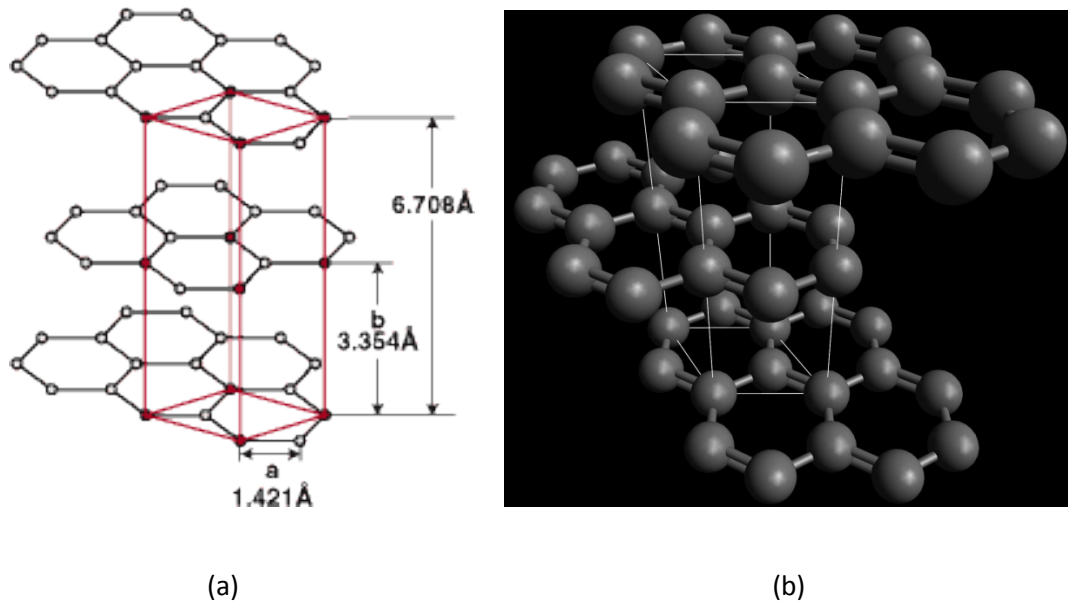
Figure 4. A (a) schematic and (b) graphical representation of the graphite unit crystal structure illustrating the hexagonal ring shapes within the stacked graphene basal planes.
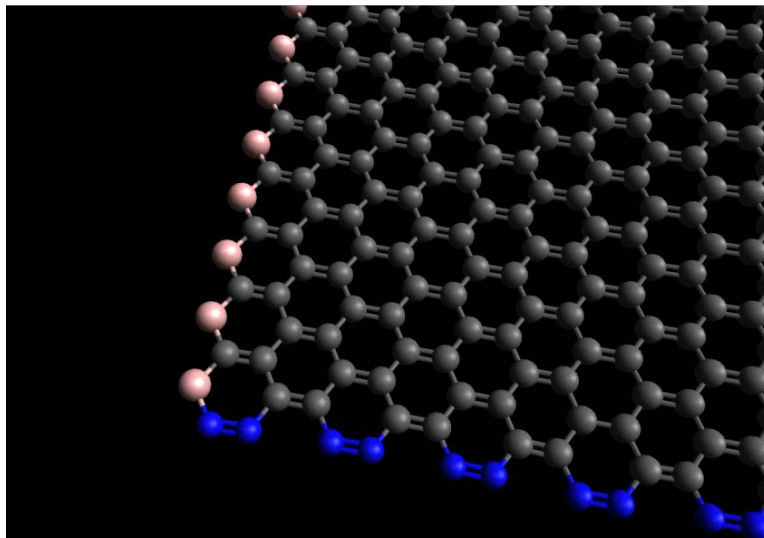
Figure 5. Single graphene sheet illustrating expected atomic bonding within the sheet. These bonds dictate the terminating carbon atoms in single bond zig-zag (pink) and double bond armchair (blue) configurations.

Graphite crystallites consist of thousands of stacked graphene planes bonded weakly to form large anisotropic crystalline blocks. These stacked and ordered individual crystallites, along with some less ordered and even amorphous structures, compose the microstructure of nuclear grade graphite. Structures with less crystallographic order are not desirable for oxidation resistance (or irradiation stability) and are minimized where possible. These structures include the small fuel 'compacts' used in prismatic core reactors and the pebbles used in pebble bed reactors, both of which encapsulate the coated fuel particles. The partially-graphitized matrix material cannot be subjected to the extremely high temperatures used to

11

fabricate large graphite blocks because of the damage it may cause to the fuel particles. The oxidation of these graphitic structures is the controlling parameter for the overall rate of graphite oxidation. The crystallite oxidation rate is dependent upon the graphite-oxygen kinetics and specific mechanism controlling the chemical reaction, which are influenced by the crystal structure of the graphite crystallites as discussed in the following section.

2.1.2   Graphite-Oxygen Reaction Kinetics

Researchers have studied the carbon and oxygen reaction in detail for well over a century with several major contributions made over the past 50 years[13,14,15,16,17,18,19, 20]. The primary thermodynamic carbon–oxygen reactions, as presented in Equations 2 through 8, are well established and reasonably well understood. These primary chemical reactions can also be presented in a simplified form describing the possible reaction mechanism in an oxygen transfer model. These oxygen transfer mechanism for the oxidation of high purity graphite with a highly (nearly perfect) ordered crystal structure are described in Equations 10a through 15 and schematically illustrated in Figure 5 through Figure 6[19]. It should be noted that at different temperatures chemisorption and desorption reaction mechanism can occur through alternative reaction pathways, Equations 10a and 10b and 12a, 12b, and 12c. It is important to understand why the overall bulk oxidation response changes from a kinetic controlled regime to a diffusion controlled regime with changing temperatures. More detailed versions of this oxygen transfer mechanism are described in-depth by Radovic et al., and reflect all known influential factors[31,233,234,235, 27,28,29].

$$C_e + O_2(g) \xrightarrow{k_{A1}} C_e(O_2)$$ 　　　　Molecular Oxygen Chemisorption 　　　　　　　　(10a)

$$2C_e + O_2(g) \xrightarrow{k_{A2}} 2C_e(O)$$ 　　　　Oxygen Dissociative Chemisorption 　　　　　　(10b)

$$C_e(O_2) + C_b \xrightarrow{k_S} C_e(O) + C_b(O)$$ 　　Oxygen Spillove 　　　　　　　　　　　　　　　(11)

$$C_e(O) \xrightarrow{k_{D1}} CO(g) \; (+2C_e)$$ 　　　　Direct CO Desorption 　　　　　　　　　　　　(12a)

$$C_e(O) + C_b(O) \xrightarrow{k_{D2}} CO_2(g) \; (+C_e)$$ 　Indirect CO_2 Desorption 　　　　　　　　　　(12b)

$$C_e(O_2) \xrightarrow{k_{D3}} CO_2(g) \; (+2C_e)$$ 　　　Direct CO_2 Desorption 　　　　　　　　　　　(12c)
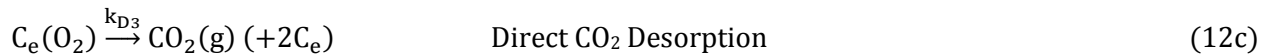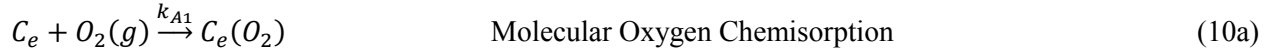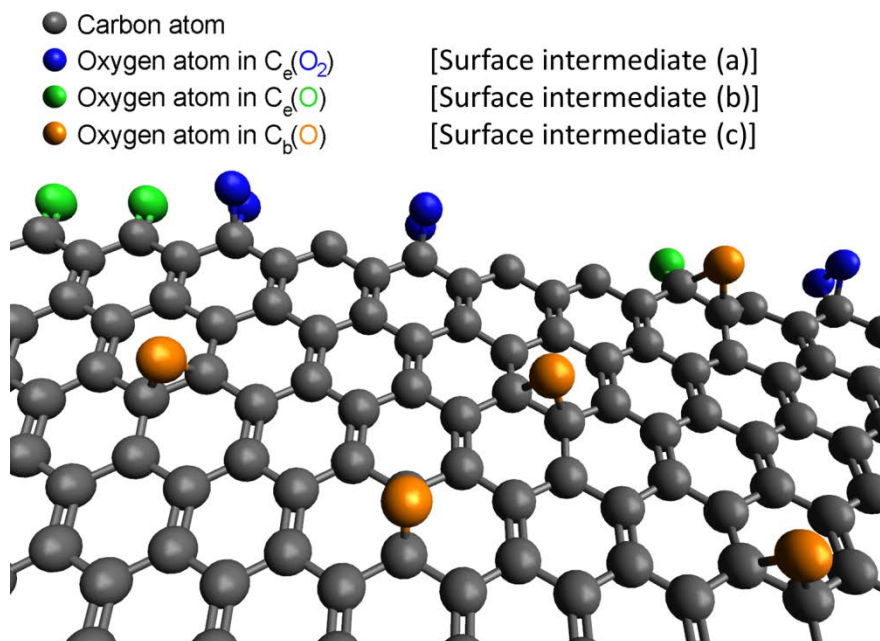
Figure 6. Reactive surface intermediates on a graphene basal plane (a) $C_e(O)$ as single bonded edge site bonds and (b) $C_e(O_2)$ as double bonded edge site bonds. Stable surface intermediate (c) $C_b(O)$ are double bonded non-edge site bonds (interior atom sites).

Atomic lattice sites designated as C_e represent an edge site, such as the zig-zag and armchair edge sites as illustrated in Figure 5 and Figure 6. Atomic sites designated as C_b represent an interior atom site of the surface of a stable basal plane configuration. The edge sites, $C_e(O)$ and $C_e(O_2)$, are the reactive surface intermediates, while $C_b(O)$ is a stable surface intermediate. Carbons from the $C_e(O)$ and $C_e(O_2)$ sites can directly desorb from the edges of the basal planes and react with oxygen to form CO or CO_2 as shown in Figure 7. The $C_b(O)$ surface intermediate site is stable and will not directly desorb from the interior of the basal planes and react with oxygen to form CO or CO_2. Thus, graphite-oxygen reactions can only occur on the edges of the basal planes where the reactive sites are located, not from the interior surface sites where the unreactive (stable) sites are located.

Molecular Oxygen Chemisorption (10a)

$$C_e + O_2 \xrightarrow{k_{A1}} C_e(O_2)$$

Direct CO_2 Desorption (12c)

$$C_e(O_2) \xrightarrow{k_{D3}} CO_2$$

Oxygen Dissociative Chemisorption (10b)

Oxygen Spillover (11)

$$C_e + O_2 \xrightarrow{k_{A2}} 2C_e(O)$$

$$C_e(O_2) + C_b \xrightarrow{k_S} C_e(O) + C_b(O)$$

Indirect CO_2 Desorption (12b)

$$C_e(O) + C_b(O) \xrightarrow{k_{D2}} CO_2$$

Direct CO Desorption (12a)

$$C_e(O) \xrightarrow{k_{D1}} CO$$

Carbon atom

Oxygen atom in gas molecule

Oxygen atom in $C_e(O_2)$

Oxygen atom in $C_e(O)$

Oxygen atom in $C_b(O)$
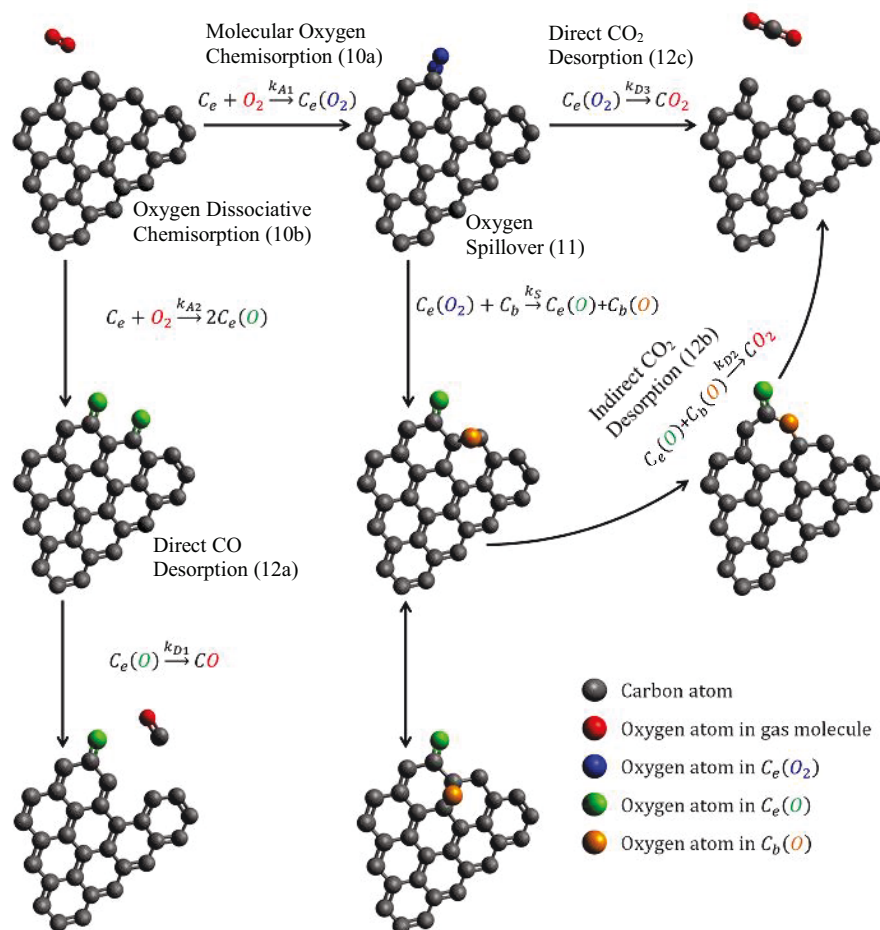
Figure 7. Schematic representation of oxygen transfer mechanism pathways proposed in Equations 10a-12c.

Under the oxygen transfer mechanism model oxygen can only adsorb to the basal plane edge sites, and any reaction products can only desorb from these edge sites[25]. These edge sites are the RSA sites as discussed previously and are the only places where the oxidation reaction can occur. This mechanism is observed with oxidized crystallites of graphite where the topmost graphene sheets have undergone more extensive edge site reactions than underlying sheets which are protected from the initial oxidation reaction, Figure 8. This terracing effect where the outermost sheets have the most extensive edge oxidation reactions is direct evidence that only the edges of the individual sheets react while the interior of the sheets are left unreacted. If interior sheet reactions were occurring, there would be no terracing shapes formed as the material would be reacted uniformly and randomly.

For an isolated oxidizing graphite crystallite, only the edge site locations can react. Carbon atoms on the remaining exposed surface area (approximately half) and in essentially all of the interior volume are unavailable for oxygen adsorption. This dramatically limits the oxidation rate, effectively eliminating the chain reaction component of the fire tetrahedron.
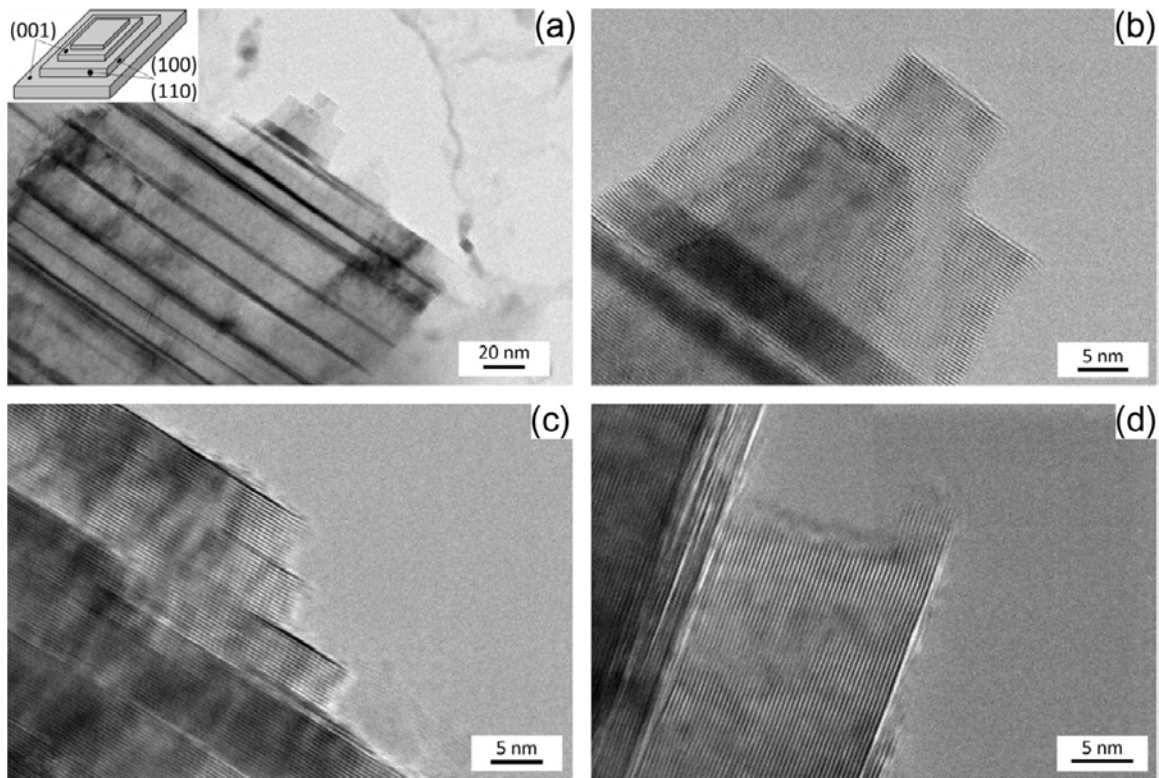
Figure 8. High resolution transmission electron micrographs of NBG-18 graphite. The reaction progression along the edge plane steps appears uniform. (a) Shows terracing commonly observed in large crystallites within the filler particles. (b) Is the tip of the crystallite from (a). (c) and (d) show the terracing at the edges of crystallites.

It must be noted that even though a self-sustained chain reaction is prevented by the limited number of available reactive sites, graphite will still oxidize at higher temperatures given a continuous supply of oxygen and an external heat source.

A simple analogy to this behavior is the oxidation of a paper book containing many pages. If a thick paper book is placed in a fire only the edges of the pages inside the book will burn; the interior page material is not exposed. The page centers do not oxidize and, if the book is removed from the heat source, the oxidation stops. A thick configuration of stacked pages can still smother a fire even though wood-based paper contains impurities, volatile species, and trapped moisture, all of which contribute to flame propagation at high temperature. Keeping the book in the fire will eventually oxidize all the pages but the process is slow and is not self-sustaining so long as the book retains many pages stacked together. Sustaining oxidation in nuclear grade graphite is even more difficult since the graphite material is largely devoid of volatile material, impurities, and moisture at the crystallite length-scale and there are many more graphene "pages" that must be sequentially exposed and oxidized.

As discussed, the overall carbon oxidation reaction ($C + O_2 \rightarrow CO + CO_2$) can occur via a number of direct or indirect chemical reaction pathways. From Equations 10a-12c, CO can only be produced via one path, Equation 12a, the direct desorption of a semiquinone intermediate, a $C_e(O)$ reaction[22,23,24]. The production of $C_e(O)$ can occur in two possible ways: direct production of two $C_e(O)$ from the dissociative chemisorption of oxygen on an exposed reactive carbon site[35] or from the spill-over of one oxygen atom from the dioxiranyl intermediate ($C_e(O_2)$) onto the basal plane, leaving the other oxygen behind in the form of $C_e(O)$[25,26].

CO_2 is produced via two pathways. The direct route starts with diatomic oxygen chemisorption to a single edge site forming a $C_e(O_2)$ intermediate[21]. The subsequent desorption of the $C_e(O_2)$ intermediate completes the direct CO_2 formation route[29]. For indirect CO_2 desorption, oxygen in the form of an epoxide, $C_b(O)$, on the basal plane will react with $C_e(O)$ to form CO_2[28].

From Equations 12a and 12c and the oxygen transfer mechanism depicted in Figure 7, the chemical reaction is shown to be dependent upon the generation of two edge sites from a single carbon atom site (via the reactive intermediaries, $C_e(O)$ and $C_e(O_2)$ respectively). However, Equation 12b is neutral in this regard, regenerating an edge site without expanding the available reactant species, thus interrupting the chain reaction process by using an available reaction site without desorbing a carbon atom. The strongly bonded carbon atoms within the graphene layers (basal plane layers) severely restrict the number of RSA sites available for the graphite-oxygen reactions to occur. In the context of burning, fewer than half of the carbon atoms in the graphite matrix are available as fuel for reaction with any available oxygen. Only the C_e reactive sites can serve as the available "carbon fuel" for these oxidation reactions partially isolating the interior carbon atoms from the oxygen and eliminating the chain reaction element of the fire tetrahedron. Additionally, a gas boundary layer begins to build between the reactive sites and the surrounding oxygen atmosphere even at the crystallite length-scale. This boundary layer impedes the oxygen diffusion to the reactive sites and limits the third element of the fire tetrahedron, the oxidant, as discussed below.

2.1.3 Effects of Temperature and Oxygen Concentration on the Effective Reaction Rate Constant

The highly exothermic air-graphite interaction is the most rapid, and therefore the most conservative, oxidation reaction anticipated for a modular HTGR accident. For this reaction, the graphite-oxygen chemical reactions are dominated by the reactions accounting for molecular oxygen from air (Equations 2 and 3). These chemical reactions are described mechanistically through six oxygen transfer mechanism pathways (Equations 10a–12c). Assuming pseudo-steady-state approximations with no limitations of oxygen to the reactive sites, the overall rate of graphite oxidation is controlled by the activation energies of each chemical reaction pathway and the temperature during reaction. As shown previously, the reaction rate for oxidation is proportional to the activation energy and the temperature as $r \propto exp(-Ea/T)$ (Equation 9). In general, as the temperature rises the rate of reaction increases as well. However, higher activation energies for a chemical reaction tend to decrease the rate of reaction.

The overall (bulk) reaction rate for graphite oxidation is controlled through a complex mix of all the possible reaction pathways (Equations 12a–12c) and their associated activation energies. The activation energies at different temperatures will determine the individual rates of reactions for each reaction pathway at each temperature level. The sum of these specific pathway activation energies will combine to form an effective activation energy for the overall oxidation reaction rate of graphite over the

temperatures of interest, Figure 9. Since this is an amalgamation of all the possible reaction pathways, it should be noted the overall rate of graphite oxidation is controlled by the slowest reaction pathway within the multistep reaction pathway. In extreme cases where one pathway is significantly slower than the rest, the observed rate of the overall reaction is governed by the slowest pathway, the rate limiting step.
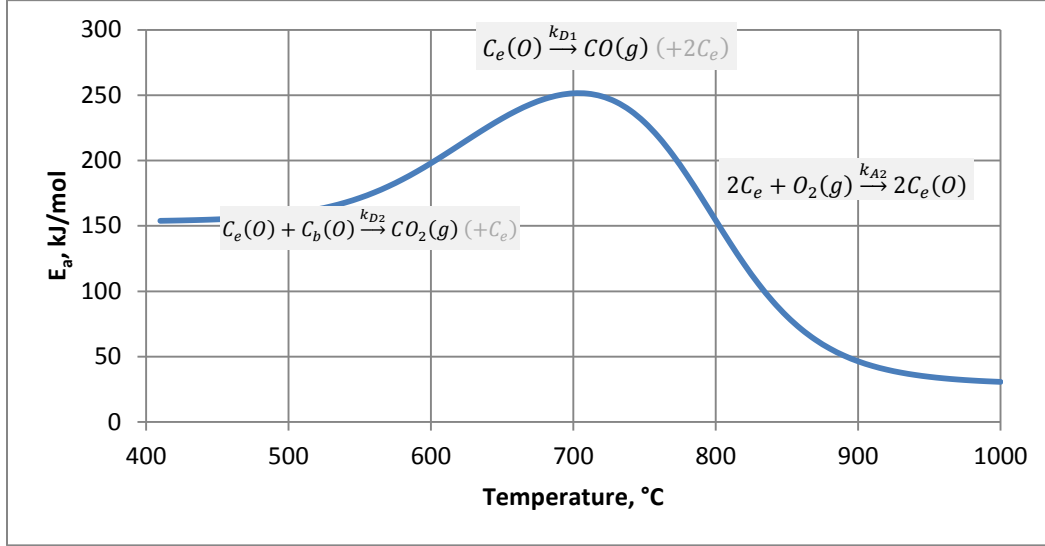
Figure 9. Effective activation energy for overall graphite oxidation reaction as a function of temperature.

The effective activation energy for the overall graphite-oxygen reaction indicates three oxygen transfer mechanism pathways dominating the chemical reaction behavior over the temperature range 400°C -1000°C. For T≤ 600°C, the activation energy is approximately 150 kJ/mol. This indicates that CO_2 production via the indirect pathway, Equation 12b, is the rate limiting reaction. Thus, at these low temperatures the primary gaseous product is CO_2. As the temperature increases to 700°C the activation energy also increases, indicating the desorption of CO pathway, Equation 12a, becomes the controlling reaction. By 800°C the effective activation energy has surpassed its peak of approximately 250 kJ/mol and begins to decrease. The rate limiting pathway is chemisorption of oxygen to the reactive sites, Equation 10b, which has a much lower activation energy than the other graphite-oxygen pathways. Since the temperature is increasing and the overall activation energy is decreasing, the reaction rate begins to increase substantially. By 900°C rate of reaction is almost entirely dominated by the dissociative chemisorption of oxygen, and the reaction rate is very rapid. As the temperatures increase, the overall activation energy for the graphite-oxygen stays low, below 50 KJ/mol.

At the very high temperatures predicted for an air-ingress accident within a large nuclear reactor, additional reactions with the graphite-oxygen reaction products (CO and CO_2) are possible within the very hottest temperature regions of the core. While dissociative chemisorption of oxygen is still the dominant reaction for graphite and oxygen, the CO_2 byproduct of this reaction pathway is expected to further oxidize the graphite at very high temperatures. The chemisorption of CO_2 on RSA edge sites or dissociation of CO_2 on the graphite surfaces forming CO are understood to be the most likely reaction mechanism for this graphite-CO_2 oxidation reaction, Equation 13[29],[30]. This oxidation event series is discussed further in Section 3.

$$CO_2 + C_e \xrightarrow{k_S} 2CO(g) \tag{13}$$

The overall graphite-oxygen reaction rate increases with increasing temperature, but the increase does not behave as a traditional chemical rate constant. Because the activation energy changes with temperature (Figure 9), the overall oxidation rate is much more temperature sensitive than would normally be expected. From Figure 9, for temperatures <600°C the effective activation energy is moderately high (150-200 kJ/mol), and the temperatures are relatively low, creating conditions for a low overall oxidation rate for graphite. However, as the temperature increases the rate limiting reaction pathway changes, and the overall effective activation energy is shown to increase as well (~250 kJ/mol). As a result, the oxidation rate is actually repressed from the expected exponential increase if the reaction pathway were not changed. At the higher temperatures, the rate limiting reaction pathway changes again with a much lower activation energy. This combination of higher temperatures and much lower effective activation energy causes the overall oxidation rate to be very rapid. In addition, at the highest temperatures (>900-1000°C) the overall rate of reaction is dominated by dissociative chemisorption of oxygen with an extremely low activation energy (<50 kJ/mol), and the overall rate of reaction becomes relatively insensitive to temperature.

Finally, the microstructure is altered during oxidation causing the oxidation rate to change. As oxidation progresses, the oxidation rate begins to accelerate as the graphite pore structure opens allowing access to more RSA sites. When the pore structure openings become so wide they reduce the available reactive sites, the overall rate will decelerate (until theoretically all material is consumed). The net progression of oxidation is therefore influenced by the combination of reaction mechanism favored by the specific microstructure encountered within each specific graphite grade as the reaction occurs. The effect of the unique microstructures encountered within each specific nuclear graphite grade must be understood before the overall reaction rate can be established.

2.2   Microscopic Level Oxidation

The oxygen transport model describes the fundamental mechanism for desorbing carbon atoms from graphite reactive atomic lattice sites. At the crystallite length-scale, the graphite-oxygen reaction rate is shown to be the upper limit of oxidation rate (the maximum reaction rate possible) for all graphite grades assuming there is no limitation of oxygen to the active area sites on the crystallites. However, the overall bulk oxidation rate has been shown to vary dramatically between grades of graphite, indicating the bulk rate is dependent upon the internal microstructure rather than the crystalline structure of graphite. The bulk oxidation rate is dependent upon the oxygen concentration at the available graphene plane edge sites within a specific graphite grade. Both the available oxygen required for graphite-oxygen reactions and the number of available reactive sites for desorption of carbon atoms is controlled by the unique microstructure formed within each nuclear graphite grade.

Transport of available oxygen to the RSA sites is controlled by the pore defect microstructure in graphite. While some graphite-oxygen reaction occurs at the surface of bulk graphite material, the open porosity inherent in nuclear grade graphite permits oxygen to infiltrate into the interior and be exposed to a much greater surface area where it reacts with any available internal reactive sites. The efficiency of this oxygen transport is controlled by the pore size, pore interconnectivity, and diffusion path tortuosity of the open pore structure.

The number of available reactive edge sites depends upon the size and uniformity of the stacked graphene planes within the graphite microstructure. For large, perfectly formed graphite crystallite formations a minimum of active surface sites is available since only those carbon atoms on the outer

18

surfaces of the crystallite have been shown to react with the available oxygen. Crystal structures with higher disorder will increase the number of available reaction sites, leading to a higher rate of graphite oxidation.

The microstructure within nuclear grade graphite is an aggregate of ordered and disordered graphite crystal structures surrounded by a unique pore defect structure. The density of the reactive surface sites and the amount of oxygen able to diffuse through the pore structure is dependent upon the feedstock material (coke and binder material) and the billet forming process (billet formation, impregnation, bake-out temperature, and graphitization temperature). These microstructure features control the overall rate of graphite oxidation and are responsible for the different oxidation rates in nuclear grade graphites.

Nuclear grade graphite is a manufactured, nearly isotropic, polycrystalline material consisting of filler material, binder material, and pores[31]. Filler material is composed of coke particles derived from either petroleum oil refining processes or through coal tar refinement. Binder material is also derived from oil or coal tar refinement but is a thermoplastic liquid which acts to bind the coke particle filler materials together into a solid mass. In nuclear grade graphite, approximately 15-20% of the volume is in the form of closed and open porosity, which provides graphite with its excellent thermal shock resistance and irradiation stability.

The pore microstructure is one of the integral features of nuclear grade graphite promoting irradiation dimensional stability, thermal shock resistance, and lower thermal expansion at high temperatures. This pore structure is complex, with a variety of pores forming under different steps in the fabrication process. In general, three primary pore structures form within nuclear grade graphite which range in size from nanometers to millimeter depending upon the raw materials used and the specific fabrication process.

- *Calcination cracks* – To form a more ordered, graphitic structure the coke (filler) particles are calcined usually to about 1400-1600°C. During calcination shrinkage cracks are formed within the coke particles. These are generally closed pores contained within the individual filler particles.

- *Gas entrainment pores* – If the fabrication process uses a liquid thermoplastic binder to bind the coke particles into a solid structure, pores can form during bake-out when volatile hydrocarbon gases are driven from the liquid binder (temperatures range from 900°C – 1200°C). As the gas is first formed and then driven from the coke-binder mixture, an open pore structure is created as the entrained gas escapes from the microstructure.

- *Graphitization (Mrozowski) cracks* – During the final process step of graphitization, nanocracks form between and within ordered crystallites due to thermal expansion under the extreme temperatures (≥3000°C). Thermal expansion perpendicular to the stacked graphene basal planes is very high, allowing significant expansion to occur at high temperatures. After graphitization the crystallites contract creating nanosized gaps or cracks between crystallites.

Pores from all three sources are illustrated in Figure 10.
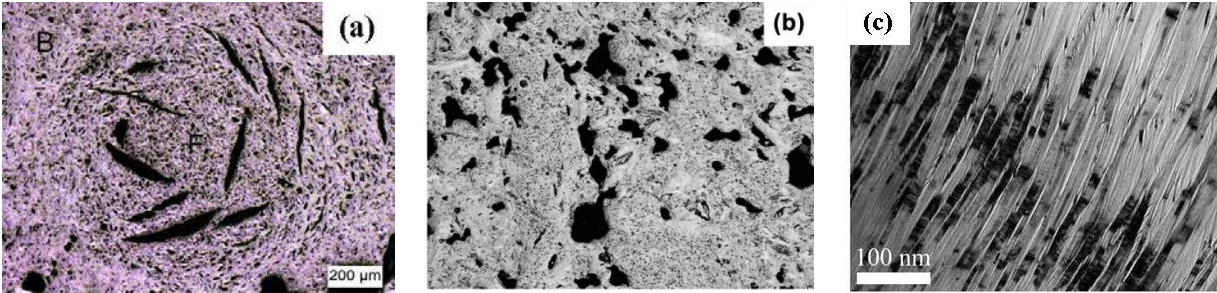
Figure 10. Pore defect structures illustrating a) calcination shrinkage cracks inside coke particles, b) gas evolution pores from bake-out, and c) Mrozowski microcracks at the crystallite length-scale.

Filler particles in nuclear grade graphite fall into two main types; petroleum and pitch-based cokes. Petroleum coke particles are generally more brittle and acicular in shape than pitch coke particles, which tend to form more spherical particles, Figure 11[32]. The more ordered structure of petroleum coke forms highly brittle, crystalline configurations that, when originally formed or when ground to the desired size, produce needle-shaped particles. Within each particle, the ordered crystallites are primarily aligned parallel to the long axis. Pitch-based coke particles are less ordered, resulting in slightly less brittle particles that are generally spherical in nature. The pitch particles display more order in the outer perimeter than inside the particle, with the crystallites tending to form with their long axis parallel to the circumference of the spherical particle.
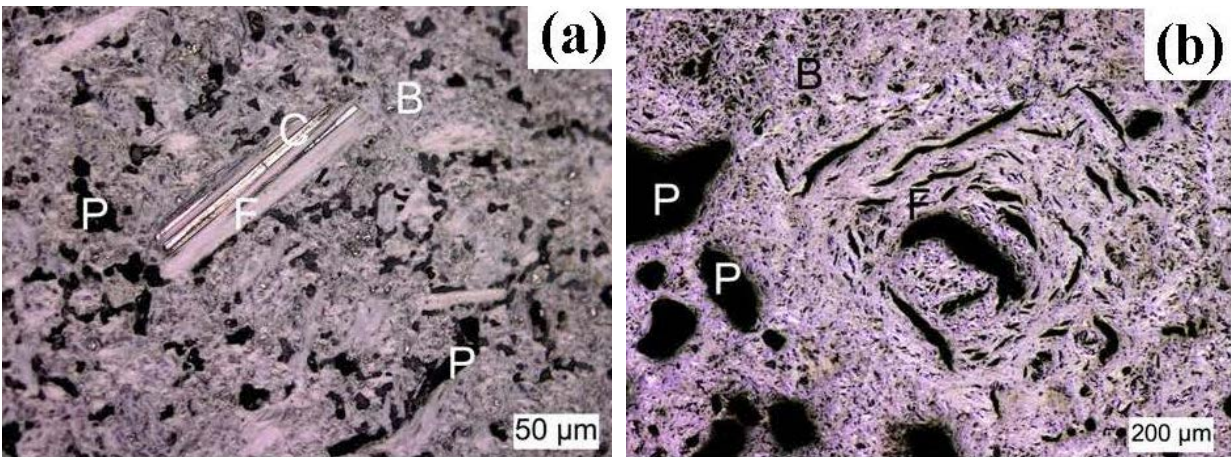
Figure 11. Petroleum and pitch based coke particles showing a) acicular and b) spherical formations (P = pore, F = filler particle, B = binder, and C = calcine shrinkage crack).

The thermoplastic binder material is used to fill the interstitial spaces between the filler particles and bind them into a solid mass. Generally, filler particles are mixed with the binder material at temperatures high enough to allow the binder to flow and thoroughly mix with the solid filler particles. This mixture is then formed into billets utilizing three primary methods: extrusion, vibration molding, and isostatic molding. The billets are heated (bake-out), during which the liquid binder breaks down and hardens into a solid. During this heated stage, hydrocarbon gases are generated within the binder phase, forming gas pockets where the gas is entrained in the material. Eventually, the gas escapes from the binder material forming a complex network of open porosity within the microstructure. Depending upon the forming process or the desired final material properties, the gas evolution pores can be filled with additional liquid binder material through a process step called impregnation, thus increasing the overall density of the

20

graphite grade. Impregnation and bake-out can be performed multiple times, effectively creating smaller gas entrainment pores and increasing the density, Figure 12.
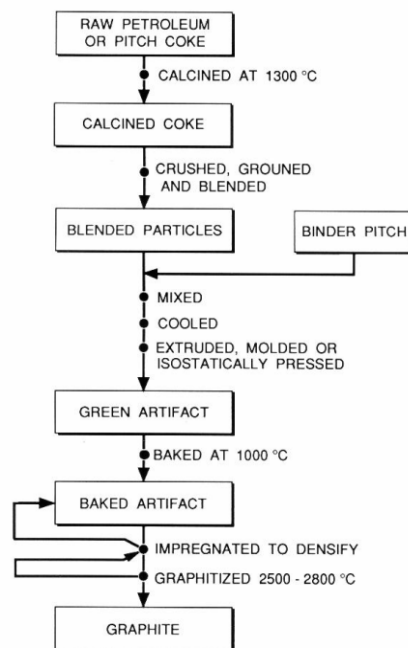
Figure 12. Typical process steps in the manufacturing of nuclear grade graphite.

Binder is a complex material comprised of thousands of compounds, mainly polyaromatic hydrocarbons and their heterocyclic analogs. These aromatic hydrocarbons are recognized as the precursor to graphene planar structures created during the graphitization step in nuclear grade graphite production. While these precursor materials can form graphene crystal structures, however, they do not create the highly ordered, stacked graphene crystallite structures that are formed within the filler particles. As such, the binder phase in graphite has significantly more RSA sites available for oxidation than the more ordered filler particles. Since the binder phase has the highest density of RSA sites it is the preferred phase for oxidation and is preferentially oxidized over the filler particles, as seen in numerous bulk oxidation studies[33,34,35].

Oxidation transport theory establishes the rate of oxidation by the RSAs sites available along the edges of the graphene crystal planes. Lower amounts of ordered graphene planes within the microstructure will yield more RSA sites and thus higher rates of oxidation. The amount of aromatic hydrocarbons in the precursor binder material dictates the amounts of graphene crystal planes formed during the graphitization process step. Thus, the rate of oxidation of the binder phase is dependent on the amount of aromatic hydrocarbon contained within the binder precursor material. This implies the overall bulk oxidation rate of each specific grade of graphite is strongly influenced by the composition of the binder material. Binder material with a more ordered crystal structure would be expected to have a slower bulk oxidation rate while binder with less ordered crystal structure would oxidize more rapidly, Figure 13.
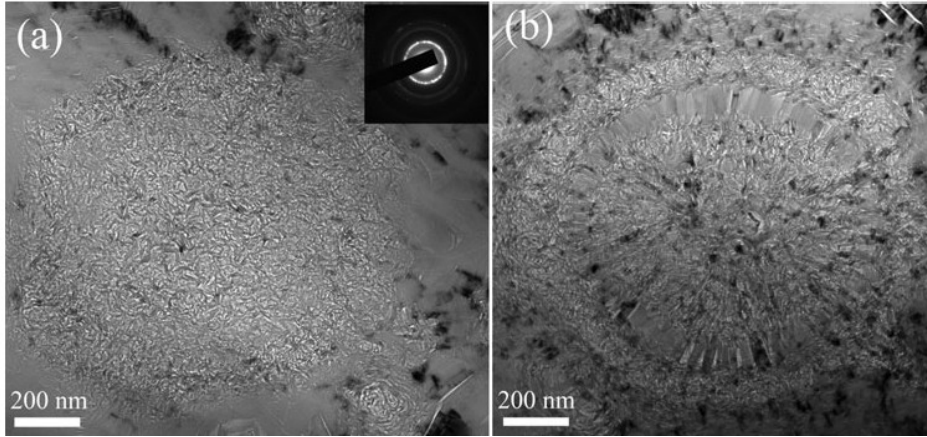
Figure 13. Examples of (a) a less ordered binder crystal structure region and (b) a higher ordered binder region within a graphite microstructure.

The filler particles and binder phase within the microstructure are much larger than single crystallites. Both filler particles and binder phase are significantly less ordered than a single crystallite and have a corresponding greater ratio of RSA to unit volume. This much larger RSA ratio will tend to increase the overall oxidation rate for the same solid volume but only if the oxygen can be transported to these available active sites within the microstructure.

Oxygen diffusion to the RSA sites is controlled by the pore structures, specifically the open porosity generated from the volatile gas evolution during binder bake-out and impregnation. Calcination shrinkage cracks, and even Mrozowski microcracks, may also contribute to oxygen diffusion if connected to the gas evolved open pore structure. The overall bulk oxidation rate is dependent upon the transport of oxygen through the increasingly restrictive open porosity structure within all graphite microstructures. This implies that the limiting action for the overall graphite oxidation rate is the transport efficiency of oxygen to the available RSA sites within the microstructure of the graphite[4].

Oxygen transport efficiency is further limited due to the transport of product gases (CO and CO_2) out of the microstructure through the same restricted open porosity structure. Mixing of oxygen and product gases gradually limits the transport of the oxygen to a finite penetration depth dependent upon the unique graphite microstructure, the temperature, and the oxidizing environment (air or water oxidation). So while there are RSA sites at the graphene planer edges within the filler and binder phases, the rate of reaction is severely restricted by the ability of the available oxygen to diffuse to these RSA sites. This severe restriction of available oxygen starves the oxidation reaction and creates conditions incapable of self-sustained oxidation within nuclear grade graphite.

2.3   Macroscopic Oxidation

Macroscopic oxidation, or overall bulk oxidation of small samples of manufactured graphite, is observed as an averaging of the RSA oxidation across the entire microstructure volume (including both binder and filler material) and the oxygen transport efficiency through the pore defect structures to the reactive sites of the crystallites. Macroscopic oxidation rates are based upon empirical data from bench scale experiments performed on small samples of assorted sizes, geometries, and nuclear grade graphite types. Bulk oxidation rate behavior, controlled by the specific graphite grade microstructure, is described by observed oxidation rate regimes from bulk specimen testing (as discussed in Section 2.0). These

22

averaging oxidation regimes summarize the bulk oxidation behavior for graphite and are most useful for generalizing the oxidation performance of large components in engineering design.

2.3.1   Bulk Oxidation Regimes

Bulk oxidation testing is used to determine the specific oxidation rates of different graphite grades through testing of small specimens. The primary assumption underlying these bulk tests is that if the oxidizing conditions are similar (temperature, oxygen content, specimen geometry) the specific rate of oxidation for each graphite grade can be determined, allowing the different grades to be compared to each other. All bulk oxidation testing uses this methodology, allowing comparisons between the different graphite grades so long as the oxidation conditions are similar.

As discussed in Section 2.0, during bulk oxidation testing three distinct regimes have been identified; kinetic controlled regime (low temperatures), transition regime, and diffusion controlled regime (high temperatures)[5]. At higher temperatures (diffusion controlled regime) the rate of oxidation reaction is very high, creating conditions where the graphite on the specimen surface is immediately oxidized as soon as it comes in contact with oxygen. Oxygen penetration into the open porosity of the graphite is limited, and oxidation is primarily limited to only a thin "film" of graphite on the surface of the graphite. Diffusion of oxygen into the open pore structure of the graphite is severely limited due to the large boundary layer of product material (CO and CO_2) from the rapid oxidation reaction on the surface of the specimen. The overall bulk oxidation rate is therefore controlled by the available reaction area sites directly on the specimen surface, with the interior RSA sites unavailable for oxidation at these higher temperatures.

For low temperature oxidation (kinetic controlled regime) the rate of oxidation is much lower, allowing maximum diffusion of the oxygen into the graphite microstructure. If these conditions are achieved, it has been shown only about 2% of the observed reaction occurs at the sample surface, and the other 98% occurs within the internal pore structure. The conservative assumption is that the oxygen diffuses completely through the specimen, allowing a maximum interaction of oxygen with the RSA sites throughout the graphite specimen. This effectively eliminates any oxygen transport restrictions from the pore microstructure. Bulk oxidation at lower temperatures is controlled by the rate of oxygen diffusion to the available RSA sites within the graphite microstructure. Higher rates of oxygen diffusion to microstructures with higher densities of RSA sites will produce higher overall bulk oxidation rates, while lower oxygen diffusion rates will produce slower oxidation rates[36,37].

While each nuclear grade graphite demonstrates these three oxidation regimes, however, the specific temperatures where each regime ends and begins can vary between them. These differences can be attributed to the unique microstructures of each graphite grade and the fact that the specific pore structures create different oxygen diffusion behavior in the graphite microstructure. The three regimes were originally intended as convenient visualization tools to illustrate the balance between oxygen diffusion efficiency into the interior of the graphite open pore structure and the rate of oxidation reaction at the RSA sites. Rather than distinct transition points of the overall bulk oxidation where one mechanism takes control, the oxidation rate is a continuous function of the diffusion and reaction rates for each specific graphite grade.

2.3.2   Oxidation Reactions Within Bulk Graphite

Depending upon the microstructure of the specific graphite, the oxygen diffusion length and reaction rate will vary depending upon the density of the reaction area sites available, the pore structure (pore size,

connectivity, and path tortuosity), and the temperature. For a microstructure with a small open pore structure and higher RSA site density (a higher binder content), the oxygen diffusion into the specimen interior is expected to be the limiting factor for bulk oxidation rate. For graphite microstructures with large pore structures and low RSA site density (larger filler particle content), the RSA site density will control the overall oxidation rate of the bulk specimens. At a constant temperature, the depth the oxygen penetrates into each specific graphite grade interior will be constant (after the initial onset period) but will differ among graphite grades.

For bulk oxidation specimens with geometries larger than the depth of oxygen penetration, a "rind" of oxidation, extending from the outer surface into the interior, results from the oxygen diffusion depth, Figure 14[9,38]. The oxygen diffusion depth is finite and will be consistent for all large graphite oxidation specimens, including specimen sizes similar to reactor components. Due to the consistent penetration depth the oxidation test results for larger graphite specimens are valid for the large reactor components used in VHTR designs.
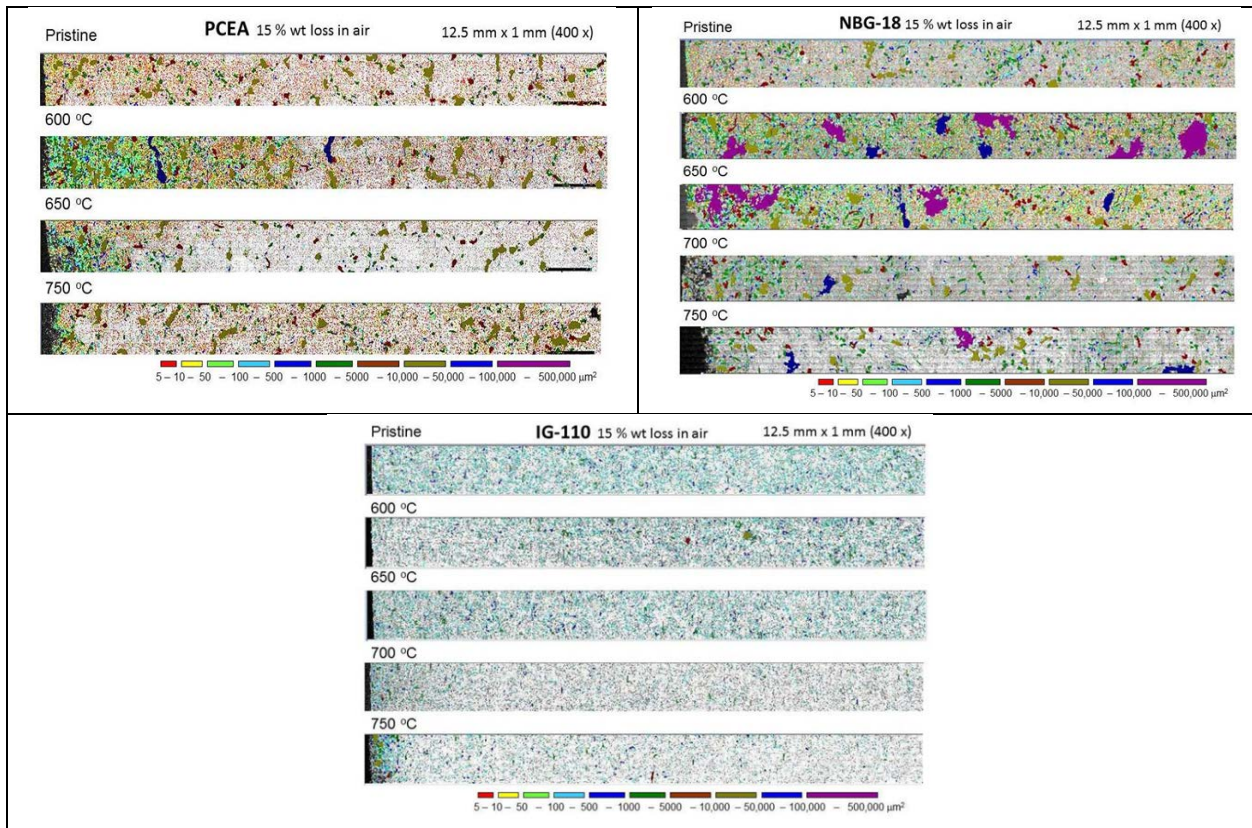
Figure 14. Penetration depth seen for PCEA, NBG-18, and IG-110 graphite grades over a temperature range of 600 – 750°C for the same amount of mass loss.

2.4   Component Level Oxidation

The large size of nuclear core components (up to 1 meter in thickness) creates very slow oxidation rates due to limited RSA sites, limited oxygen diffusion into the graphite interior, limited air supply within the helium gas mixture surrounding the individual components resulting from the plant design, as well as the slow intrinsic oxidation rate of bulk graphite material. As components in a nuclear core, the irradiation

effects, impurity levels of the component graphite, and high temperatures from the nuclear reactor must be considered as additional factors for oxidation potential for the graphite elements containing the fuel, the reflector blocks, and of the core support components. The graphite components act as a large carbon mass to absorb and mitigate any oxidants introduced into the core region. Oxidation of the graphite during air ingress accidents are furthermore limited by the several engineering and core design principles and will be discussed in Section 3.

2.4.1   Graphite Component Size and Geometry

Graphite components within a modular HTGR design typically are in the form of large bricks or blocks (50 – 150 cm in length and/or thickness) which are stacked to form an interconnected, 3-dimensional cylindrical core configuration, Figure 15. Pebble bed plant designs utilize the same shaped reflector blocks to form the structure of the core, but the fuel is contained within spherical "pebbles" composed of nuclear particles, graphite flake and binder material (see description in Section 3). The fuel matrix material containing the fuel particles is surrounded by a 3-5mm thick outer layer containing no fuel particles which acts as a protective shell for the pebble.

As discussed in Section 2.1 the outer protective layer of the pebbles is composed of partially-graphitized carbonaceous precursor material. This outer layer cannot be subjected to the high graphitization temperatures required to produce highly ordered crystallite structures (>2800°C) due to potential damage of the nuclear fuel particles. As a consequence, the oxidation behavior of these graphitic structures is expected to be similar to, but not the same as, components made from graphite heat treated to graphitization temperatures. The pebble matrix material oxidation rate will still be dependent upon the same graphite-oxygen thermodynamics and specific mechanism controlling the chemical reaction, but the overall reaction rate will be increased due to a reduction in the amount of fully graphitized crystallites within the pebble protective layer.. Few oxidation studies on fuel matrix or pebble protective layer material are available in the literature, simply resulting from the fact that these materials are more specialized to fuel requirements than to established reactor graphite component requirements. Since modular HTGR fuel fabrication is still undergoing development in several countries the oxidation response for these non-graphitized carbonaceous materials have not yet been firmly established. As such, oxidation discussions for the fuel matrix material are limited in this paper.
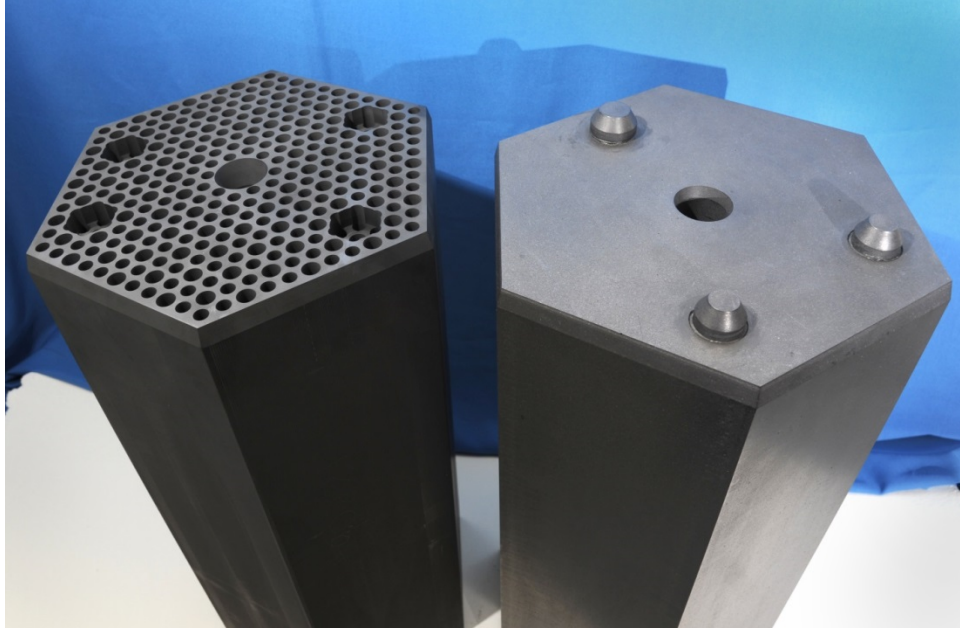
Figure 15. Typical prismatic fuel block (left) and a reflector block generic to both a prismatic and pebble bed design (right).

While the mass of the graphite components conceptually provides ample fuel for an oxidation reaction, the oxygen penetration into the interior has been shown to be small due to diffusion restrictions from the open porosity existing in all nuclear grade graphite. Relative to the large physical size of the block components, the oxygen diffusion depth is minimal. Core components within an mHTGR are stacked very close together, effectively creating an oxygen starved environment as described in Section 3. This further reduces the oxidation reaction rate within core components since the oxygen levels are reduced even before the air diffuses through the tortuous graphite pore microstructure. Thus, for air-ingress events, the overall graphite oxidation rate is further reduced due to the large size of the components and the available oxygen supply within the reactor core. This eliminates the possibility that the entire graphite mass within a nuclear core is capable of oxidizing all at once.

2.4.2 Graphite Impurity Effects on Component Oxidation

Trace additions of metals in graphite produce a wide array of catalytic effects enhancing or inhibiting the rate of oxidation[39,40]. The effect on the oxidation rate depends upon the impurity type and the content of the impurity. Generally most metals are catalysts for the oxidation of graphite while non-metals or materials exhibiting non-metallic behavior are known inhibitors[41,412]. Most metals enhance the graphite-oxygen reaction by facilitating a faster path for oxygen transfer to the RSA sites, increasing the overall oxidation rate. This enhancement is achieved through two primary mechanisms; non-dissociative and dissociative.

Metals such as Pd, Ag, Pt, and Au adsorb oxygen non-dissociatively, enhancing oxidation by carving channels or pitting the carbon (parallel or perpendicular to the basal plane) and allowing faster oxygen transfer to the RSA sites. The impurities do not interact with the carbon structure directly but merely facilitate the transport of oxygen to the available RSA sites.

Metals such as Ti, V, Cr, Fe, Mo, W, Re, Ru, Rh, Ir, Cu, and Zn adsorb oxygen by dissociation and increasing the contact along the edges of the graphene sheets (wetting). Catalytic oxidation proceeds by recession of the graphene sheets and is primarily due to the fast and low energy barrier dissociation and transfer of atomic oxygen to the RSA sites. Second row transition metals are also catalytically active, but tend to become significantly less active over time due to their transformation to stable carbides, which are significantly less active catalytically.

Depending upon the impurity levels in specific graphite grades the oxidation rate can be increased by a factor of 2-3 times due to trace impurities. The effect of impurity on graphite oxidation is well known and nuclear grade graphite standards specify a maximum impurity level to mitigate enhanced oxidation[3]. High purity grades require a maximum total impurity level of 300 ppm, and low purity grades are allowed a maximum total impurity level of 1,000 ppm. All current nuclear grade graphite meets or exceeds these specified levels to ensure minimal enhancement of graphite oxidation.

2.4.3   Heat Sources in Graphite Components

At the component level, heat sources and heat transfer mechanism are evaluated to address component temperatures and component oxidation. Any heat generated from oxidation chemical reaction will be transported away from the component surface due to the large thermal diffusivity of graphite. The large mass of the components and the high heat capacity of the graphite allow for significant heat to be transported away from any RSA sites and stored within the large components without significantly raising the overall temperature of the component. This prevents heat generated in a local area undergoing oxidation from producing a large localized escalation in temperature.

Radioactive decay heat significantly increases the component temperatures, providing additional heat to the graphite material within the nuclear grade graphite blocks. This increased temperature will promote higher rates of oxidation of the components. During an air-ingress event, the nuclear decay heat is generated from the nuclear fuel and transported outward to the graphite component surfaces. This internal heat will slow the heat transport from the outer oxidation reaction areas on the nuclear fuel blocks and allow the temperature to rise in the oxidizing area.

If the nuclear decay heat is high enough to raise the temperatures within the blocks significantly, oxidation will continue to occur if sufficient oxygen is available at the component surfaces. However, this is not self-sustained oxidation, since this rapid oxidation of the graphite is only possible while the graphite temperatures remain high enough to induce oxidation. Once the nuclear decay heat has decreased and the temperatures are lowered, the oxidation reaction will stop due to loss of reaction heat and limited oxygen transport necessary to sustain the reaction. Reactor engineering systems designed to reduce decay heat induced oxidation of the core components are discussed in Section 3.

The ability of graphite to conduct heat away from an oxidizing area in large graphite components has been illustrated through simple experimental studies[43]. Utilizing oxy-acetylene torches to locally heat and oxidize an area on a large graphite block component, it was observed that once the heat source was removed the region below the torch nozzle stopped oxidizing almost immediately and the area cooled quickly. While simplistic, these studies illustrate the significant heat conductivity of graphite and the difficulty of imposing self-sustained oxidation of nuclear grade graphite components.

2.4.4   Irradiation Effects on Component Oxidation

Since graphite is the primary structural material containing the nuclear fuel in a modular HTGR, the irradiation induced changes to the graphite need to be addressed. Irradiation damage to the graphite crystal structure, changes to the material properties, and additional factors such as high temperatures experienced in the nuclear core can change the oxidation response. Extensive work has been conducted and is ongoing on irradiation effects on the thermal, mechanical, physical, and chemical properties of graphite[44,45,46,47,48].

2.4.4.1   Irradiation Damage to Graphite Crystal Structure

In general, irradiation damage in graphite material should have minimal effect on the oxidation mechanism or rate. Irradiation damage occurs within the graphite atomic crystal structure, creating atomic and crystallite level defects within the crystallite structure[49,50,51]. With increasing irradiation dose, the microstructure begins to become denser as the crystallites swell perpendicular to the direction of the graphene basal planes. This closes the Mrozowski microcracks and creates a denser, less open pore microstructure throughout the graphite. At very high irradiation dose, typically after 15- 20 years of service, crystallite growth continues to expand, and eventually the crystals begin to intersect with each other, forcing them apart and causing new cracks to form within the microstructure[48,51].

Irradiation damage to the crystal structure will create more RSA sites, but these sites will primarily be in the interior of the crystallite, not on the outer surfaces of the crystallites. Since oxygen can only react with RSA sites directly on the surfaces of the crystallites, any increase in RSA sites from irradiation damage will be minimal. Any effect on the oxidation rate from increased RSA site formation would also be minimized as the microcracks and pores close under irradiation. Diffusion of oxygen into the microstructure would gradually be reduced as the open porosity is closed, supporting the idea that graphite oxidation rate decreases under irradiation. Oxidation rates for graphite at the end of life (15-20 irradiation service years) may increase due to the increased open porosity. However, there is little to no experimental data to support a significant change to graphite oxidation at these irradiation dose levels.

Most irradiated graphite oxidation data comes from studies in the United Kingdom on the Magnox and Advanced Graphite Reactor (AGR) designs[52,53]. These designs use a CO_2 coolant that dissociates under irradiation, creating constant low levels of oxygen within the graphite microstructure at normal reactor core temperatures. Gradual, chronic graphite mass loss from irradiation induced oxidation is the life-limiting mechanism for the AGR and Magnox graphite core components and is under constant monitoring by the utility. However, under an air or steam ingress accident, the same mitigating mechanism for acute oxidation shown to be inherent in nuclear grade graphite still apply. The AGR graphite microstructure may have greater open porosity from the chronic oxidation, but that is the only difference from graphite that has not been exposed to chronic oxidation.

2.4.4.2   Wigner Energy

Irradiation damage to the graphite crystal structure physically removes carbon atoms from the crystal lattice positions within the graphene basal planes. These displaced carbon atoms (interstitial atoms) are left to freely move about the crystal structure while the crystal lattice adjusts to accommodate these missing atoms (vacancy sites). Because these interstitial atoms are not in the ideal location (inside the crystal lattice position) they have an energy associated with them, much like a ball at the top of a hill has gravitational potential energy.

If all displaced carbon atoms are allowed to return back to vacancy sites within the atomic crystal structure at once, the energy associated with them would be released suddenly. This "Wigner stored energy release" phenomenon is a common problem with low temperature graphite core reactors. The stored energy can be substantial, and when it is released, the temperature of the material can rise significantly. Annealing the irradiated graphite to temperature levels where the interstitials move freely to the vacancy sites in a slow and controlled manner will reduce the stored energy and avert any significant sudden rise in temperature. Annealing temperatures are usually about 200-250°C, the temperature where free movement of interstitials can easily move to the closest vacancy site, as discussed in Section 2.4.4.1.

Several studies demonstrate the total stored energy increases with irradiation dose and appears to reach a saturation limit after long exposures, for a given irradiation temperature. A characteristic release peak at around 200°C was found for some graphite grades irradiated at a low temperature. This peak shifts to higher temperatures and diminishes in magnitude (to almost undetectable levels), as the irradiation temperature increases[52]. Graphite irradiated at temperatures at or above 250°C should not accumulate significant Wigner energy stored in the crystal structure. These trends, however, are only supported experimentally with data for irradiation temperatures of up to 450°C and doses of <2 dpa.

Evidence was found to indicate not all of the stored energy is released even after annealing temperatures up to 1000°C . Some stored energy remains in the graphite, which can produce a smaller second release peak at temperatures in the range of 1200–1500°C. However, all these indications are for graphites irradiated at low temperature, which contains large amounts of stored energy. Higher irradiation temperatures provide very little stored energy as the defect structures are annealed during irradiation.

Modular HTGR designs are operated at temperatures significantly higher (400°C – 1000°C) than the irradiation temperatures where Wigner energy is demonstrated to be stored. This prevents a significant buildup of internal stored energy. Minimal stored energy will therefore be available in the event of an accident, with no significant increase in temperature of the graphite core components.

2.4.4.3   Graphite Dimensional Change and the Formation of Gas Gaps

Under irradiation, graphite material tends to become denser, which is manifested as macroscopic shrinkage in the core components. Under irradiation, the graphite core block components can be expected to shrink as much as 7-8% from their original dimensions. This irradiation-induced shrinkage can increase gaps between stacked block components, leading to an increase in gas bypass and a subsequent increase in available oxygen to diffuse into the microstructure of the graphite. The maximum 7-8% gap increase will occur slowly as the neutron dose is accumulated and will not be present until near the end of life for the graphite components. Most irradiation induced dimensional effects on graphite oxidation will occur later in the life of the graphite core and can be mitigated by replacing core components at appropriate

intervals. To determine the safety implications from these increasing gas gaps between components, reactor core safety analyses are performed as discussed in Section 3.

2.5 Factors Necessary for Self-Sustained Graphite Oxidation

The oxidation of graphite is a complex phenomenon requiring specific knowledge of the chemical as well as material properties of nuclear grade graphite at all length scales to determine accurate oxidation behavior. The mechanism and factors underlying graphite-oxygen chemical reactions have been discussed in detail in all of Section 2, from the oxygen transport theory at the atomic and crystallite length scale, to graphite microstructural effects, to nuclear component size and irradiation effects. As discussed, the rate of graphite oxidation is dependent not just upon the theoretical oxidation rate at the crystallite length scale, which assumes unlimited oxygen available, but also the diffusion efficiency of the oxygen to the RSA sites throughout the entire volume of graphite.

Utilizing these graphite oxidation principles and the factors required to sustain a fire for a combustible material, the likelihood of self-sustained graphite oxidation (graphite burning) can be determined. The mechanism underlying the graphite-oxygen transport theory, the pertinent microstructural features in nuclear grade graphite, and relevant nuclear considerations such as irradiation damage and reactor core design features will now be discussed within the context of each of the fire tetrahedron requirements required for self-sustained combustion.

2.5.1 Carbonaceous Fuel

Combustion or burning, as defined by the NFPA, is the sequence of chemical reactions between a carbonaceous fuel and oxidant accompanied by the production of heat and conversion of chemical species. At the atomic scale, every carbon atom may be assumed to potentially be fuel for a carbon-oxygen chemical reaction. However, as discussed in Section 2.0 and 2.1, the carbon atoms are ordered within graphene basal planes stacked within graphite crystallites, and only those atoms at RSA sites are actually available for the graphite-oxygen reaction. This severely limits the available fuel for the oxidation reaction as RSA sites occur only on the outer edges of the crystallites and oxygen cannot diffuse into the crystallite structure to complete the chemical reaction. Thus only a fraction of the available carbon atoms react within graphite, which severely limits the rate of reaction at any temperature.

RSA sites can be increased with more disorder in the crystal structures. As discussed in Section 2.2, the binder region within nuclear grade graphite microstructures can have a greater number of RSA sites than found within filler particles. This is the primary reason why binder is preferentially oxidized before filler particles in nuclear grade graphite. However, oxygen must be able to diffuse into the interior microstructure of the graphite to these RSA site locations. The oxygen diffusion restriction from the tortuous open pore structures within nuclear grade graphite creates significant limitations on transporting oxygen to the regions with a higher density of RSA sites, limiting the increase in overall bulk oxidation rate for graphite grades with higher levels of binder in the microstructure. Theoretically, irradiation induced damage to the crystal structures may also produce more RSA sites, increasing the amount of available fuel. In Section 2.4.4.2, irradiation damage is shown to occur mainly in the interior of the graphite crystal structure. Only minimal disruption is expected on the edges of the ordered crystallite structures where graphite-oxygen reactions occur. While a change to the number of RSA sites may increase the potential fuel for chemical reactions, the diffusion of oxygen to these sites remains the rate limiting factor.

The overall reaction rate may also be increased with the introduction of catalytic impurities in the graphite microstructure, lowering the reaction activation energy and making more carbon atoms available as fuel for the reaction. As discussed in Section 2.4.2, even small impurity levels, mainly from metallic elements, can significantly affect the bulk oxidation rate of graphite. To eliminate this acceleration potential, the feedstock material or the nuclear grade graphite components are purified prior to use. Total impurity levels are reduced to levels below 300 ppm, reducing the enhanced oxidation rates from impurities.

Finally, the number of RSA sites provides an upper bound for the oxidation rate of graphite. Small increases to the number of reactive sites are possible if more binder material is used or if considerable irradiation damage is incurred, but these increases are small (a maximum of a few percentage). A minimal increase in RSA sites may increase the overall rate of oxidation, but the chemical reaction is still controlled by the reaction of carbon atoms on along the basal places edges and not in the interior of the crystallites. Thus, unlimited, self-sustaining consumption of the carbon atoms within a nuclear grade graphite microstructure is not possible under any oxidizing condition.

2.5.2   Oxidant

A continuous chemical reaction between the carbonaceous fuel and an oxidant (air or steam for nuclear reactor conditions) is required for combustion or burning. The ability of oxygen to diffuse into the graphite microstructure and react with the available carbon atoms at the RSA sites is the key parameter to determining the overall rate of graphite oxidation. Section 2.1 shows oxygen only reacts with the outer RSA sites along the surfaces of the crystallites and cannot diffuse into the crystal structure. Sections 2.2, 2.3, and 2.4 illustrate oxygen diffusion to the available RSA sites is restricted at the microscopic, bulk, and component length-scales. Diffusion through the graphite pore structure is dramatically reduced as the open porosity is gradually restricted. Oxygen diffusion is further impeded by diffusion of the reaction products, CO and CO_2, out of the microstructure, which becomes significant at high temperatures. Finally, the amount of oxygen available to diffuse into the graphite microstructure is severely restricted by the component block stacking configurations. Tight gas gaps between the core components blocks severely restrict the amount of oxygen or steam that can diffuse into the interior of the graphite microstructure, further limiting the amount of oxygen available at RSA sites.

Oxygen diffusion to RSA sites can be enhanced by irradiation dimensional change in the graphite. As Section 2.4.4 discusses, irradiation can create larger gaps between core component blocks, allowing more air or steam to become available for diffusion into the graphite microstructure. In addition, at very high dose levels, new porosity within the microstructure occurs due to irradiation-induced swelling of the crystallites. The increase to oxygen diffusion is, however, modest at best and only begins to occur at very high dose levels, very close to the end of useful life for the core components.

The diffusion of oxygen to RSA sites is the critical requirement for self-sustained oxidation of graphite. The severe restriction of oxygen diffusion within the nuclear grade graphite microstructure marks it as the controlling requirement for the graphite-oxygen chemical reaction. Oxidation can and does occur in air or steam environments at high temperatures, but the extremely slow rate of oxygen diffusion to the limited number of RSA sites limits the chemical reaction severely, and the reaction cannot be sustained.

2.5.3   Heat

The carbon-oxygen chemical reaction is an exothermic reaction, implying that heat is generated during graphite oxidation which can raise the local temperature and allow further oxidation to occur. However, the thermal conductivity of graphite is higher than that of most metallic materials, and the heat can be expected to be conducted away from the local RSA. Even when heated from the nuclear reactor, the large thermal conductivity and large mass of the core components will remove the heat from the local regions as discussed in Section 2.4. This is illustrated through experimental data demonstrating the temperature is immediately reduced after oxidation, indicating the heat of reaction is conducted from the local oxidation site, as shown in Figure 16.

Self-Limiting Oxidation, Not Burning
for constant 10 liter per minute total gas flow

—Graphite sample exhibits 1% mass loss in 10% air in helium maintained at 750°C
—Further mass loss tapers off in 100% air for naturally decaying temperature from 750 to 300°C
—Gas Temperature Near Graphite Sample
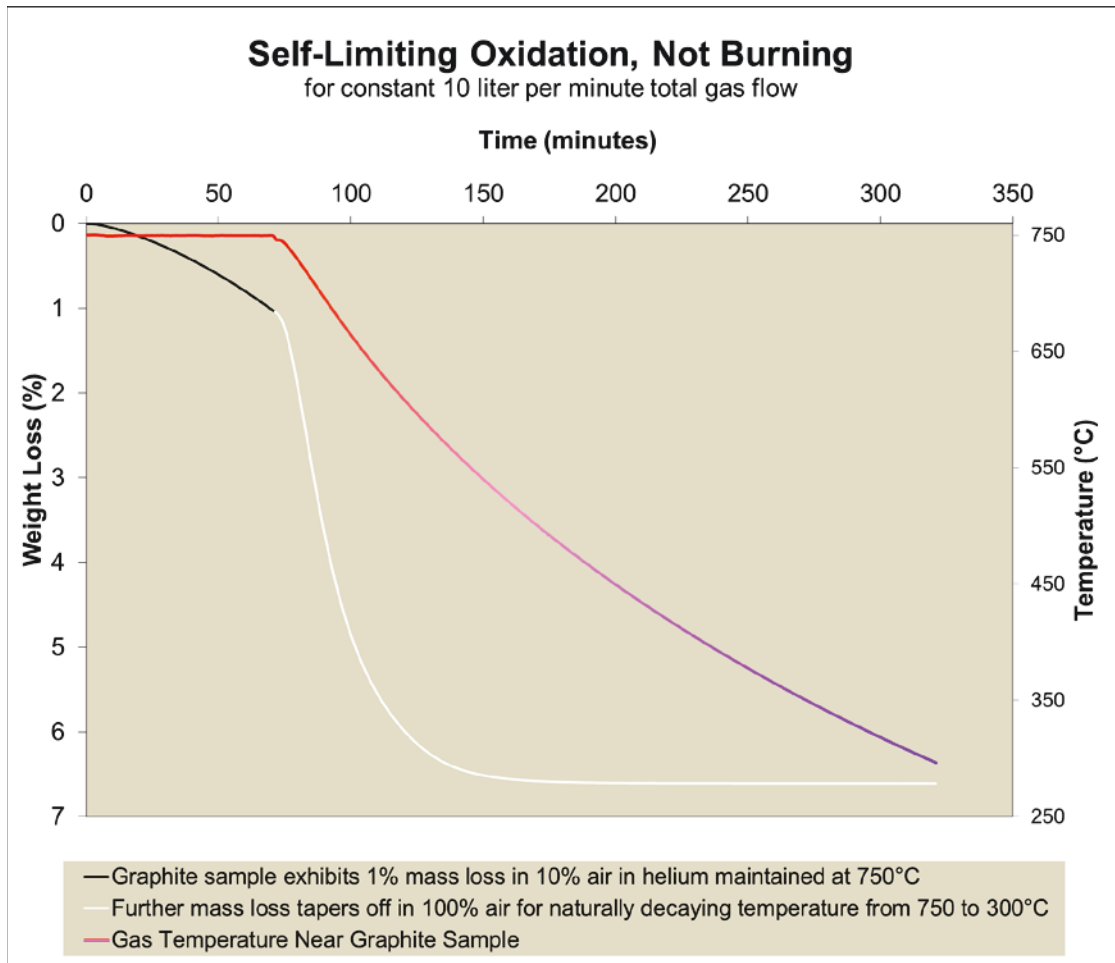
Figure 16. Graphite sample oxidizes with available oxygen from air leak at 750°C, but reaction is self-limiting, even in 100% air, once furnace heaters are shut down.

2.5.4   Chemical Chain Reaction

The chemical chain reaction, necessary for self-sustained oxidation, is dependent upon a continuous supply of available carbon atoms, unrestricted oxygen to react with the carbon atoms, and a high temperature necessary for a high rate of reaction. As discussed throughout all of Section 2, the carbon atom availability is restricted to only RSA sites, and the oxygen supply is severely restricted through the graphite microstructure. While the temperatures achieved within a nuclear reactor are quite high and can

maintain a rapid oxidation rate, once the heat has been lowered, graphite oxidation has been shown to stop. Even at the highest temperatures anticipated for an air or steam ingress accident, the oxidation of graphite is shown to be self-limiting at the crystallite length-scale level, and a chemical chain reaction cannot be maintained. Self-sustained oxidation is physically not possible due to these material restrictions.

Significant effort has been spent on designing modular HTGRs to limit oxidation of the graphite components in the event of steam or air ingress during an accident. These engineering design controls provide yet another level of oxidation protection to the graphite components in addition to the physical and thermal properties of the graphite itself. A detailed discussion of these modular HTGR engineered features specifically designed to limit the oxidation of graphite components is presented in the following section.

3. OVERVIEW OF MODULAR HTGR OFF-NORMAL EVENTS INVOLVING GRAPHITE OXIDATION

The overall design process of modular HTGRs integrates the major objectives of safe, reliable, economic generation of power and/or process steam. One of the primary objectives addressed during the modular HTGR safety design is control of chemical attack. In this regard, the central design selections are the chemically compatible ceramic-coated fuel, the nuclear-grade graphite moderator, and the chemically-inert high purity helium. From the point of view of offsite radiological consequences to the public during rare off-normal events, the progression and extent of the nuclear-grade graphite oxidation in a modular HTGR, due to either ingress of air from the reactor building or of water from the steam generators, is important since it could lead to the release of radionuclides within the helium primary circuit, as well as a degradation of the reactor core structural support.

While events that result in air and water ingress can both lead to graphite oxidation, the spectrum of events involving water ingress are more risk-significant. The first reason for this is the water in the steam generators is pressurized considerably higher than the helium in the primary circuit which is much higher than the atmospheric air in the reactor building. A leak in the steam generator portion of the helium pressure boundary immediately results in water/steam ingress, whereas a leak in the other portions of the HPB results in a relatively slow depressurization of the helium that expels most of the air in the vented low pressure reactor building. Additional reasons for off-normal events involving water ingress being of more risk significance is that the pressurized water results in steam-induced liftoff of radionuclides plated out on metallic surfaces of the primary circuit during normal operation, and the addition of the higher pressure water/steam may result in the opening of a transport path and mass transport mechanism for the radionuclides into the reactor building, possibly opening the reactor building vent to the environment. Thus, although graphite oxidation by air is an exothermic reaction (producing heat) whereas the graphite oxidation by water is an endothermic reaction (requiring heat), this factor is insignificant compared to the likelihood of plentiful water ingress and the resulting potential for radionuclide transport offsite. The focus of this section is the off-normal events involving the oxidation of air with graphite, but a few remarks will be included on steam ingress.

The spectrum of off-normal events involving air ingress and graphite oxidation include: Anticipated Events (AE) expected in the life of a multiple reactor plant, Design Basis Events (DBE) not expected in the plant lifetime or Beyond Design Basis Events (BDBE) not expected in a fleet of several hundred plants. In all these events, a sequence of initiating events are evaluated, which then leads to an outcome determined by the response of the plant systems to take corrective actions, for example by shutting the reactor down and cooling the core. In the case of off-normal events involving air ingress, the initiating event is typically a leak (e.g., from an instrument line or break from the helium purification connecting pipe) in the helium pressure boundary. The size and location of the initiating leak or break is important in how the helium-air gas mixture enters the HPB after the time for the helium to depressurize. Additionally, a crucial plant response is the success of the active core cooling systems to remove the residual heat as the oxidation reaction is temperature dependent. Finally, if the passive core cooling system is relied on to remove the residual heat, then the timing for the helium-air gas mixture to reenter the HPB is delayed.

Analysis of these reactor accidents is required as part of the reactor licensing process. This is achieved by utilizing predictive reactor simulation software tools, which use data validated on experimental and similar operating reactors and are verified with code-to-code and numerical benchmarks. Sophisticated models are used to predict the total kinetic rate of oxidation in the graphite regions. These models utilize a combination of the thermodynamic equations in Section 2.0 and 2.1, accounting for the availability of oxygen due to fluid flow characteristics, graphite temperatures expected from the nuclear decay heat source, as well as the design of the core components and core configuration.

As discussed in Section 2, self-sustained oxidation or burning is not possible for graphite components, and the extent and severity of the oxidation of graphite components within the core are controlled by the graphite-oxygen mechanism. In this section an overview of modular HTGR air ingress accident analyses is provided, and a few design-specific examples of simulated graphite oxidation events are also included for prismatic and pebble bed modular HTGRs (e.g., spatial distributions of gas compositions, mass flow rates, and temperatures). These simulations illustrate the influence of the limitations on oxidation of graphite discussed in Section 2 and the effects of reactor system design selections on the progression of accidents involving graphite oxidation. It should be stressed the examples presented here are only a sub-set of the available literature, and the validation status of the various codes is unknown. It should be noted that no new analyses were performed for this review.

3.1   Modular HTGR Core Design Overview

The operational design envelope and assumed boundary conditions are of primary importance for accurate modeling of modular HTGR graphite oxidation. A comparison of design parameters for two pebble and prismatic reactors is presented in Table 1. The High Temperature Reactor Pebble Bed Module (HTR-PM)[55] is a two-module 250 MWt pebble bed design currently under construction in China. The 350 MWt four-module MHTGR is a General Atomics prismatic design from the 1980s that was recently selected for two international code-to-code benchmark exercises[56,57]. The layouts of a typical pebble bed HTR and the MHTGR-350 are shown in Figure 17 and Figure 18, respectively.
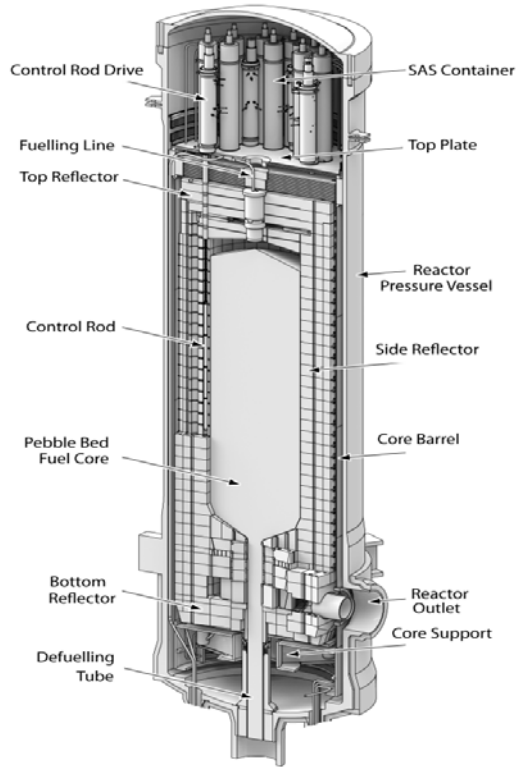
Figure 17. Reactor vessel geometrical representation for the pebble bed HTR-PM design.
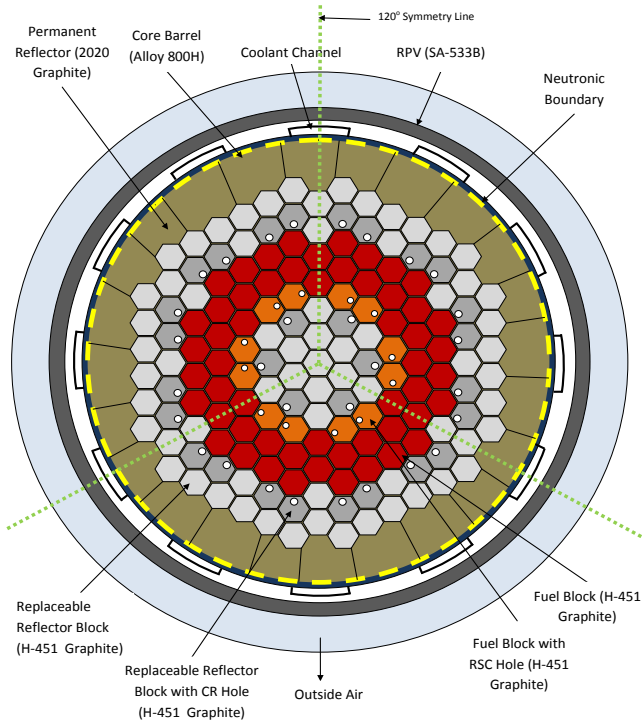
Figure 18. Radial core layout for the prismatic MHTGR design.

Both core designs contain several hundred tons of nuclear-grade graphite. Graphite blocks form the reflector region, while the active nuclear fuel "core" region consist of either prismatic blocks (MHTGR) or graphite pebbles (HTR-PM), as shown in Figure 19 and Figure 20. The prismatic and pebble bed designs use UCO and UO_2 nuclear fuel, respectively, embedded in the form of several thousand tristructural isotropic (TRISO) coated fuel particles inside a graphite matrix, which is then packed into the active core region as either hexagonal fuel blocks (660 in total for the MHTGR) or 6 cm fuel pebbles (approximately 420,000 for the HTR-PM).
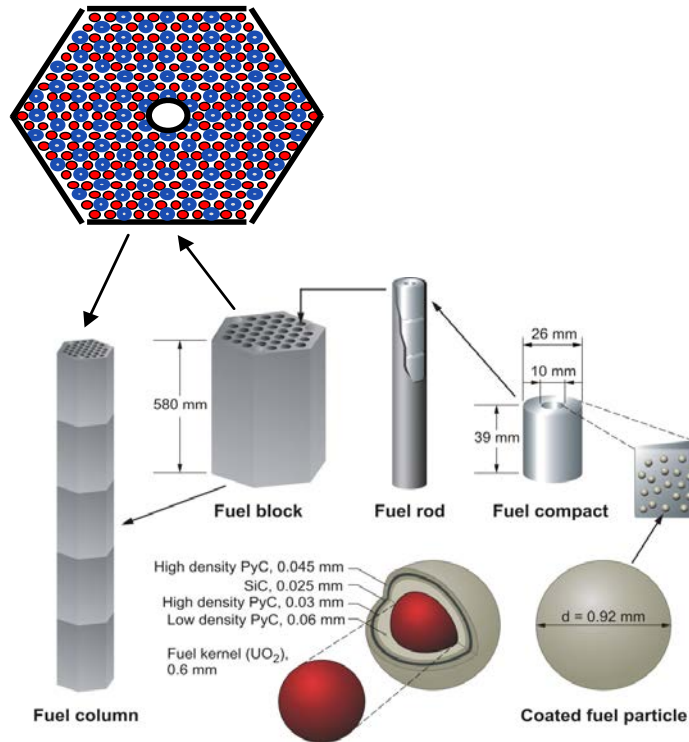
Figure 19. TRISO fuel, compact and block in a prismatic modular HTGR.
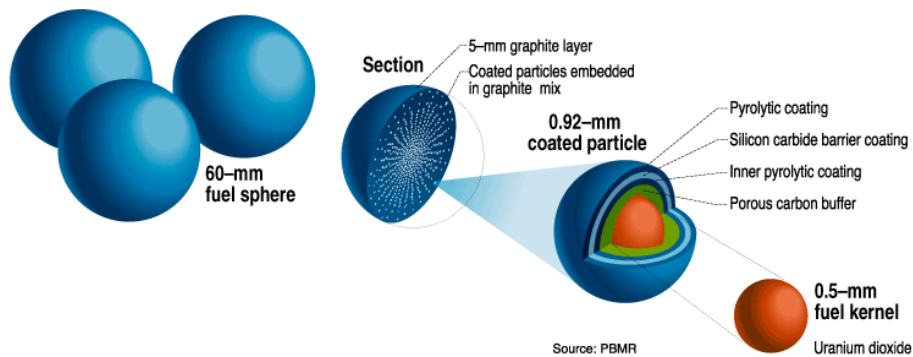
Figure 20. TRISO fuel particles in a pebble bed modular HTGR.

In the prismatic design, heat generated by fuel elements during normal operation (shown in red in Figure 18) is removed by forced helium cooling through coolant channels in the fuel elements. The MHTGR nuclear fuel blocks each contain approximately 108 of these coolant channels, but the reflector blocks in the central and outer reflector regions are solid. During an off-normal event, oxygen can reach the graphite surfaces via the engineered coolant channels inside the nuclear fuel blocks or via gaps that exist between the fuel blocks and between the graphite reflector blocks in the reactor. The flow path of the helium coolant in the MHTGR design is presented in Figure 21.
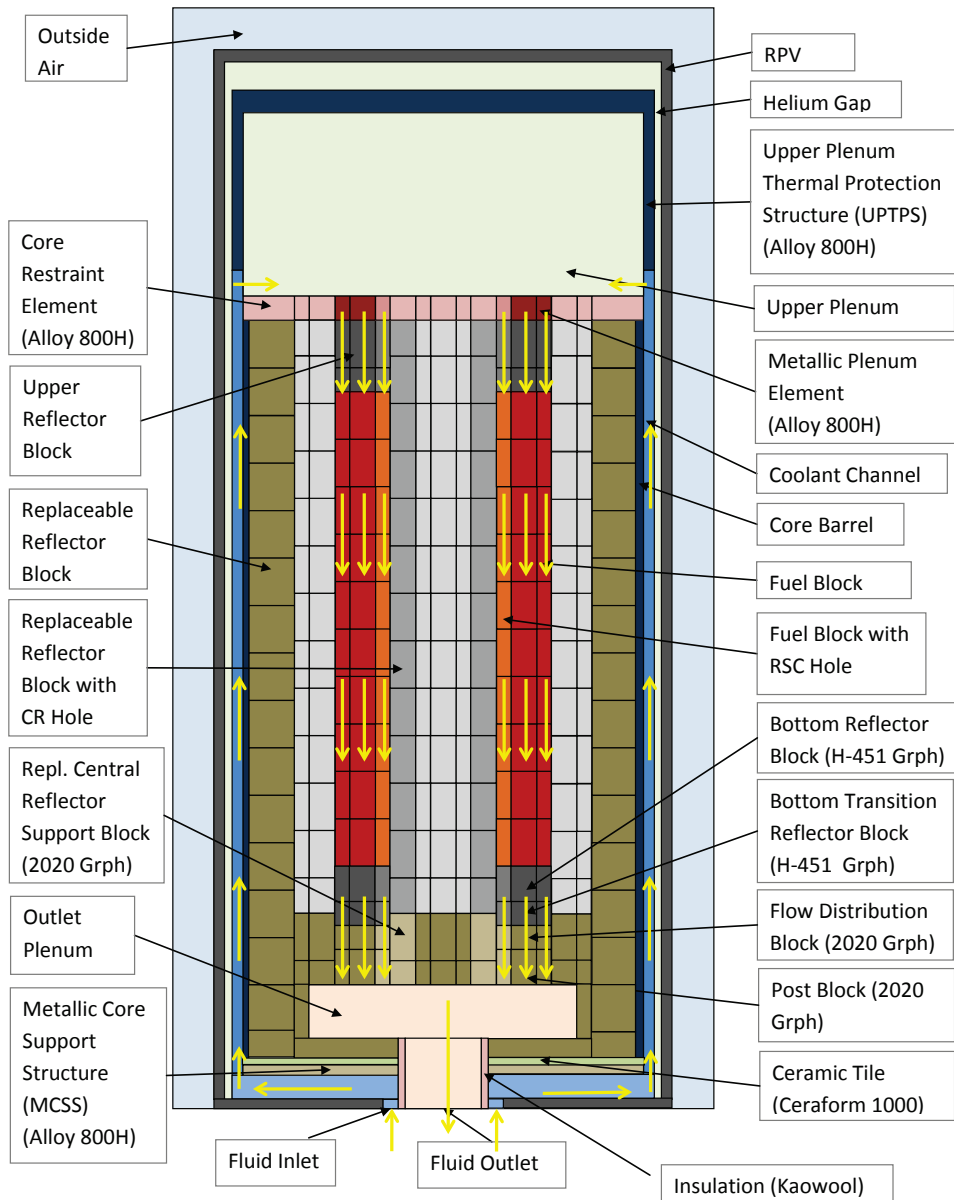
Figure 21. MHTGR Helium Flow Path.

In the case of pebble bed modular HTGRs, helium flow in the core is more torturous through the packed pebble bed, and the total available graphite surface area in the pebble bed core is approximately 35% higher compared to the prismatic design (Table 1). It is also shown in Table 1 the graphite layer between the fuel and helium coolant is thicker (1 cm) for the pebble type fuel compared to the 0.45-0.61 cm for the prismatic type fuel.

Table 1. Design parameters for two modular HTGR designs.

Parameter	HTR-PM	MHTGR-350
Thermal power	2×250 MWt	4×350 MWt
Core diameter	3 m	3 m
Core height	11 m	10 m
Number of fuel elements	420,000 fuel spheres	660 fuel blocks
Inlet/outlet gas temperature	250/750 oC	259/687 oC
Primary helium pressure	7 MPa	6.39 MPa
Mass flow rate	96 kg/s	157 kg/s
Pebble radius/block pitch	3.0 cm	36 cm
Thickness of graphite region separating helium coolant from fuel	1 cm radial outer surface layer on each fuel sphere	0.45 cm (large coolant holes) 0.61 cm (small coolant holes)
Core graphite surface area (fuel region only)	~ 50 m2	~ 37 m2

3.2   Parameters That Influence Graphite Oxidation

Since a typical modular HTGR operates at a very high helium pressure (Table 1), air ingress is only possible if it is preceded by a breach in the helium pressure boundary. The most probable type of breach is a small line leak, which could take several hours to depressurize the primary system (see Section 3.3.1). During this "blowdown" period, the helium enters the reactor building, where it mixes with air before the mixture is released through the building pressure relief system when the system's set point is reached. A generic air ingress simulation would further assume a mixture of air and helium would start to enter into the helium pressure boundary at some point after the system has reached atmospheric pressure. This hot gas mixture will then follow a flow path through the core and reflector regions determined by the complex combination of fluid dynamics (natural convection, flow resistance, gas density and temperature), heat generation (from nuclear decay heat as well as exothermic oxidation processes), and oxidation kinetics (as described in Section 2).

In the case of indirect steam cycle designs such as the HTR-PM and MHTGR, the secondary steam generator operates under very high pressure, in excess of 15 MPa, so a possible failure in this case is one of the steam generator tubes. A limited volume of steam then enters the primary system very rapidly and provides an additional source of oxidants that can be distributed in the core and reflector regions.

The parameters listed in the three sections below determine the progression and final outcome of an air or steam ingress event. (This discussion follows the structure implemented in Section 2.5, where graphite oxidation is described in terms of the fire tetrahedron).

3.2.1 Carbonaceous Fuel

The reflector dimensions in modular HTGR cores are sized to obtain optimal neutron economy (i.e., to maximize neutron thermalization and backscatter into the fuel region and minimize neutron leakage). The core designers therefore do not have a lot of freedom regarding the total graphite mass in the core. However, the total graphite surface area in contact with helium flow is a more relevant parameter in air ingress events than the total available mass, because as discussed in Section 2.4, only the reactive sites close to the graphite block surfaces are available for oxygen interactions. The MHTGR design contains approximately 450 tons (250 m^3) of graphite in the form of $79 \times 36 \times 36$ cm hexagonal reflector blocks, as well as 80 tons of graphite in fuel blocks.

A common erroneous assumption in regard to air ingress events by those who are not familiar with modular HTGR design and with the details of nuclear grade graphite oxidation phenomena is the complete oxidation of all this graphite, with the exothermic heat load this would represent, and the resultant loss of core structural integrity and increased fission product release. In reality the oxidation of graphite occurs only in a thin surface layer at the available oxygen interface surfaces, and the "bulk" graphite inventory is therefore not available for oxidation. The areas that will experience oxidation first include the graphite in the plenums and then the engineered flow paths (fuel coolant channels, control rod channels), as well as unintended bypass flow paths (e.g., in the 2-7 mm gaps that exist between the reflector blocks to allow for graphite expansion).

Evaluations of events involving graphite oxidation show the bottom reflector graphite structures play a "sacrificial" role because this region experiences oxidation first. By removing the oxygen the bottom reflector actually protects the core region for some period of time in the event sequence (see Section 4.3 for more detail). Even if the oxygen eventually reaches the coated fuel particles, a fundamental difference exists between modular HTGR fuel designs and any other nuclear reactor fuel type: the UO$_2$ or UCO fuel is embedded in the form of billions of TRISO coated fuel particles inside a graphite matrix, as shown in Figure 19. In the case of an air or water ingress, the oxidation front will first react with the surrounding matrix graphite before the TRISO particles are reached. The TRISO particles present in the MHTGR core therefore act as individual containers of the fission products that build up during reactor operation.

3.2.2 Oxidant

In the case of overly simplified air ingress analyses, 100% air is sometimes assumed to enter the core through a break in the primary pressure boundary as an enveloping safety case. In reality, the reactor primary system is situated inside a reactor building, where the helium inventory contained in the primary system is vented into the building volume in case of a pressure boundary breach. Instead of 100% air, a mixture of helium and air will then enter the core after the depressurization case, leading to a significant reduction in the available reaction agent inventory. This factor is taken into account in all realistic mechanistic helium-air gas mixture ingress analyses.

An important difference between direct Brayton modular HTGR cycle designs (e.g., the pebble bed PBMR-400) and indirect steam cycles (e.g., the MHTGR) is the increase in the total water inventory for the second type of design. This factor directly influences the amount of oxygen available for interaction

with the core and reflector graphite via a steam ingress accident. Similar to the available graphite surface area, the full water inventory does not participate in the ingress event: of the theoretical 17,000 kg of water present in the 200 MW HTR Module secondary system, only 600 kg of water could actually reach the primary system in the case of multiple steam generator tube ruptures[58].

3.2.3   Heat

The core state at the time of accident initiation determines the temperature distribution and heat source behavior during air ingress events. Accident analysis is usually performed for all initial core states to determine the bounding case. An air ingress event will lead to different results if it occurs when the core is in a cold-shutdown, hot start-up, or full operating power state. Since graphite oxidation kinetics depend on temperature, it makes most sense to examine oxidation events when the reactor has been operating for some time and has reached its equilibrium state.

As shown in Section 2, graphite oxidation kinetics is highly dependent on the graphite temperature. The main heat source during a pressure boundary break is the nuclear decay heat generated by the decay of fission products (see Section 3.3.2.2 for more detail). The decay heat is distributed throughout the core and reflector graphite components via conduction, radiation and convection. For a helium pressure boundary breach that leads to a Depressurized Loss of Forced Coolant (DLOFC) accident, two of the parameters that influence the eventual peak fuel temperatures are the height and radius of the core. A tall, thin modular HTGR core will typically reach lower peak temperatures compared to a shorter, thicker core, since the heat transfer surface area is much larger, and the resistance path to the final heat sink for the inner fuel regions is also shorter.

3.3   Modular HTGR Air Ingress Analysis

As described in the introduction to this section, air ingress events are evaluated as part of the modular HTGR licensing safety case. The accident analysis utilizes a set of postulated initiating events and boundary conditions to simulate the progression and outcome of various air ingress events. A large number of air and water ingress simulation analyses have been performed for graphite moderated systems over a period of more than five decades. A comprehensive literature review of the general graphite oxidation field covering more than 130 sources was performed in 1990[59]. This section, therefore, discusses a few examples of the more recent work performed with modern simulation codes to illustrate how the graphite oxidation kinetics discussed in Section 2 are utilized in accident simulations. Instead of limiting the discussion to a single design, a limited set of results reported for five prismatic and pebble bed designs (Table 2) are included in this section to show the general trend in simulation predictions.

Table 2. Overview of modular HTGR designs discussed in Section 3.

HTGR Design	Description (origin, thermal power, cycle type, fuel geometry)
HTR-PM	China, 250 MW, indirect cycle, pebble bed
HTR Module	Germany, 200 MW, indirect cycle, pebble bed
PBMR-400	South Africa, 400 MW, direct cycle, pebble bed
ANTARES	France, 600 MW, indirect cycle, prismatic
MHTGR	United States, 350 MW, indirect cycle, prismatic

3.3.1   Event Classification

Licensing basis events are classified in three broad categories, depending on the expected occurrence frequency. Events entailing ingress of air involve a breach of the helium pressure boundary and depressurization of the helium coolant. In this section, a few examples are provided from the MHTGR Preliminary Safety Information Document (PSID)[60] to illustrate how an air ingress event can be classified.

3.3.1.1   Normal Operation

This category covers all operational states of the reactor unit (i.e., cold and hot zero power testing, hot intermediate power operation, and hot full power operation). In the absence of air as a source of oxygen, water vapor could still be present during normal operation as a trace-level contaminant in the helium coolant flow, or from outgassing of the graphite during the initial start-up phase, resulting in possible chronic oxidation of the graphite along the helium flow paths. The possibility of chronic oxidation is usually mitigated by design (e.g., a helium purification system (HPS) usually maintains impurity levels within limits, and a reactor shutdown will be required if impurity levels exceeded limits). A conservative calculation of the graphite strength degradation during prolonged exposure to trace amounts of oxygen found that the stress increases in the MHTGR supporting structures remained within the allowable limits, and that no loss of structural integrity would occur[61]. Subsequent work found that the normal operation of the MHTGR would not be impacted by the continued ingress of a maximum expected value of 0.1 ppm steam in the helium coolant[61]. This paper therefore focuses on the *accidental* ingress of air into the reactor primary system as the sources of oxygen that can interact with graphite.

3.3.1.2   Anticipated Events (AE)

An AE is typically expected to occur with a frequency of less than 10-2 per plant year (i.e., once in a plant lifetime). The MHTGR PSID[71] included two "chemical attack" scenarios in the AE category: a small steam generator leak that released 18 kg of water into the primary coolant, and a small breach (<650 mm^2 or 1 in^2) in the helium pressure boundary that causes a helium depressurization lasting about an hour. Both of these events lead to insignificant graphite oxidation and no additional radiological releases, according to analysis results.

3.3.1.3   Design Basis Events (DBE)

Air and water ingress events in the DBE class represent the most serious accident conditions the nuclear reactor designers have to plan for. Although the frequency of these events is very low (10^{-2} - 10^{-4} events per plant year), the consequences could include radioactive releases to the public within the authorized radiological limits. Two specific examples of the graphite oxidation simulation scenarios in the MHTGR DBE category are described below. Similar data sets have been utilized for other pebble and prismatic modular HTGR designs.

- DBE example 1: A moderate steam generator leak of 6 kg/s resulted in a total mass of 272 kg steam entering the reactor vessel over a period of several hours. In the most conservative case, where no core cooling was assumed, only 75 kg steam reacted with a total of 50 kg graphite. The bottom reflector region below the active core experienced most of this mass loss, but it was still limited to less than 0.04% of the total structural mass, while the hottest fuel coolant channel recorded a mass loss of 0.08%. The resulting 0.5% loss of strength in these channels was insignificant when compared to the safety margins of the core.

- DBE example 2: A small break results in a DLOFC and subsequent 100% air ingress over a period of 40 days. (As indicated before, these conservative licensing scenarios do not assume operator intervention during this period.) Displacement of the helium in the reactor vessel with 172 kg air over the first 6 days resulted in a total graphite oxidation fraction of only 0.005%. The decrease in the core temperature in the period between 6-40 days drew an additional 95 kg air into the vessel, oxidizing another 0.003% of the total core graphite inventory. The exothermic chemical reactions added an insignificant 0.12 MWh of heat to the total heat source, compared to the nuclear decay heat contribution of more than 900 MWh over the same period.

3.3.1.4   *Beyond Design Basis Events (BDBE)*

BDBE events are included in safety analysis studies to investigate system performance in very infrequent events (10^{-4} to 5×10^{-7} per plant year) to determine whether the systems behavior and the event consequences would drastically change if the event boundary conditions are modified beyond the DBE assumptions.

3.3.2   Modular HTGR Air and Water Ingress Analysis

3.3.2.1   *Experimental Validation Data*

Progress has been made in recent years regarding the modeling of modular HTGR graphite oxidation during air or water ingress events, mainly due to an improvement in Computational Fluid Dynamics (CFD) tools that led to improved gas flow and temperature prediction capabilities and the availability of experimental data for validation purposes. In general, reactor simulation codes can be verified through comparison with analytic solutions and code-to-code benchmarks and validated by comparison with experimental and operating facilities. Significant uncertainties remain, however, on the direct applicability of these data sets to the validation basis of current modular HTGR simulation codes.. Integral and separate effects experiments, therefore, provide valuable data sets used to verify and validate the graphite oxidation modules in various core simulation codes. A few examples of graphite oxidation validation data sources are provided below, but it should be noted that data from these facilities provided only partial validation of the typical operational envelope of modern modular HTGR designs, and in some cases were highly simplified representations of the accident conditions.

- Schweitzer (Brookhaven National Laboratory): A set of graphite oxidation experiments were performed for the graphite moderated and air cooled BNL reactor in the early 1960s[63]. Several important observations and criteria were determined that are still of great value today, and Schweitzer also produced two seminal summaries on graphite oxidation in 1987 and 1995[56,64].

- SUPERNOVA, KORA, INDEX and THERA (Research Center Jülich): The Research Center Jülich (FZJ) performed several smaller scale experiments on graphite oxidation since the 1980s. The sample sizes typically tested ranged between a few milligrams up to several kilograms, and a variety of reflector blocks, matrix material and nuclear grade graphite types were tested. An example of the typical data produced, in this case for the South African Pebble Bed Modular Reactor (PBMR)[65], is shown in Figure 22. In this example, the oxidation rates of reflector graphite types NBG-10 and NBG-18 are compared for a 100% air environment at 750°C.
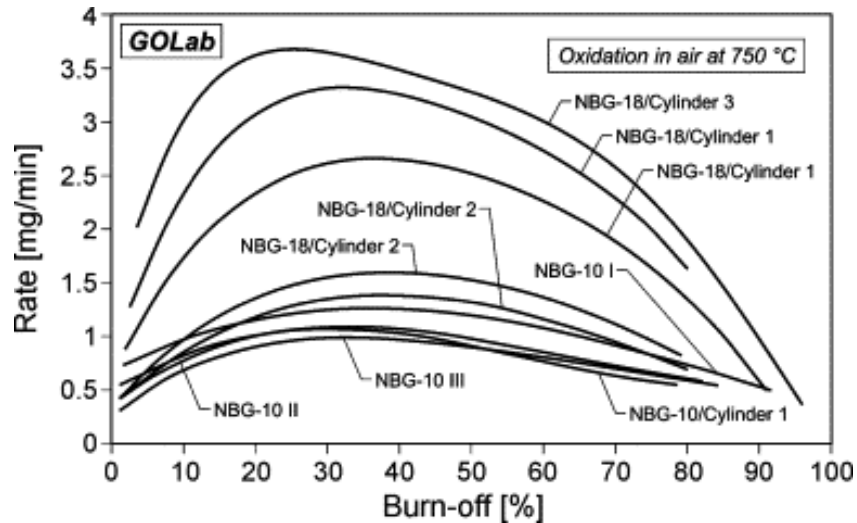
Figure 22. Comparison of NBG-10 and NBG-18 oxidation rates in 100% air at 750°C.

- The NACOK ("Naturzug im Core mit Korrosion") facility at FZJ was a significantly larger experiment (it featured a pebble bed of 5 m height) dedicated to study of graphite oxidation in the natural convection flow regime[66]. The data generated by this facility have been used extensively by several modular HTGR core simulation codes to validate their predictive results (e.g., the analysis of the detailed temperature and flow distributions using the commercial CFD code FLUENT-6[67] and a RELAP5 and GAMMA code comparison study[68]).

- Reverse U-shaped tube experiments (JAERI)[69]: A relatively simple reverse U-tube experimental setup was used by Takeda and Hishida to study the combined phenomena of molecular diffusion phenomena and the natural convection of a gas mixture during graphite oxidation. The influential data set from this complex combination of phenomena were used extensively by several modular HTGR core simulation codes for validation of their oxidation and gas mixing routines[68,69].

Although code development and improvements will continue, the primary phenomena of graphite oxidation are reasonably well understood, and a sufficient validation basis of bulk graphite oxidation exists to provide a degree of fidelity and assurance that air ingress events can be assessed with a number of reactor simulation tools. The main graphite oxidation core simulation challenge currently remaining are the high-fidelity modeling of the gas mixture flows, especially during low velocity natural convection events (e.g., Pressurized Loss of Cooling event).The importance of these two variables on large-scale graphite oxidation simulation is shown in the next two sections.

3.3.2.2   Heat Source Distribution: Graphite and Gas Temperatures

As indicated in Section 2, the temperature of graphite plays a critical role in oxidation kinetics. The solid and gas temperature of the active fuel core and reflector graphite structures are determined by the spatial heat source distribution and the net effect of heat removal mechanism. During normal operation, the heat source in modular HTGRs consists of the instantaneous fission energy and the decay heat from short and long lived fission products. When the core enters a sub-critical state (e.g., when a reactor trip is performed), the only heat source remaining is the decay of short- and long-lived fission products. The fission product decay heat term is nominally around 6% of the total thermal power at the beginning of the depressurization event (e.g., 21 MW for the MHTGR-350[66]), where after it decreases to less than 1%

43

within a few hours. Most of this heat is deposited in the nuclear fuel kernels and surrounding graphite material, but approximately 6% of the total decay heat is deposited directly in the reflector structures via fast neutron and gamma radiation energy deposition. This "non-local" reflector heating effect has been shown[70] to be important in modular HTGR reactor simulations, since this phenomenon increases the inner and outer reflector temperatures significantly during DLOFC accidents.

In this section, a few typical temperature profile examples from different modular HTGR designs are presented (the examples are intentionally selected from various sources to generalize the discussion). An example of the predicted graphite temperature distribution of the 250 MWt HTR-PM core during normal operation[71] is shown in Figure 23. The highest temperatures are reached in the bottom regions of the core (inside the red rectangle) due to the downwards forced helium flow (shown with black arrows). This region of higher temperatures also extends into the bottom reflector blocks. In the case of a helium pressure boundary breach below the core, the higher temperatures in this region result in a higher rate of oxidization of these graphite components compared to the active core region. The next section shows that the bottom reflector acts as a protective layer to the active fuel region in these cases by converting molecular oxygen into less reactive species (CO_2 or CO). For a breach above the core, the heavier 100% air will reach the active core region faster, but from Figure 23 the top region of the core is clearly much cooler than the bottom half, and the subsequent graphite oxidation rate is limited by the lower temperatures.

The normal operation temperature distribution shown in Figure 23 is, however, only the starting condition for the changes that occur during the DLOFC event. As soon as a break occurs, the primary system depressurizes within a few seconds (for very low frequency breaches larger than 20 cm in diameter) or over a period of hours for small breaches (less than 2 mm diameter). Over the subsequent 30-50 hours, the mismatch between the decay heat production rate and the heat removal rate at the reactor vessel boundary results in the fuel temperature rising, as shown in Figure 24 for the 250 MW HTR-Module design[72]. The data shown here was created for a DLOFC uncertainty study that consisted of running 200 separate DLOFC calculations with the PEBBED code, each of which sampled different input values of eight input parameters. The rise in graphite temperature reverses as soon as the decay heat production equals the heat removal rate at the reactor vessel boundary. This increase in graphite temperatures acts as the main driver for the increase in the graphite oxidation rate, as discussed in the next section.
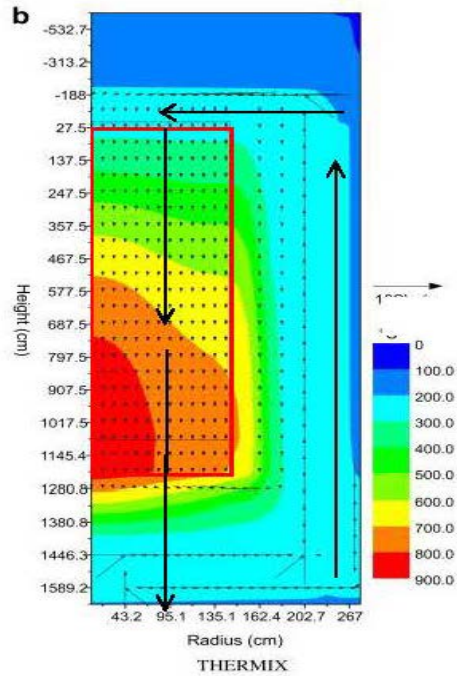
Figure 23. THERMIX graphite normal operation temperature profile (°C) of the HTR-PM[69].
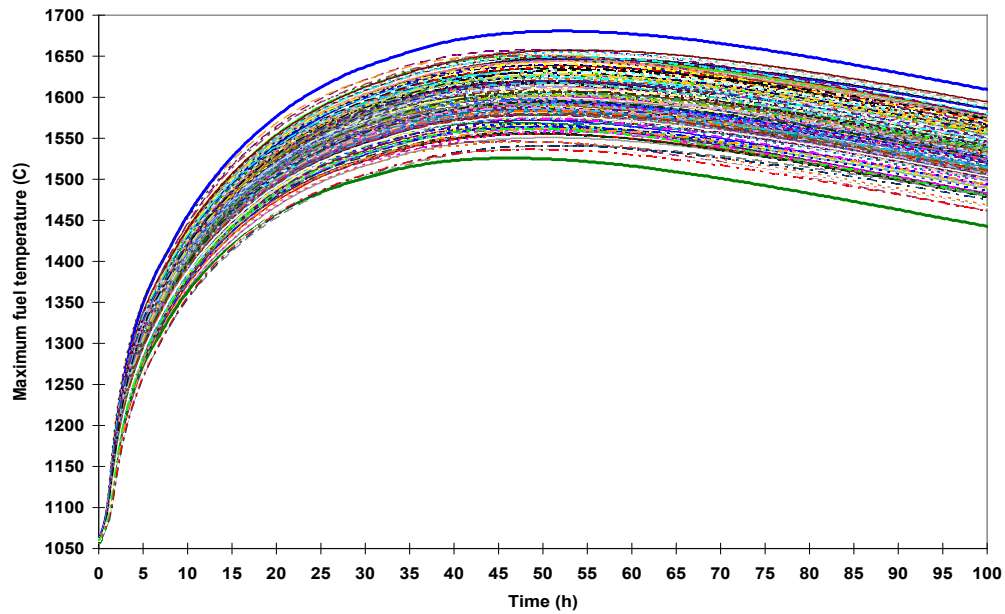
Figure 24. HTR-Module DLOFC maximum fuel temperature (°C) vs. time for 200 uncertainty variation cases[70].

The data shown in Figure 24 only represents a small volume of graphite in the core. This is illustrated in Figure 25, where the volumetric distribution of the fuel temperature is shown for three model variations at the time point when the peak DLOFC fuel temperatures are reached (e.g., around 50 h in Figure 24). (The fuel and graphite temperatures are identical at this point in time). As illustrated in Figure 25, less

45

than 5% of the graphite in the HTR-Module core reaches temperatures between 1400-1600°C, (i.e., 95% of the UO_2 fuel and its associated graphite temperatures were lower than 1400°C.) More than 60% of the graphite temperatures were in fact lower than 1000°C at this time point. Since the graphite temperature is one of the main drivers that determine the bulk oxidation rate, the temperature vs. volume distribution is an important factor in core simulation studies. As a second example, the spatial variance in the core region graphite temperatures is further illustrated in Figure 26 by the temperature distribution at 100 h into the PBMR-400 DLOFC event[73]. This temperature profile clearly shows the upward movement of the peak fuel temperature, which is now located in a small region at an axial height of 400 cm. This change is caused by the termination of the downward helium gas flow and the characteristic decay heat distribution in the PBMR-400 core.
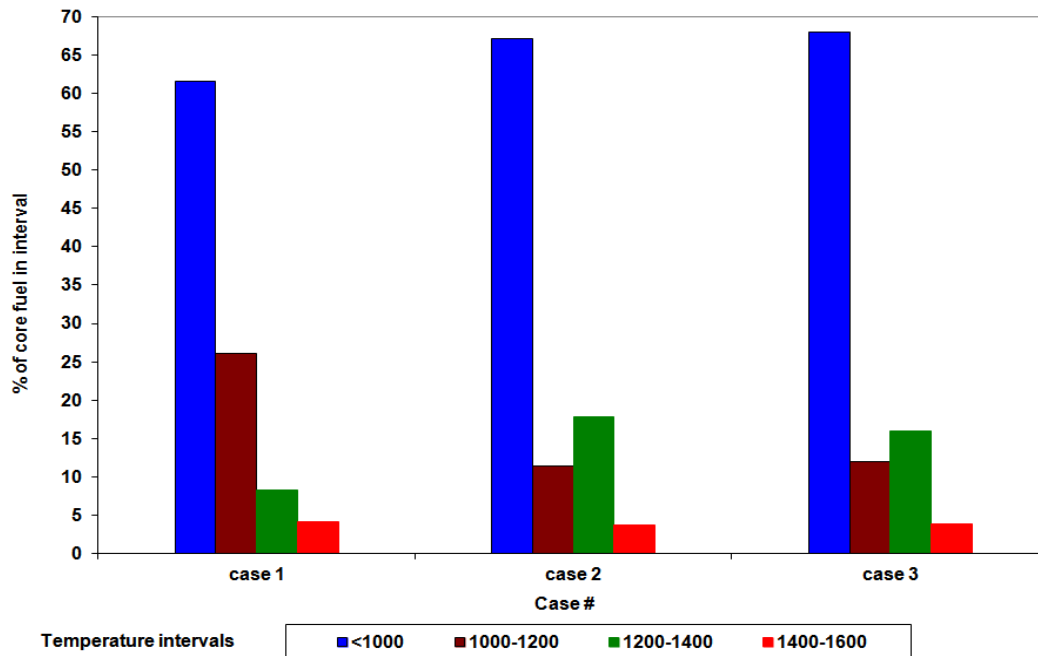
Figure 25. Maximum graphite temperature volumetric distribution for three HTR-Module DLOFC cases at the time of peak fuel temperatures (% of total fuel volume)[68].
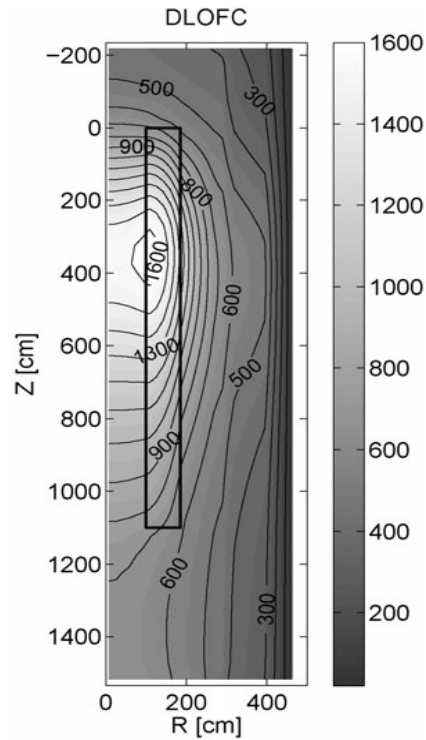
Figure 26. DALTON-THERMIX graphite temperature profile (°C) of the PBMR-400 at 100 h[71].

    The change in graphite temperatures in the bottom reflector is quite different from the core region. The data presented in Figure 27 for four variations on an air ingress scenario show[74] the bottom reflector starts to cool down immediately after a DLOFC event occurs, in contrast to the increase in fuel temperatures, Figure 28. The ingress delay times are a function of the size of the helium pressure boundary breach: a small breach will take up to 72 hours to depressurize the core sufficiently for air ingress to commence, while a large breach can lead to air ingress within a few seconds. The variation in the time of air ingress results in different rates of temperature decrease due to the exothermic heat generated by the oxidation reactions. (For this scenario, 22% oxygen was assumed to enter the break location).

Figure 27. DLOFC bottom graphite temperature (°C) for the PBMR-400 for four air ingress start time variations[72].

Figure 28. DLOFC maximum fuel temperature (°C) for the PBMR-400 for four air ingress start time variations[72].

3.3.2.3   Oxidant and Product Distributions

The parameters of interest for graphite oxidation analyses are the graphite oxidation rate and the total mass of graphite oxidized. The sample results presented in this section are the combined outcome when all the parameters discussed in Sections 2 and 3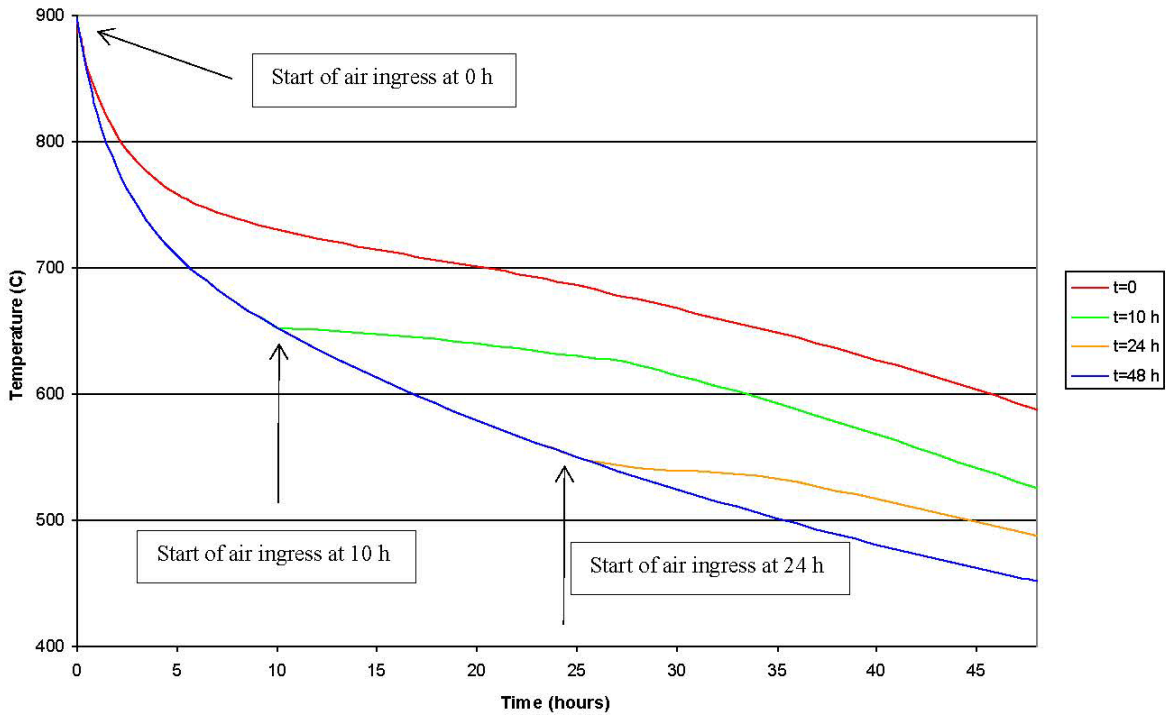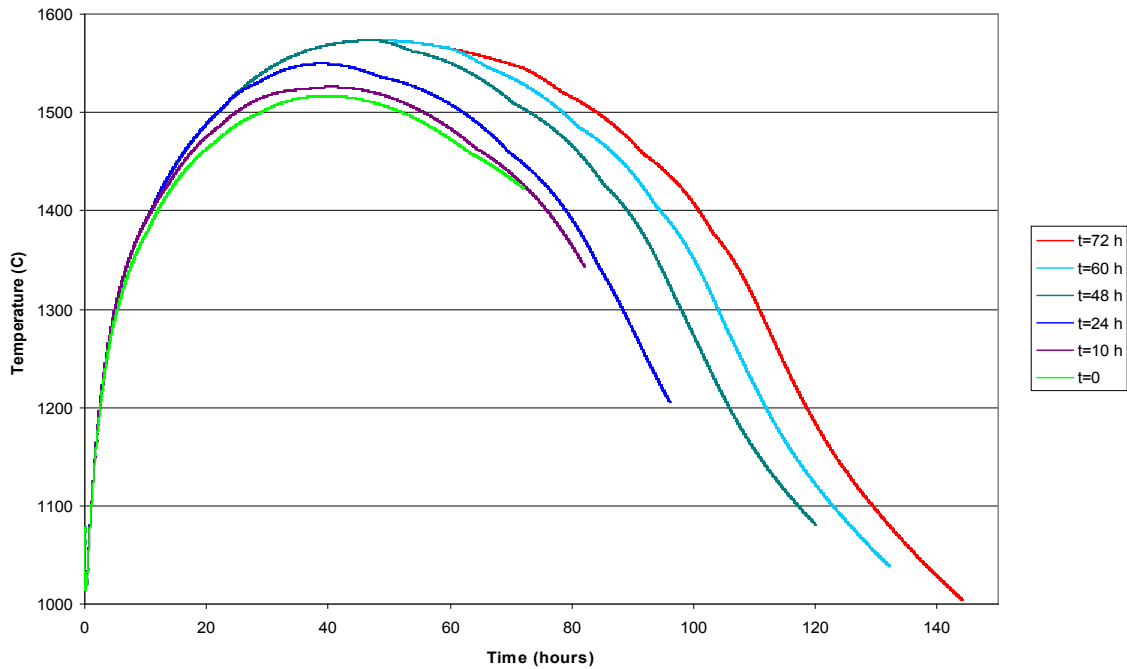 are addressed. A typical air ingress simulation consists of solving the parameters listed below in a mesh-by-mesh iterative or simultaneous coupled scheme.

- *Thermal fluids*: The thermal fluid module provides the spatially dependent velocities, temperature and other properties of all gasses (helium, oxygen and product gas) and solids (graphite, nuclear fuel).

- *Heat source*: The neutronics module calculates the total heat source from fission product decay and fission processes, and in the case of water ingress scenarios, also the increase in fission power. The exothermic heat source generated by the oxidation processes are also added to the homogenized solid material mesh.

- *Chemical interactions*: The chemistry module of a coupled core simulator combines the graphite oxidation kinetics (the equation set in Section 2.1.1) with reaction energy requirements, available gas mixture composition, graphite temperatures, and validated correlations for graphite oxidation rates to determine an effective graphite oxidation rate in a specific spatial mesh location. The converged solution in the current location is then used as input for the next downstream mesh.

The outcomes of this process are spatially dependent "maps" of graphite temperatures (a few examples were shown in the previous section), oxidation product concentrations (e.g., CO/CO_2 molar densities) and graphite oxidation rates in all affected regions. A typical graphite oxidation distribution is presented in Figure 29 for the PBMR-400 design in the case of a hypothetical bottom break in the pressure boundary[88]. (The mass of graphite oxidized is shown here in kilogram unit. The oxygen content of air was assumed to be 22%. As a matter of perspective, it should be kept in mind that the core and reflectors contain more than 700 *tons* of graphite in total).
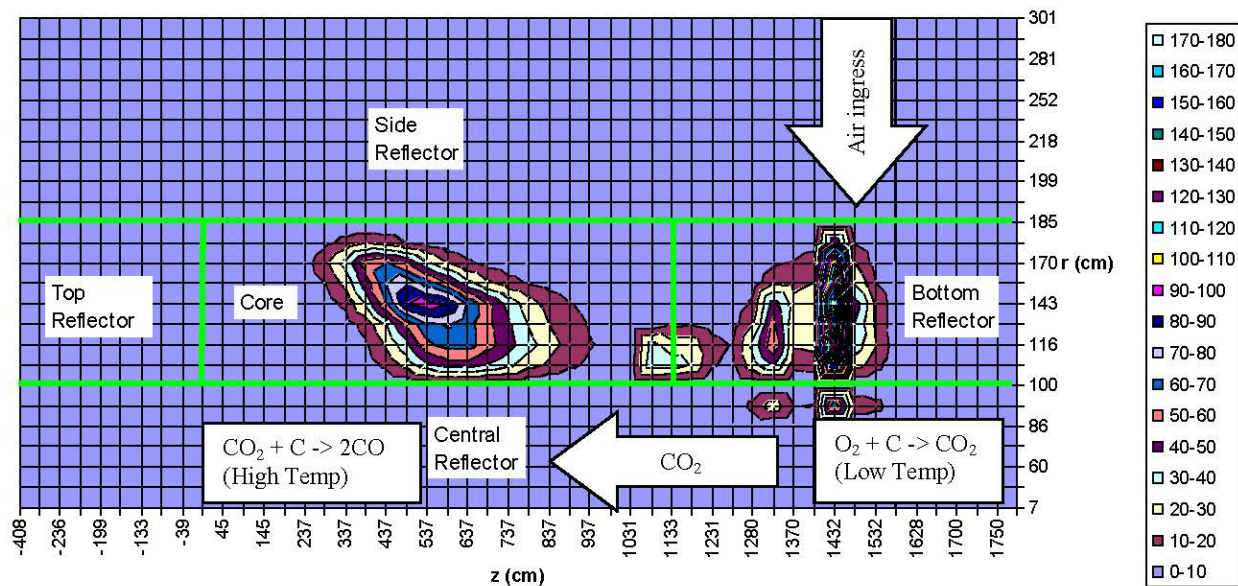

Figure 29. Spatial distribution of graphite oxidized (kg) in the PBMR-400 at 72 h: air ingress at bottom break location at 0.208 kg/s[72].

In Figure 29, the top of the core is located at z=90 cm, and the air ingress location is in the bottom inlet plenum at z=1432 cm. Natural convection forces the gas flow upwards through the coolant channels in the core, and down through the helium riser channels in the side reflector, so that a convection loop is formed that effectively transports heat and gas products through the core at low flow rates (a few grams per second). The contour map shows that the bottom reflector graphite (up to 180 kg in certain regions) and the center region of the active fuel core (up to 100 kg) experienced the most oxidation over a period of 72 hours and at a sustained air ingress rate of 0.208 kg/s. It is important to stress the very limited extent of graphite oxidation that these values represent. Figure 32 shows that the total fraction of graphite oxidized during the event is less than 1.5% of the total graphite inventory.

An important difference between the two regions is the dominant oxidation reactions: in the bottom reflector graphite region the oxygen in air reacts with graphite mainly via the conversion to CO_2 (Equation 2 in Section 2), whereas the conversion to CO via Equations 3 and 4 dominates in the center core region. The oxygen content of the inlet air decreases as it flows upwards through the core, and since the conversion to CO_2 is a stable product, further reactions are limited. From an oxygen supply point of view, there is therefore much less O_2 available in the upper regions of the core. Any remaining O_2 will still react with graphite, but begins to favor Equation 3 to form CO as the temperature increases. Since the CO_2 gas is also transported upwards into the active fuel region, at these very high temperatures, this inventory can be converted into CO via the CO_2 reaction from Equation 4, $CO_2 + C \rightarrow 2CO$. The increase in graphite temperature from the bottom graphite structure into the core region is significant (up to 1000°C). This temperature differential acts as the primary driver for the natural convection of all the gasses, as well as the increase in the graphite oxidation reaction rate.

Two further examples are provided here to illustrate the highly spatial-dependent nature of graphite oxidation and the effect of a change in temperature and boundary conditions on the progression of a graphite oxidation event. The first example is of steam ingress into the same bottom inlet region after a steam generator tube rupture. From the graphite oxidation distribution 72 hours into the event, Figure 29, the location of the primary oxidation region can be seen significantly lower in the bottom region of core,. This is caused by a significant graphite temperature difference that exists between the air and steam ingress cases, because the water ingress event assumed continued functioning of the PBMR Core Conditioning System (CCS) that rapidly cooled down the core after the start of the steam ingress phase.

The total mass of graphite that reacted with the steam is also an order of magnitude less than in the air ingress case (i.e., if the legends are compared). For comparison, the steam ingress rate was selected to be identical to the air ingress rate in the previous example. In this case, the combination of temperature profile and gaseous species (H, O_2, and C) available to react in the bottom regions of the core results in no graphite oxidation in the upper core regions, in contrast to the calculated distribution in Figure 30. This example illustrates the "buffer" effect of the bottom reflector in case of a breach below the core (i.e., the oxidation is in a graphite region that does not lead to the release of fission products from the nuclear fuel region). The consequences of this steam ingress scenario will therefore be much less severe than those of the first air ingress example.

Figure 30. Spatial distribution of graphite oxidized (kg) in the PBMR-400 at 72 h: steam ingress at bottom break location at 0.277 kg/s[72].

The final example of a graphite oxidation distribution is shown in Figure 31. In this scenario, a small breach is assumed for one of the lines connected to the top inlet plenum. In spite of a very low air ingress rate (9 g/s), this accident leads to the oxidation of a larger mass of graphite than the steam ingress example. It is still significantly lower than first air ingress example, and the main reason is the lower graphite temperatures in the upper core region. A second area of oxidation can be seen in the lower regions of the core, as air is transported downward through an air-helium density differential in combination with natural convection.
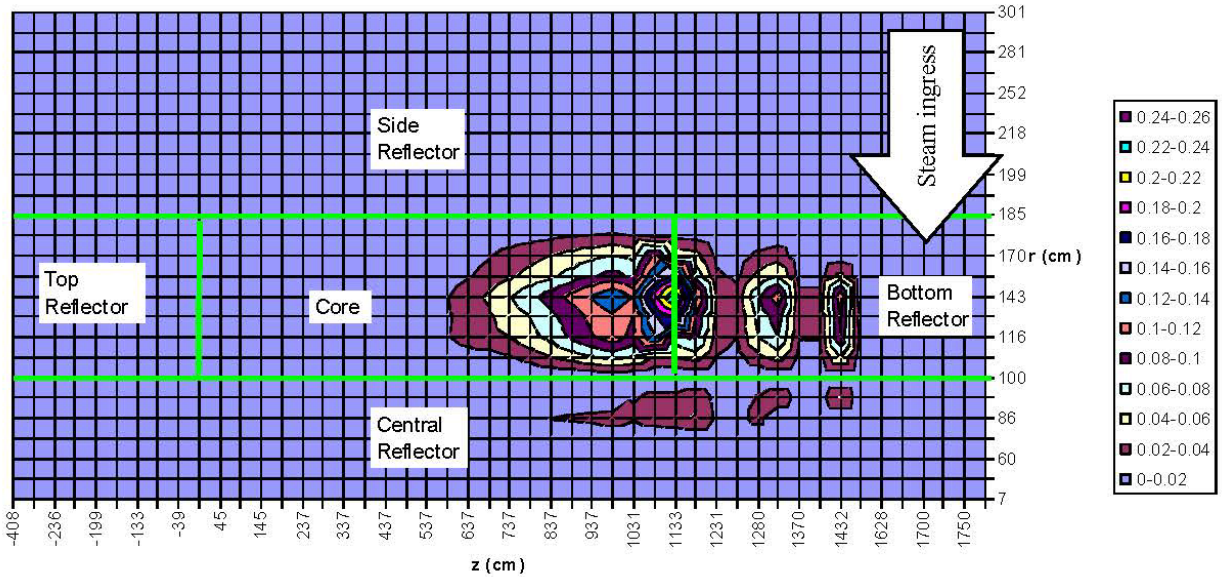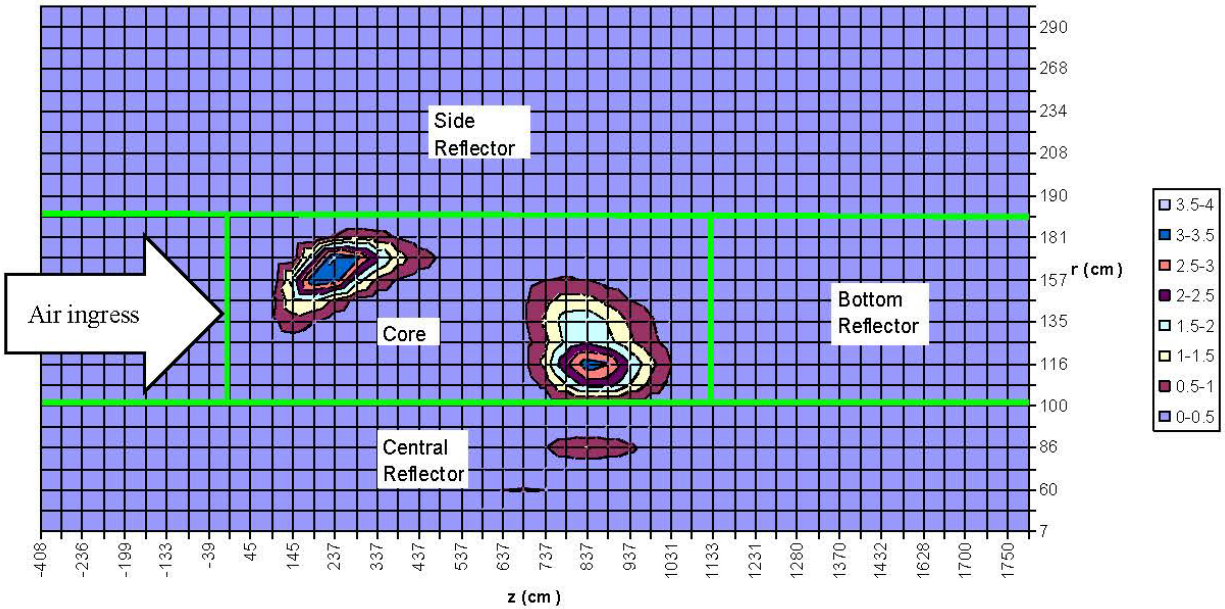
Figure 31. Spatial distribution of graphite oxidized (kg) in the PBMR-400 at 72 h: air ingress at top break location at 0.009 kg/s[72].

The combined effect of a decreasing decay heat source and the spatial variation in the graphite structure temperatures on graphite oxidation is illustrated in Figure 32. For this study, six air ingress variations of the PBMR-400 large inlet/outlet pipe break were performed with the start of air ingress delayed by 0, 10, 24, 48, 60, and 72 hours[88]. The corresponding graphite temperature data for this study was presented in Figure 23. These delay times are a function of the size of the breach, as mentioned previously, since air cannot ingress into the core before the outflow of helium through the break location is completed. Figure 22 shows that the total graphite oxidation of all bottom reflector graphite reaches approximately 1% of the total bottom reflector mass when the air ingress starts immediately, but only 0.2% when the ingress is delayed for 3 days. The longer delay times leads to a decrease in the bottom reflector graphite temperature, which is sufficient to limit the total rate of oxidation in this region. The data in Figure 32 also show that the oxidation rates decrease significantly when the bottom reflector graphite temperature is too low to sustain significant oxidation – beyond these time points, oxidation is limited to the high temperature fuel region, as can be seen when Figure 32 and Figure 33 are compared. The total bottom reflector graphite mass oxidized during this event is only a fraction of its total mass (1%) and is well within the safety margins of structural damage.

The graphite oxidation in the active core region (Figure 33) shows trends similar to the bottom reflector oxidation progression. Since the fuel is much hotter than the bottom reflector for a longer time (Figure 28), oxidation continues for a longer period and eventually involves a larger fraction of the core graphite inventory (up to 3.2% at the point when the calculation was terminated). Only a very small volume of the total core region graphite inventory is involved in this process. It can also be seen how critical the starting point of the ingress is to the graphite oxidation rate: the decrease in fuel temperatures for the longer delay time transients (e.g., starting at 72 h) led to a decrease in the oxidation rate, whereas the shorter delay time cases produced a more sustained oxidation rate for a longer period.
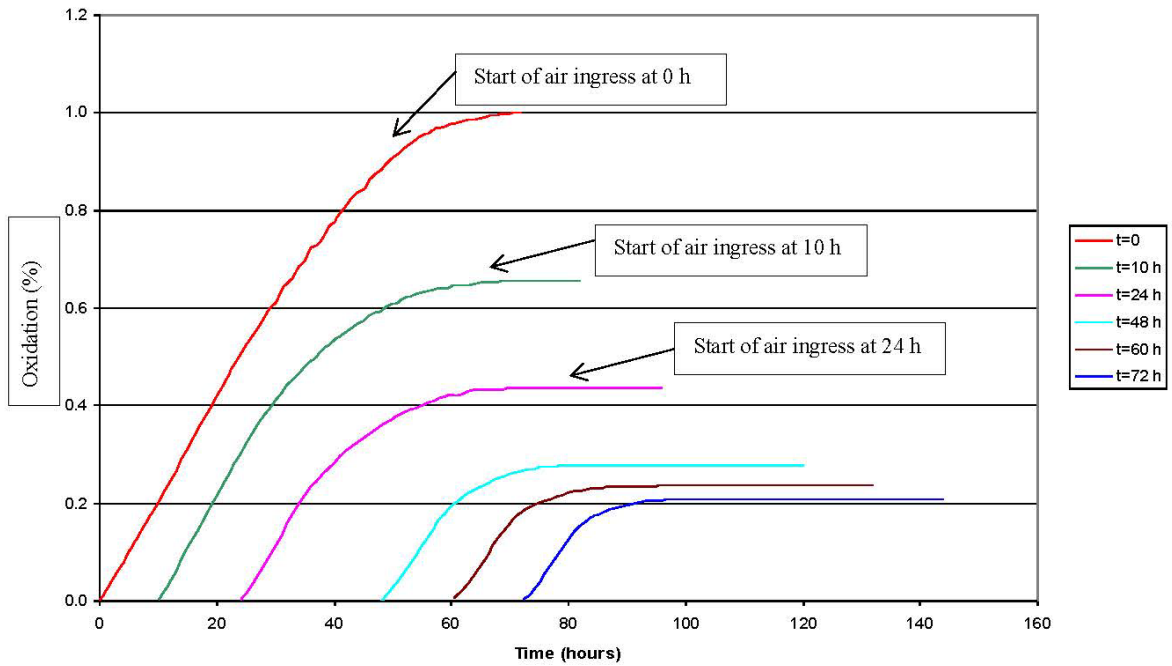
52

Figure 32. Graphite oxidation (%) in the bottom reflector vs. time for 6 air ingress start time variations[72].
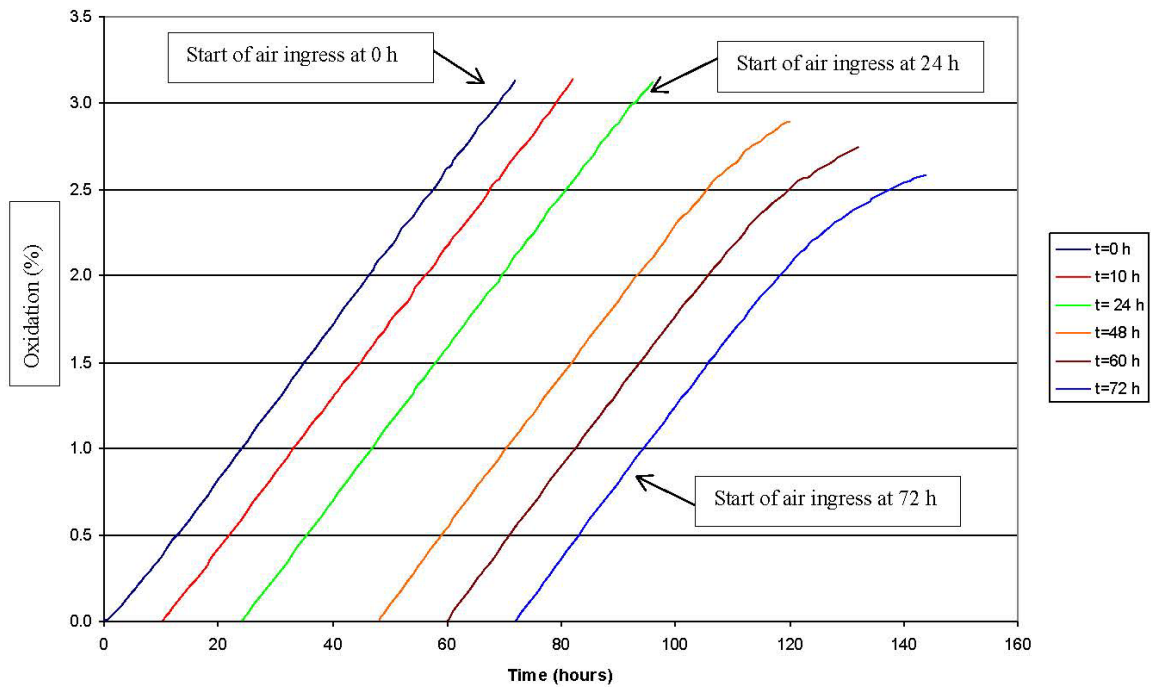

Figure 33. Graphite oxidation (%) in the active core region vs. time for 6 air ingress start time variations[72].

Although the focus of this paper is primarily on graphite oxidation in a generic sense, not all regions in the core are equally important in terms of the consequences of events entailing graphite oxidation. If the graphite oxidation is limited to the inner or outer reflector blocks, very few structural issues or radiological fission product releases can be expected. In these regions, the main concern would be to assess whether the control rods can still be safely inserted to ensure core shutdown after an ingress event. Oxidation of the bottom support structures likewise carries no radiological risk, but the structural integrity of the graphite columns needs to be assessed for an air ingress event to assess the safety margins. The main licensing and regulatory concern with graphite oxidation events is focused on the release of fission products from the active fuel region during and after ingress events.

Estimates of the active fuel region exposure during large break air ingress events were calculated by the ORNL code GRSAC[75] for both pebble bed and prismatic modular HTGR designs. It was found that for the pebble bed design 992 kg graphite was oxidized in the bottom fuelled region of the core, which represents an average loss of 25% of a typical fuel pebble's 0.5 cm thick outer graphite layer. On average, 75% of the protective outer graphite layer still remained. The ORNL study further calculated that for the 600 MW prismatic MHTGR-600 design, the graphite loss in the active fuel region was 1,211 kg (~3%) due to the lower flow resistance in the prismatic fuel blocks. (This is in agreement with the TINTE calculations presented in the preceding paragraphs).

A useful parameter in the case of fuel particle exposure would be an estimate on how long it would take for the oxidation front to reach the first particle location. A study performed on the AREVA 600 MW prismatic ANTARES design[76] concluded the graphite oxidation front would reach the first fuel kernels within 60-70 hours after the start of the air ingress event. It was, however, pointed out that even if oxygen reaches a coated fuel particle, fission products will remain confined as the silicon carbide coating has a very limited reaction with oxygen even at elevated temperatures. The axial temperature and graphite oxidation profiles are shown for ANTARES in Figure 34 and Figure 35. The change from the normal operation temperature profile (in blue) to the DLOFC profile without air ingress (purple) is apparent from Figure 34, as well as the large axial profile change that occurs between the 0.05 kg/s and 0.6 kg/s air ingress curves. The effect of this temperature difference between the two cases is shown in Figure 35, where the air ingress case at 0.05 kg/s resulted in a sharply defined oxidation region in the bottom of the core (black line). The AREVA study used a unit of Mol/m^2 to quantify graphite oxidation; where $1,000 \ Mol/m2 = 1.2 \ g/cm_2$. The two higher ingress flow rates did not change this axial profile significantly, but the higher sustained air flow rates did oxidize a larger volume of the fuel matrix graphite in the upper areas of the core.

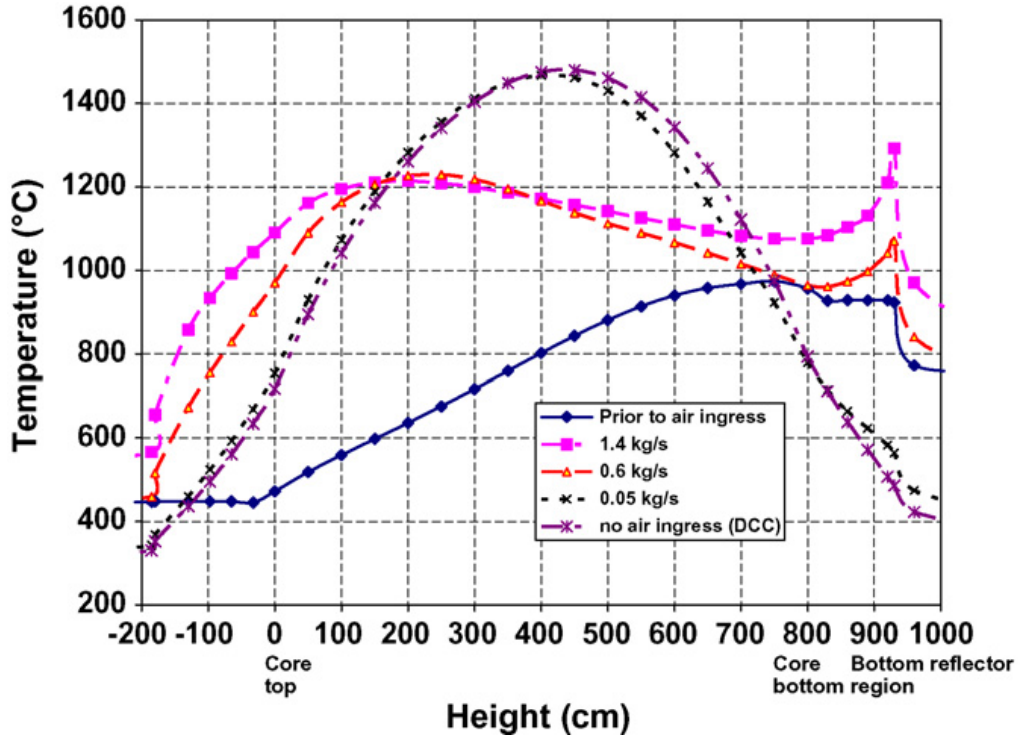Figure 34. Axial temperature (°C) distribution in the ANTARES reactor at 70 h for various air flow rates[74].

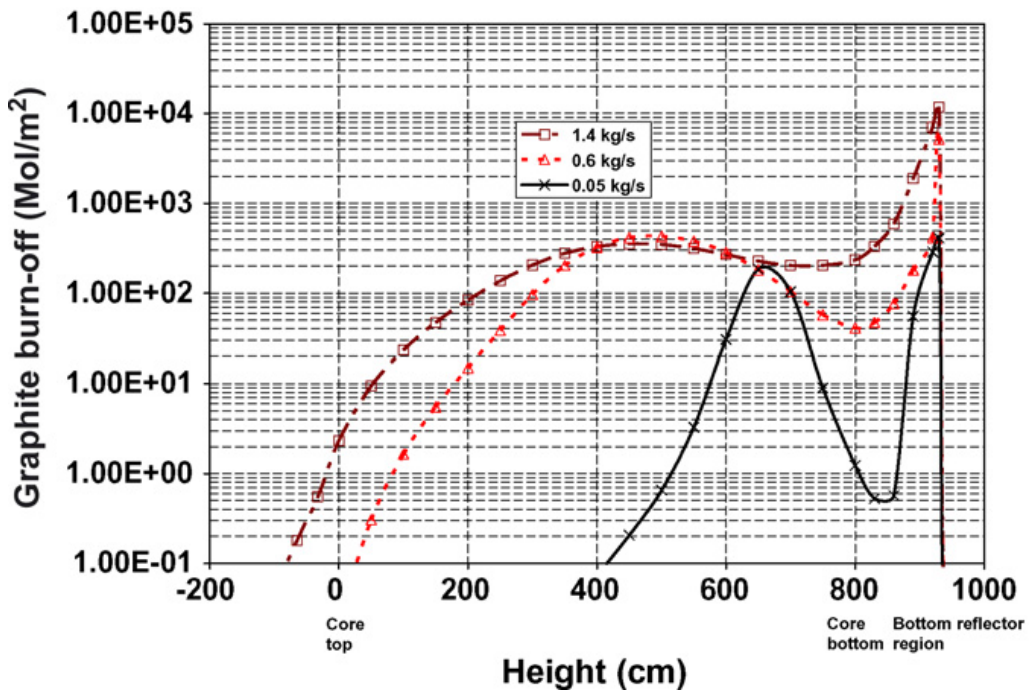

Figure 35. Axial graphite oxidation distribution (Mol/m^2) in the ANTARES reactor at 70 h for various air flow rates[74]. (1000 Mol/m^2 = 1.2 g/cm^2)

Several examples of graphite oxidation simulations performed in the past for various modular HTGR designs were presented in this section. In all cases, the amount of graphite oxidized was limited to a small fraction of the total mass (less than 1% in the bottom reflector region, and less than 3.5% in the core region). All of these cases assumed 100% air entering the break locations, and in some cases a very low frequency pressure boundary break event was also simulated as a demonstration of a bounding event. The protective role of the bottom graphite structures during the more extreme bottom helium pressure boundary breach scenarios was also highlighted.

The sustained presence of an oxygen source and sufficiently high graphite temperatures were shown to be critical requirements of the oxidation propagation – as soon as one of these requirements decreased, oxidation was terminated. Self-sustained oxidation of graphite is not predicted by any of the reactor simulation tools utilized in reactor licensing, since the decay heat is a decreasing source and the oxygen source is always limited. The concept of graphite "fire" defined in Section 1 as self-sustained oxidation of graphite, does therefore not apply to these scenarios.

Nevertheless, despite the multiple physical barriers preventing graphite combustion, significant oxidation of graphite is possible if it is exposed to sufficient quantities of oxygen and external heat sources. Unwarranted assumptions and contradictory language used to explain the two most dramatic examples of large scale accidental graphite oxidation have contributed to common misconceptions about the role played by graphite during an accident. The Windscale and Chernobyl accidents are discussed in Appendix A in the context of the arguments presented in Sections 2 and 3.

4. CONCLUSIONS

Numerous studies have shown self-sustained oxidation or burning of nuclear grade graphite is not possible[56,77]. Self-sustained oxidation is physically impossible in nuclear grade graphite due to the reduced reaction kinetics from the limited number of RSA sites within a graphite crystal structure, the very low oxygen diffusion rate to the RSA sites, and the small volume of graphite available for chemical reaction due to limited oxygen penetration into the interior microstructure of graphite. The oxidation rate is limited even at the atomic crystallite scale since only edge sites along the outer surface of crystallites are reactive and oxygen cannot diffuse and react with carbon atoms inside the graphite crystal structure. The oxidation rate is further reduced by the significant limitations of oxygen diffusion into the graphite microstructure at to the available RSA sites. Thus, few available reactive sites and severely limited oxygen available for the chemical reaction naturally arrest any self-sustained oxidation reactions in graphite.

Catalytic impurities within the graphite microstructure and high temperatures from the nuclear fuel can potentially accelerate the oxidation rate of graphite, but these are not enough to sustain the chemical chain reaction needed for self-sustained oxidation. Further, nuclear grade graphite is purified before use minimizing the amount of non-carbon trace elements within nuclear graphite. Low temperature irradiation damage to the graphite structure resulting in Wigner stored energy is minimized by the high temperatures of current power reactors (> 250°C operating temperatures). Only at extremely high dose levels (close to the end of service for nuclear components) where irradiation damage begins to produce porosity within the graphite microstructure could irradiation damage begin to increase the oxidation rate of graphite. However, while the oxidation may be increased, the conditions for self-sustained oxidation will remain unachievable even for highly irradiated graphite since irradiation damage manifests itself within the interior of crystallites which are not accessible to the oxygen.

Significant oxidation of graphite is possible given certain conditions inside a reactor (high core temperatures and a continuous supply of air). However, the engineered design of a nuclear graphite core results in an oxygen-starved environment surrounding the majority of the components. This severely limits any oxygen available for diffusion into the graphite components and significantly reduces oxidation of the total core. Further, the oxidation product materials (CO and CO_2) will generally displace the available air in the reactor, effectively halting the oxidation reaction inside the reactor vessel itself. Any oxygen that does reach the hot core during an air or steam ingress accident will still have limited reactivity due to the material and kinetic chemical reaction constraints discussed previously (limited RSA sites, limited oxygen diffusion, and minimal catalytic impurities accelerating oxidation).

Extensive accident simulations all predict limited damage within allowable tolerances to the fuel and reflector graphite structures, which leads to the conclusion that a core collapse during these events is highly unlikely. The large thermal heat capacity of graphite and the protective role of the bottom and top reflector structures have also been shown for several accident scenarios to limit the availability of oxygen in the active fuel region and to limit any possible damage to the fuel, which is the primary function of the graphite during an accident event.

Physical factors prevent nuclear graphite from achieving self-sustained oxidation for all conditions, either normal or accident operations. Graphite fires, graphite component burning, and other self-sustained oxidation events are not possible. While oxidation can and does occur during an air ingress accident, graphite material properties and engineering barriers limit the oxidation of graphite core components and the nuclear fuel contained within the core. These inherent properties of graphite within a modular HTGR provide significant protection to the fuel during all operating conditions, especially air ingress accident conditions.

5.   REFERENCES

1. Moormann R., Phenomenology of Graphite Burning in Air Ingress Accidents of HTRs, Science and Technology of Nuclear Installations 2011, article ID 589747.

2. H. Kouts, "The Chernobyl Accident", BNL-52033 UC-80 (General Reactor Technology TIC-4500), Lecture number 227, September 24, 1986

3. ASTM D7219, Standard Specification for Isotropic and Near-isotropic Nuclear Graphites

4. NFPA 10, Standard for Portable Fire Extinguishers, National Fire Protection Association, 2013 Edition.

5. Walker, P. L., F. Rusinko, and L. G. Austin, Gas Reactions of Carbon, Advances in Catalysis, Vol. 11, 1958, pp. 133-221.

6. Propp, W. A. Graphite Oxidation Thermodynamics/Reactions, DOE/SNF/REP-018, September 1998.

7. Clark, T. J., R. E. Woodley, D. R. deHalas, Gas-Graphite Systems, Gas-Graphite Systems, in: R. E. Nightingale (Ed.), Nuclear Graphite, Academic Press, New York, 1962, p. 387-444.

8. CRC Handbook of Chemistry and Physics, Haynes, W. M., Editor-In-Chief, 95th Edition, Internet Version 2015, http://www.hbcpnetbase.com/, 2014-2015.

9. Cristian Contescu et al., "Graphite oxidation studies at Oak Ridge National Laboratory", presented at VHTR R&D FY12 Technical Review Meeting, Salt Lake City, Utah, May 22-24, 2012

10. Cullis, C.F. and J. G. Yates, Reaction of carbon with nitrogen, Vol. 60, Transactions of the Faraday Society, 1964, pp. 141-148. DOI: 10.1039/TF9646000141.

11. Kühn, K., Hinssen, H.-K, Moormann, R., Behaviour of C-based materials in contact to oxidising gases, Proceedings of the International Congress on Advances in Nuclear Power Plants (ICAPP 03), Cordoba, Spain, 4 May – 7 May 2003

12. Wichner, Robert P., Timothy D. Burchell, and Cristian I Contescu, Penetration depth and transient oxidation of graphite by oxygen and water vapor, Journal of Nuclear Materials, Vol 393, 2009, pp. 518-521

13. Walker Jr. P. L. Carbon: An old but new material revisited. Carbon 1990; 28: 261-279.

14. Thomas J. M. Reactivity of Carbon: Some current problems and trends. Carbon 1970; 8: 413-421.

15. Walker Jr. P. L., Taylor T. L., Ranish J. M. An update on the graphite-oxygen reaction. Carbon 1991; 29:411-421.

16. Radovic L. R. Carbon and Graphite Reactivity. In: Buschow K.H.J., Cahn R. W., Flemings M. C., Ilschner B., Kramer E. J., Mahajan S. Editors. Encyclopedia of Materials: Science and Technology, New York; Elsevier; 2001.

17. Laine N.R. A mass spectrometric study of the graphite-oxygen reaction-27 years later. Carbon 1991; 29(6):729-733.

18. Radovic L. R., Active Sites in Graphene and the Mechansim of CO_2 Formation in Carbon Oxidation. J AM CHEM SOC 2009; 131: 17166-17175.

19. Radovic L. R., Silva-Villalobos A. F., Silva-tapia A. B., Vallejos-Burgos F., On the mechanism of nascent site deactivation in graphene. Carbon 2011; 49: 3471-3487.

20. Silva-Tapia A. B., García-Carmona X., Radovic L. R. Similarities and differences in O_2 chemisorption on graphenenanoribbon vs. carbon nanotube. Carbon 2012; 50: 1152-1162.

21. Kane J. J., Karthik K., Ubic R., Windes W. E., Butt D. P.. An oxygen transfer model for high purity graphite oxidation. Carbon 2013; 59: 46-64.

22. Back M. H. Comment on an update on the graphite-oxygen reaction. Carbon 1991; 29:1290-1.

23. Montoya A., Mondragón F., Truong T. N. First-principles kinetics of CO desorption from oxygen species on carbonaceous surface. J. Phys. Chem. A 2002; 106: 4236-4239.

24. Chen S. G., Yang R. T., Kapeteijn F., Moulihn J. A. A new surface oxygen complex on carbon: Toward a unified mechanism for carbon gasification reactions. Ind Eng Chem Res 1993; 32: 2835-2840.

25. Radovic L. R., Suarez A., Vallejos-Burgos F., Sofo J. O. Oxygen migration on the graphene surface. 2. Thermochemistry of basal-plane diffusion (hopping). Carbon 2011; 49(13): 4226-4238.

26. Radovic L. R., Silva-Tapia AB, Vallejos-Burgos F. Oxygen migration on the graphene surface. 1. Origin of epoxide groups. Carbon 2011; 49(11): 4218-4225.

27. Sánchez A., Mondragón F. Role of the epoxy group in the heterogeneous CO_2 evolution in carbon oxidation reactions. J. Phys. Chem. C 2007; 111: 612-617.

28. Orrego J. F., Zapata F., Truong T. N., Mondragón F. Heterogeneous CO_2 evolution from oxidation of aromatic carbon based materials. J. Phys. Chem. A 2009; 113: 8415-8420.

29. Radovic et. al., The mechanism of CO_2 chemisorption on zigzag carbon active sites: A computational chemistry study, Carbon 43 (2005) 907–915

30. E. T. Turkdogan, et. al., "Effect of carbon monoxide on the rate of oxidation of charcoal, graphite and coke in carbon dioxide", Carbon 1970, Vol. 8, pp. 39-53

31. R. E. Nightingale (Ed.), Nuclear Graphite, Academic Press, New York, 1962, pp. 387-444

32. J. Kane, C. Karthik, D. P. Butt, W. E. Windes, R. Ubic, "Microstructural characterization and pore structure analysis of nuclear graphite", JNM, Vol 415, Issue 2, 15 August 2011, pp 189-197

33. Thrower, P. A., Progress Report, 1 Feb. 1976 – 31 Jan. 1977, COO-2712-2.

34. Thrower, P. A., J. C. Bognet and G. K. Mathew, The influence of oxidation on the structure and strength of graphite - I. Materials of different structure, Carbon Vol. 20, No. 6, 1982, pp. 457-464.

35. Moormann, Rainer, H. K. Hinssen, and K. Kühn, Oxidation behaviour of an HTR fuel element matrix graphite in oxygen compared to a standard nuclear graphite, Nuclear Engineering and Design, Vol. 227, 2004, pp. 281-284.

36. Octave Levenspiel, "The Chemical Reactor Omnibook", OSU Book Stores, Inc. Corvallis, Oregon, July 1996

37. Octave Levenspiel, "Chemical Reactor Engineering, 3rd Edition", John Wiley and Sons, 1999

38. M. S. El-Genk and J. M. P. Tournier, "Comparison of oxidation model predictions with gasification data of IG-110, IG-430 and NBG-25 nuclear graphite", Journal of Nuclear Materials 420 (2012) 141-158

39. McKee, Douglas W., Chemistry and Physics of Carbon, Oxidation Protection of Carbon Materials, No. 1, Vol. 16, 1981, pp. 1-118.

40. Ryan, B. A., and D. R. de Halas, Graphite Burnout, Interim Report ON IP-25-A (PT-105-532-E), HW-62273 Rev. 2, Hanford Laboratories, March 15, 1960, (Declassified, 49 pp.).

41. Q. Wang, Effect of boron on graphite oxidation – a theoretical study", Carbon 35 [2] pp307-313, 1997

42. J. F. Rakszawski and W. E. Parker, "The effect of group IIIA to VIA elements and their oxides on graphite oxidation", 6th Biennial conference on Carbon, Pittsburgh, P A, June 17-21, 1963

43. D. G. Schweitzer et al., "A Safety Assessment of the Use of Graphite in Nuclear Reactors Licensed by the US Nuclear Regulatory Commission", Brookhaven National Laboratory Report BNL-NUREG-52092, NUREG/CR-4981 (1987).

44. B.T. Kelly, Physics of Graphite, Applied Science Publishers LTD, London and New Jersey, 1981, Chapter 6, pp 362-385.

45. T. Burchell (Ed.), Carbon Materials for Advanced Technologies, Elsevier Science LTD, Oxford, 1999, Chapter 13, pp 429-484.

46. Kelly, B. T., Radiation damage in graphite and its relevance to reactor design, Progress in Nuclear Energy, Vol. 2, 1978, pp. 219-269.

47. Davidson, H. W., and H. H. W. Losty, The Effects of Neutron Irradiation on the Mechanical Properties of Graphite, Second United Nations International Conference on the Peaceful Uses of Atomic Energy, A/CONF.15/P/28, February 1958.

48. M. Bradford and M. Davies, A revised description of graphite irradiation induced creep, Journal of Nuclear Materials 381 (2008) 39–45

49. IAEA, Irradiation Damage in Graphite due to fast neutrons in fission and fusion systems, IAEA-TECDOC-1154, Austria, September 2000.

50. Thrower, P. A., Final Report, May 1981, DOE-ER02712-8, COO-2712-8

51. T. D. Burchell, K. L. Murty, and J. Eapen, Irradiation Induced Creep of Graphite, Journal of Materials, Vol. 62 No. 9, pp 93-99.

52. Blanchard, A., Appendix 2, The Thermal Oxidation of Graphite, Irradiation Damage in Graphite due to Fast Neutrons in Fission and Fusion Systems, IAEA-TECDOC-1154, April 2000

53. Hennig, Gerhart, A Comparison of the Effects of Oxidation and the Effects of Neutron Irradiation on Graphite, ANL-4765, February 22, 1952.

54. N. C. Gallego and T. D. Burchell, "A Review of Stored Energy Release of Irradiated Graphite", ORNL/TM-2011/378, September 2011.

55. Z. Zhang et al., "Current Status and Technical Description of Chinese 2x250 MWth HTR-PM Demonstration Plant", Nuclear Engineering and Design 239 pp. 1212-1219 (2009).

56. J. Ortensi et al., "Prismatic Core Coupled Transient Benchmark", Transactions of the American Nuclear Society, Vol. 104, pp. 854 (2011).

57. F. Reitsma et al., "The IAEA Coordinated Research Program on HTGR Reactor Physics, Thermal-Hydraulics and Depletion Uncertainty Analysis: Description of the Benchmark Test Cases and Phases", INL/CON-12-26565, Idaho National Laboratory (2012).

58. G. Strydom, H. Gougar, "Preliminary Reactor Physics Assessment of the HTR Module with 14% enriched UCO Fuel", Nuclear Engineering and Design 256, pp. 304-321 (2013).

59. J. W. Stairmand, "Graphite Oxidation - a Literature Survey", AEA Technology Report, AEA-FUS-83 (1990).

60. Bechtel National, Inc., et al., "Preliminary Safety Information Document for the Standard MHTGR", HTGR-86-024 (1986).

61. Y. Zhou et al., "Thermal Hydraulic Simulation of Reactor of HTR-PM Based on Thermal-Fluid Network and SIMPLE Algorithm", Progress in Nuclear Energy 62, pp. 83-93 (2013).

62. M. B. Richards, "Reaction of Nuclear-Grade Graphite with Low Concentrations of Steam in the Helium Coolant of an MHTGR", Energy Vol. 15, No. 9, pp. 729-739 (1990).

63. D. Schweitzer et al., "Oxidation and Heat Transfer Studies in Graphite Channels", Nuclear Science and Engineering 12, pp. 39-62 (1962).

64. D. G. Schweitzer, "Experimental Results of Air Ingress in Heated Graphite Channels: A Summary of American Analyses of the Windscale and Chernobyl Accidents", (Proceedings Technical Committee Meeting, Beijing, China), IAEA-TECDOC-784, IAEA, Vienna, pp. 50–54 (1995).

65. H.-K. Hinssen et al., "Oxidation Experiments and Theoretical Examinations on Graphite Materials relevant for the PBMR", Nuclear Engineering and Design 238, pp. 3018-3025 (2008).

66. M. B. Kuhlmann, "Experiments to Investigate Flow Transfer and Graphite Corrosion in Case of Air Ingress Accidents in a High-temperature Reactor", Jülich Research Centre, JUL-4003, ISSN 0944-2952 (2002).

67. A. C. Kadak, T. Zhai, "Air Ingress Benchmarking with Computational Fluid Dynamics Analysis", Nuclear Engineering and Design 236, pp. 587-602 (2006).

68. H. C. No et al., "Multi-Component Diffusion Analysis and Assessment of GAMMA code and Improved RELAP5 Code", Nuclear Engineering and Design 237, pp. 997-1008 (2007).

69. T. Takeda, "Air Ingress Phenomena in a Depressurization Accident of the Very-High-Temperature Reactor", Nuclear Engineering and Design 240, pp. 2443-2450 (2010).

70. G. Strydom, "TINTE Uncertainty Analysis of the Maximum Fuel Temperature During a DLOFC Event for the 400 MW Pebble Bed Modular Reactor", Proceedings of ICAPP 2004, Pittsburg, USA (2004).

71. Y. Zhou et al., "Thermal Hydraulic Simulation of Reactor of HTR-PM Based on Thermal-Fluid Network and SIMPLE Algorithm", Progress in Nuclear Energy 62, pp. 83-93 (2013).

72. G. Strydom, "Uncertainty and Sensitivity Analysis of a Pebble Bed HTGR Loss of Cooling Event", Science and Technology of Nuclear Installations, Vol. 2013, Article ID 426356 (2013).

73. B. Boer et al., "Validation of the DALTON-THERMIX Code system with Transient Analysis of the HTR-10 and Application to the PBMR", Nuclear technology, Vol. 170, pp. 306-321 (2010).

74. U. E. Sikik, "Simulations of Air and Water Ingress Transients for the Pebble Bed Modular Reactor (PBMR) by Means of the TINTE Code", Proceedings of ICAPP 2008, Washington, USA (2008).

75. S. Ball et al., "Sensitivity Studies of Air Ingress Accidents in Modular HTGRs", Nuclear Engineering and Design 238, pp. 2935-2942 (2008).

76. H. Haque, "Consequences of Delayed Air Ingress Following a Depressurisation Accident in a High Temperature Reactor", Nuclear Engineering and Design 238, pp. 3041-3046 (2008).

77. H. B. Palmer, M. Sibulkin, R. A. StrehIow, and C. H. Yang, "An Appraisal of Possible Combustion Hazards Associated With A High-Temperature Gas-Cooled Reactor," BNL-NUREG-50764, March 1978.

78. W. Botzem, J. Worner (NUKEM Nuklear GmbH, Alzenau, Germany) (2001-06-14). "Inert Annealing of Irradiated Graphite by Inductive Heating"

79. Nuclear Safety Advisory Committee, Nuclear Safety Advisory Committee Meeting of RG2 with Windscale Pile 1 Decommissioning Project Team 29/09/2005, NuSAC (2005) pp. 18.

80. M. Srinivasan, USNRC, "Advanced Reactor Research Plan and Status for Graphite Materials", presented at ACRS Future Plant Designs Subcommittee, May 13, 2011.

81. Summary Report on the Post-Accident Review Meeting on the Chernobyl Accident, Report by the International Nuclear Safety Advisory Group, Safety Series No. 75-INSAG-1, International Atomic Energy Agency, 1986, (ISBN: 9201231865)

82. INSAG-7, The Chernobyl Accident: Updating of INSAG-1, A report by the International Nuclear Safety Advisory Group, International Atomic Energy Agency, Safety Series No. 75-INSAG-7, 1992, (ISBN: 9201046928).

83. Chernobyl Reactor Accident Source Term [The]. Development of a Consensus View NEA/CSNI/R(95)24,

84. C. Wood, "Graphite Decommissioning: Options for graphite treatment, recycling, or disposal, including a discussion of safety-related issues", EPRI Technical Report 1013091, March 2006.

85. General Atomics graphite material properties website, http://gt-mhr.ga.com/safety.php

86. Young, J. "Chernobyl: The Accident Sequence", the Proceedings of a Seminary organized by the British Nuclear Energy Society, London, October 3 1986, BNES 1987, pp 27-41.

87. Sich, A. R., "The Chernobyl Active Phase – Why the Official View is Wrong", Nuclear Engineering International, April 1996, pp 22-25.

88. M. B. Richards, "Combustability of High-Purity Nuclear Grade Graphite", Proc. 22nd Biennial Conference on Carbon, San Diego, 16-21 July, 1995, American Carbon Society, 598-599.

89. Legasov V. A., reported in Pravda, Moscow, May 20 1988, pp 3 and 8.

Appendix A

Oxidation in Graphite-Moderated Reactor Accidents

Appendix A
Oxidation in Graphite-Moderated Reactor Accidents

This section discusses the only two historical examples of large scale severe graphite oxidation events in nuclear reactors, the October 1957 accident at Windscale Pile Number 1 and the Chernobyl accident in April 1986. In both cases it is shown that although massive oxidation of the graphite structures did occur, the presence of additional fuel sources in Chernobyl (roof tar and fuel rod cladding) and excess heat in the Windscale core (from a uranium metal fire) were the crucial parameters, and that the oxidation was not self-sustained at any point, even with a continuous fresh air supply. The use of the misnomer "graphite fires" can be traced back to the first of these events (Windscale) and even aubsequent revisions of the accounts and analyses of these accidents by expert panels differed greatly on the use of this terminology.

As argued in this paper, graphite components within a nuclear reactor are not capable of self-sustained oxidation or burning as defined by the NFPA. Observations and initial reports of these two accidents ostensibly appear to contradict this conclusion. Unfortunately, even expert commissions initially described these events as graphite fires because of severe oxidation observed in the graphite components. After further analysis and considerably more data were obtained, it is now understood the initial descriptions were incorrect. Numerous studies and expert commissions investigating both accidents have come to the conclusion that while the graphite components sustained significant oxidation, there is no evidence to conclude the oxidation was self-sustained. Rather, significant evidence illustrates the graphite continued to oxidize only as long as the high temperatures (from the nuclear fuel) sustained the reactions. When the nuclear generated decay heat was reduced, graphite oxidation terminated as was discussed in Section 2. Both accidents are discussed here with the latest analysis of the factors underlying the oxidation of the graphite components. . It should also be noted that both of these designs differ substantially from modern modular HTGRs (air-cooled, uranium metal fuel for Windscale and high power densities, water cooled in Chernobyl's case compared to a low power density, TRISO fuel, helium coolant of modern modular HTGRs.).

5.1   Windscale Accident

Windscale Units 1 and 2 were low temperature, air-cooled, graphite-moderated reactors built in 1950 near Sellafield, Cumbria, England. The aluminum clad, uranium metal fuel rods (and isotope production cartridges) were inserted into horizontal channels machined in the graphite core components. The reactor was cooled by passing outside air over the graphite core with the hot air exhausted out of the back of the core and up through a filtered chimney stack.

To remove the Wigner stored energy from irradiation damage in the graphite, the Windscale pile required annealing. During the annealing procedure the graphite core was heated to 250°C by raising the temperature of the entire core using fission as the heat source. This allowed any displaced carbon atoms to slowly move back into irradiation induced vacancies within the atomic crystal structure and ensured a slow, gradual energy release of the energy stored in the irradiated graphite[78]. Although scheduled annealing was known to prevent buildup of Wigner energy, the reactor (specifically the cooling system) was not designed to undergo the procedure. During the annealing, hotspots were formed in the core which caused significantly higher temperatures to occur within the metal fuel rods in those regions. During the last annealing cycle in Windscale, the metal fuel within these hot regions attained temperatures high

enough to ignite the fuel; leading to significant radioactive material release and severe oxidation damage to the graphite core. The Windscale accident was a uranium-fueled fire, not a fire of the graphite moderator as is widely assumed[79].

A 2005 remote visual inspection of the core showed that graphite damage was localized around burning fuel elements and did not spread into the main graphite moderator[80]. The resulting heat from this metallic fire provided sufficient energy (heat) to oxidize the graphite immediately surrounding the fuel. Estimated radial temperature gradients from the fuel show that temperatures in excess of 400°C were possible only a few millimeters from the outer surface of the uranium metal fuel rods. Visual inspection of the graphite core verified that the surrounding graphite material experienced severe oxidation directly adjacent to the outer surface of the uranium fuel rods. The heat from the uranium metal fire enlarged the diameter of the fuel channels, joining the adjacent channel in a few places. At the back of the core, where the oxygen was depleted, there was little visible damage, indicating the graphite stopped oxidizing when the nuclear generated heat sources fell below 400°C. Modern modular HTGR designs do not use metallic uranium fuel, instead using a more robust ceramic and encapsulated (TRISO) fuel form. Furthermore, they operate at much higher temperatures at which periodic annealing of the graphite core is not needed.
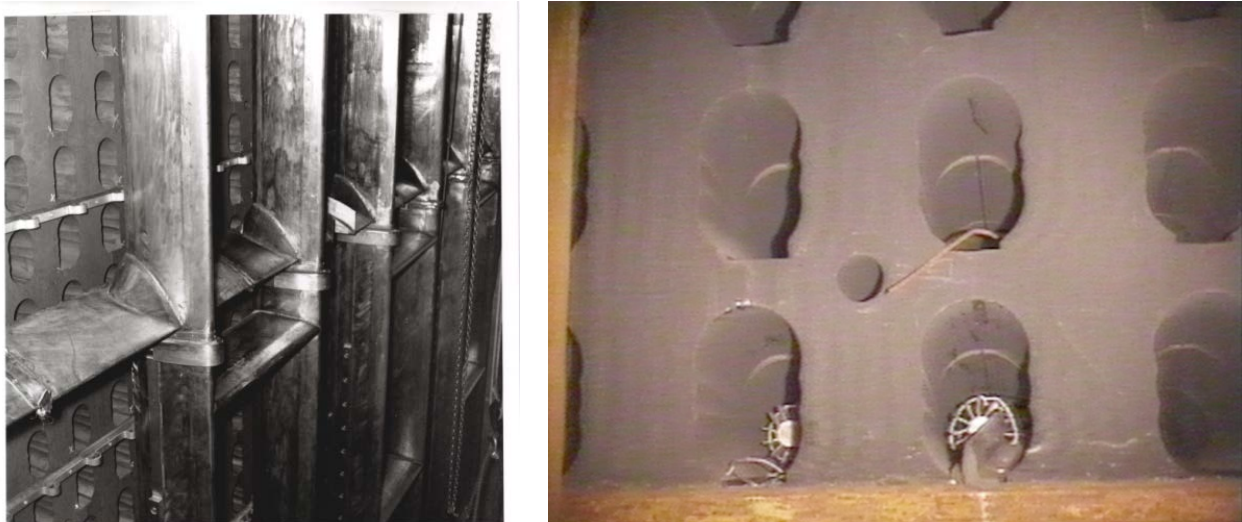

Figure 36. Windscale reactor internal before the accident (left image) and after the metal fire accident (right image). Inspection showed no indication that the fire spread into the graphite moderator material.

While severe oxidation of the graphite did occur during this air-ingress accident, the actual fire and subsequent radioactive material release resulted from the uranium fuel fire. From visual examination and extensive post-accident analysis data it is apparent oxidation in the graphite stopped once the heat from the uranium metal fires were extinguished. The graphite oxidation was not self-sustaining and was unable to continue the chemical chain reaction necessary to sustain a "fire", as defined in the NFPA specifications.

5.2   The Chernobyl (*Ukrainian Chornobyl*) Accident

The Chernobyl accident resulted from a series of events and design flaws that combined to cause an explosion during an experiment conducted to test the design operation of the independent power supply in the event of the loss of external power sources. The test required the reactor to be run at low power

(200 MWt). For unknown reasons, the core power actually dropped to about 30 MWt which, as was known by the designers, leaves the core in a thermal-hydraulically unstable state (positive void coefficient). Efforts to increase the power were frustrated by high xenon levels, reduced voiding of the coolant, and graphite cool-down. In order to increase power, the operators pulled out more control rods than were allowed to maintain the minimum operating reactivity margin. Reinserting the rods under these conditions, however, actually injected reactivity into the core because the graphite followers at the ends of the control rods preceded the absorber material upon insertion. The sudden injection of positive reactivity into the unstable core resulted in a large fission power spike, causing severe fuel damage and instantly vaporizing the water coolant. The resulting steam explosion was followed by another explosion a few seconds later, probably due to the combustion of the hydrogen released from the zirconium-steam reaction. This second explosion expelled additional fragments from the fuel channels and hot graphite from the reactor core. It should be note that none of these vapor/gas explosions can be termed "nuclear" explosions. The two explosions fractured the graphite core, blew off the biological shield, and expelled a significant mass of the very hot graphite, nuclear fuel, and the roof structure of Chernobyl Unit 4 out of the reactor building to the surrounding environment and over an extensive geographical area[81,82].

Much of the hot graphite core and fuel (about a quarter of the 1,200 tons available) was ejected and started a number of fires in the surrounding debris field and combustible material near the vicinity of the reactor building. The ejection of the nuclear fuel from the reactor structure caused the main release of radioactivity into the environment in the form of larger fragments (>50 µm) deposited near the Chernobyl site, smaller fragments (<20 µm) as aerosols carried well beyond the site, and as gases such as volatile fission products[83]. There are no data on any fission products released from the surrounding graphite moderator material, and based on the relative radionuclide inventory of the fuel compared to the graphite moderator, the assumption is that any release from the moderator was very small when compared to the amount of radioactive material released from the fuel.

There is a large amount of confusion and misinformation concerning the resulting "fires" and "glowing graphite core" after the steam explosion, but much of the expert graphite community agrees that this mixture of hot graphite and extremely hot nuclear fuel, along with combustible roofing material from the destroyed reactor building, produced the burning debris that was mistakenly identified as a graphite fire[84,85]. The hot graphite would be expected to rapidly oxidize once it was exposed to air[86] and would continue to oxidize when exposed to external heat sources, but as discussed in Section 2, self-sustained graphite fires are not possible due to the limited RSA sites and restrictions of oxygen transport through the graphite microstructure.

During the initial post-accident evaluation it was incorrectly assumed the fires on the bitumen coated rooftops of the adjacent containment buildings, fires among the building debris, and fires in the surrounding vegetation where large fragments of graphite/fuel observed glowing in the darkness were graphite-fueled. However, as was pointed out by later observations, bitumen, construction material, and surrounding vegetation is highly flammable. Mixing hot fragments of nuclear fuel and graphite with these flammable materials would cause these materials to ignite and create self-sustained fires. While the hot graphite and nuclear fuel may have initiated the fires they were not the material producing the self-sustained combustion, rather only the ignition source.

Finally, the red glow observed during the Chernobyl accident that was initially characterized as a large-scale graphite fire was actually the expected color of luminescence for graphite at >650°C and not a graphite fire[87,88]. One of the observations from a witness of the Chernobyl accident describing "a column

of white combustion products (white smoke) rising several hundreds of metres into the sky"[89] is indicative of the mistakes made when assuming graphite is capable of self-sustained fires. Graphite oxidation produces CO/CO_2 – colorless and odorless gases. The visual observation of a "white combustion product" is indirect evidence that the hot graphite ignited other combustible materials after it was ejected from the reactor core, and provides no evidence that the graphite oxidation itself was self-sustained. Much of the later analysis of the Chernobyl accident has refuted the initial statements that the graphite suffered self-sustained oxidation (burning) and does not consider this a credible event for graphite components, but the misconceptions and confusion on this topic persist to the conundrum of nuclear graphite experts.

In recent decades, a number of modular HTGRs have been designed with a two-unit pebble bed reactor currently under construction in China. These new designs feature very high coolant gas temperatures to enable high efficiency electricity generation and process heat for industrial applications. They also feature a robust coated particle fuel form and a tall, slim core geometry that allows passive core heat removal under all postulated accident conditions. The very low power densities of the new modular HTGR designs (5 MW/m^3 for a typical HTGR, compared with more than 80 MW/m^3 for Chernobyl), lack of coolant feedback mechanisms and significantly lower excess reactivity also limit the potential energy release during potential accidents. Modular HTGRs are also designed to limit the oxidation potential of their graphite components in the event of steam or air ingress, as described in Section 3. These engineering design controls provide yet another level of protection to the graphite components in addition to the physical and thermal properties of the graphite itself.